

**WAVE-INDUCED STEM BREAKAGE IN A VEGETATED
FORESHORE AND ITS IMPLICATION ON
PROBABILITY OF FLOODING**

Master of Science

Thesis

of

H.Y. SUH HEO

Delft University of Technology
Faculty of Civil Engineering
Specialization in Hydraulic Engineering

Special thanks to

you

Members of the graduation committee:

Chair :

prof. dr. ir. S.N.Jonkman Delft University of Technology

Supervisors :

ir. V. Vuik HKV, Delft University of Technology

dr. ir. S. van Vuren HKV, Delft University of Technology

dr. ir. B. van Prooijen Delft University of Technology

Figure 1: Partners of Project BE SAFE



UNIVERSITEIT TWENTE.

An electronic version of this dissertation is available at
<http://repository.tudelft.nl/>.

This work is part of the research programme BE SAFE, financed primarily by the Netherlands Organisation for Scientific Research (NWO).

CONTENTS

Acknowledgements	ix
Abstract	xi
1 Introduction	1
1.1 Motivation	1
1.2 Objective and research questions	4
1.3 Methodology and Approach.	5
2 Background	9
2.1 Three-point bending test and maximum allowable load	10
2.2 NIOZ field measurements of waves	12
2.3 Probabilistic model and 1-D wave energy balance	13
2.4 Wave dissipation by vegetation	14
2.5 Properties of vegetation and its effects on wave attenuation	17
2.6 Risk of flooding and dike failure.	19
3 Mechanical Analysis of Stem Breakage	21
3.1 Maximum allowable stress of vegetation stem	23
3.2 Wave-induced stress on vegetation	26
3.3 Wave data analysis and vegetation	29
3.3.1 Threshold wave height of stem breakage.	29
3.3.2 Variation in wave height attenuation.	30
3.4 Real data application of mechanical analysis	31
3.4.1 Spartina anglica	32
3.4.2 Scirpus maritimus	32
3.4.3 Limitations of mechanical approach.	33

4	Application of Stem Breakage to Wave Energy Balance	35
4.1	Wave energy balance	36
4.2	Implementation of stem breakage	39
4.2.1	Model setup	39
4.2.2	Overestimate of wave-induced stress	41
4.2.3	Correction factor.	44
4.3	Model application.	47
4.3.1	Sensitivity to wave height	47
4.3.2	Sensitivity by season	51
5	Probability of Flooding and Influence of Vegetation	57
5.1	Probabilistic model for dike failure	59
5.2	Vegetation scenarios	60
5.3	Correlation scenarios	62
5.4	Result analysis	67
5.4.1	Vegetation scenarios and probability of failure.	69
5.4.2	Correlation scenarios and Influence factors	72
5.4.3	Influence of individual vegetation characteristics	75
5.5	Recommendations	80
6	Discussion	81
7	Conclusion	83
	Bibliography	87
A	Wave Dynamics	91
A.1	Linear wave theory	91
A.2	Short-term wave statistics.	93
B	Probabilistic Methods	95
B.1	First-Order Reliability Method (FORM)	96
C	Vegetation Characteristics	99

ACKNOWLEDGEMENTS

Writing the MSc thesis, what felt to me like a complete black box at the beginning, has truly been a special experience. Many nights I fell asleep thinking of a solution for tomorrow, and ended up MATLAB coding throughout my dreams. I had nervous cycles of stress and revelation, wondering whether I would eventually reach satisfactory results that I aimed for. In the end, I realize that research is actually a never ending story, and I am not quite sure if I would ever be completely satisfied. Yet, I am satisfied. Not because I am a genius and contributed significantly to humanity, but because I matured a little more and enjoyed the discussions with friends, family, and researchers that gave me insight and also a platform to organize my thoughts.

Thanks to Kyuwon, for always making me laugh, refilling my confidence, and supporting me in so many different ways. The delicious meals, so nourishing and full of love, even seem to feed my soul. I thank my friends, Ana's, Non, Koen, and others for the productive discussions and moral support. The long days were so much more fun and enjoyable with such great people. Also special thanks to my sister Lina, for being such an awesome writing mentor. I used to dread writing, but over the years of constructive criticism, I now even receive compliments (which I thought would never happen). I give thanks to my family and friends abroad, especially Mom, Dad, Bird, Jungwoo, Mother-in-law, sister-in-law, Yungjin, Byul, for the encouragement and love from so far away.

Last, but not least, I would like to thank my committee members for guiding me through this research. Vincent, thank you for always answering my questions, and pointing me in the right direction. Even my friends were impressed at how kind and supportive you are. Professor Jonkman, I really appreciate your time out of your busy schedule, and even with the new excitements of life. Separate thanks to Willem who is healthy and doing well. Thank you Saskia for introducing me to this very interesting research topic, and always providing me with thorough feedback. It helped me organize and shape my research. Thank you Bram for your scientific input from a different perspective. Thanks to you I particularly made sure that I correctly stated things to make things clearer.

For those of you who I could not mention, I thank you also for making Delft a more colorful and memorable place.

Hannah

28.Aug.2016

ABSTRACT

VARIOUS flood protection measures are studied across the globe, and nature-friendly and environmentally resilient methods are gaining more attention. As part of the building with nature initiative, the project BE SAFE (**B**io-**E**ngineering for **S**AFEty) studies the effects of a vegetated foreshore as a flood protection measure which is found to be very effective. Vegetation helps to reduce wave energy as the stems and canopy work as small hurdles and obstacles that the waves need to pass. In this process, the waves lose much of its energy and the wave height reduces. As a result, the wave height is lower at the shore and less force acts on the coastal dike. From previous research, vegetation is known to be a dominant measure of wave energy dissipation, but the detailed processes of how it interacts with waves is not well known.

Until now, vegetation in the foreshore has either been completely ignored (by coastal dike managers) or considered healthy and abundant (by ecologists). This research acknowledges that vegetation exists, but its strength and stem density may vary depending on the location and time of the year. The focus of this research is understanding the interaction between vegetation and waves, as well as its implications to the probability of dike overtopping and flooding.

As waves pass through vegetation, stems break from the wave forcing which results in a variation of stem density in time (season) and space (foreshore). In this research, the mechanical interaction between vegetation stems and wave force is assessed to understand the point of stem breakage. Further, the vegetation stem breakage is implemented into the wave energy balance and in the probabilistic model of V. Vuik to quantify the probability of overtopping and dike failure. Refer to Figure 2 for the framework of this research.

Stem strength is quantified by the three-point bending test results from NIOZ (Royal Netherlands Institute for Sea Research), which is used to calculate the maximum allowable stress of the stem. This stem strength is compared to the wave-induced stress which is formulated by taking the Morison-type equation to quantify a uniform wave load acting over the submerged length of the stem. In this mechanical analysis, stems are assumed to break when the wave load exceeds stem strength.

Stem breakage is then implemented into the wave energy balance formulas, through which the stem density variation affects the amount of wave energy dissipation by influencing the wave height transformation. A correction factor is introduced to take into account leaning stems, but the correction factor could also include other simplifications that are not accounted for. Further, the performance of the wave energy balance is assessed through a sensitivity analysis of incoming wave height and seasonal vegetation data.

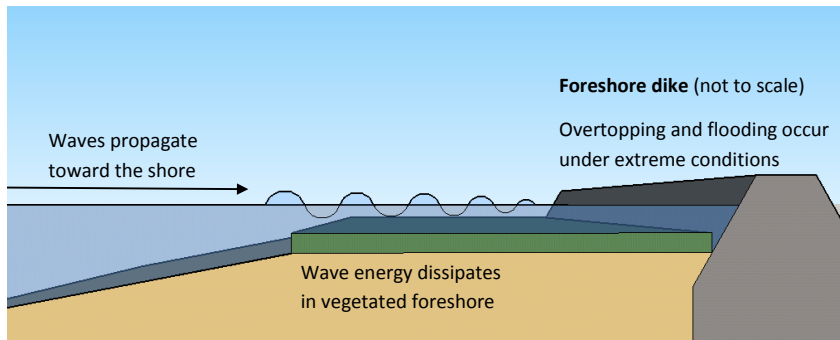


Figure 2: Framework of this research in 3D perspective. Waves propagate towards the shore, and wave energy dissipates as it travels through the vegetated marsh. If the wave height is too high when it reaches the dike (on the right), overtopping and dike failure may occur.

Seasonal vegetation data and stem breakage is implemented to the probabilistic model of V. Vuik which quantifies the probability of flooding (due to overtopping). Vegetation and correlation scenarios are tested to find the optimum approach and address the uncertainty in the result. Of the different vegetation scenarios, the most realistic approach is the percent stem breakage which evaluates wave load to the normal cumulative distribution function of stem strength. Further, the uncertainty of model results is reduced by using the correlation scenario with characteristic relations between vegetation parameters. Including vegetation stem breakage in the probabilistic model produces reasonable results, yet further research to calibrate the correction factor and to better define characteristic relations would strengthen the model result.

1

INTRODUCTION

1.1. MOTIVATION

MANY modern day engineering problems originate from the discord between natural process and artificial interference. In order to solve these problems, it has been proven that working with nature is more important than only trying to control it (Möller et al. [2014], van Slobbe et al. [2013], Van Wesenbeeck et al. [2014]). This led to the engineering concept of Building with Nature (BwN) which is receiving growing interest around the world. The **Bio-Engineering for SAFETY** using vegetated foreshores (BE SAFE) Project by Delft University of Technology, NIOZ (Royal Netherlands Institute for Sea Research), and University of Twente, is a multi-party research project investigating and quantifying the effect of vegetated foreshore in reducing flood risk. Researchers of varying fields—hydraulic engineering, ecology, bio-geomorphology, and governance—collaborate to learn the behavior and uncertainty in long-term sustainability in the respective field (TU Delft [2016]). Research institutes are included in Figure 1 in the preceding page v.

Significant progress has been made and knowledge gained regarding the effects of vegetated foreshores in low wave height situations. Yet for safety and stability of the structure, it is important to learn the governing mechanisms and effect during storm conditions which inflict the most damage. Contrary to previous research that were limited to low wave heights and mild conditions, the research by Vuik et al. [2016] proved that wave damping by vegetation is significant even for severe storm conditions. The research of Vuik addresses the limitations of previous low wave height research, and further serves as a basis for design and assessment criteria for dikes with a vegetated foreshore. Knowledge gained from this project will provide better guidance in designing a vegetated foreshore for more severe conditions and as means of flood risk reduction.

Seasonal Significance

There are yet many areas that require research and analysis, due to the complicated dynamics and lack of relevant study of extreme situations (i.e. where the most attention is needed). In particular, the seasonal variation in foreshore vegetation and its diverse effect to wave damping is not well known. Storms in most regions around the world are more likely to be seasonal than not. Depending on the geographical location, extreme conditions often occur in different seasons. For instance, in regions that are affected by the Atlantic hurricane (e.g. South-eastern coast of USA), peak season is in August through October, whereas in the North Sea of Europe severe storm conditions occur primarily from October to January. Although seasonal variation and storm conditions differ widely by region, this research focuses on locations in the Western Scheldt of the Netherlands where severe storm conditions mostly occur after the summer, and before the next spring season (broadly from September to March).

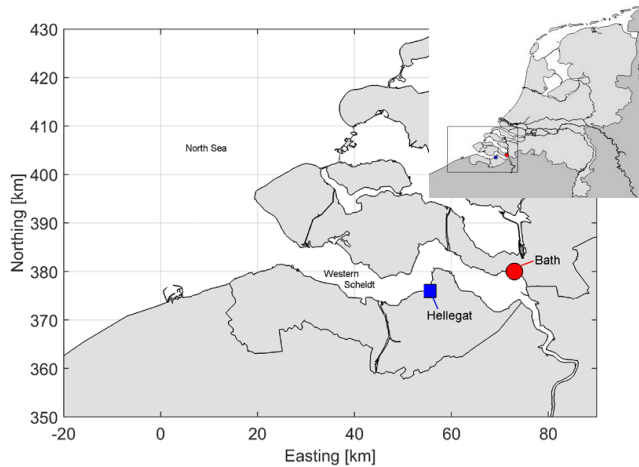


Figure 1.1: Field measurement locations Hellegat and Bath, in the Western Scheldt, of the Netherlands
*Reprinted from Vuik et al. [2016].

The winter season is of special interest in the Netherlands due to its extreme weather conditions such as storms, high wind speed, and large amount of rainfall. At the same time, the low temperature in winter causes the vegetation to be in its declining, dormant phase with no growth or development. Vegetation in its dormant winter phase easily breaks and thus reduces the rate of wave attenuation. Refer to 1.2 for photos of vegetation in winter at the field locations. This research will look into the different effects of vegetation on wave damping, and also how vegetation is affected by a significant storm.

This TU Delft MSc research, as part of the BE SAFE project, looks into seasonal stem breakage and its effect on reduction of wave damping. Relevant vegetation parameters for assessing the impact of vegetation on the foreshore include stem length, diameter, and stem density. Based on the wave conditions such as wave height and depth, the vegetation also reacts differently. Encompassing all the relevant parameters for vegetation and waves, further investigation will be made based on the resulting probability of



Figure 1.2: Site photos from February, 2016. Hellegat (left) with species: *Spartina anglica*. Bath(right) with species: *Scirpus maritimus*

flooding and uncertainty in overtopping and dike failure.

This study can be applied to other locations around the globe by understanding the location-specific wave climate as well as the respective vegetation characteristics at that location. Wave climate can be understood from wave measurement data, whereas vegetation can be studied by field measurements and three-point bending tests. These tests would provide the strength of the stems and how resilient/strong it would react to wave motion. By comparing the strength of the stem to the wave load acting on vegetation, the change in stem density could be quantified and applied to calculating wave energy dissipation. Even within the same species, vegetation length, diameter, and strength are not uniform, and instead they have a certain variation. Therefore, with a reasonable number of samples, applying the test results to the probabilistic wave model would yield a reliable prediction method for wave attenuation in the vegetated foreshore. This model can serve as a basis in determining how effective the vegetated foreshore is as an alternative for hard measures of flood protection such as a dike.

1.2. OBJECTIVE AND RESEARCH QUESTIONS

Objective

This research focuses on understanding the mechanism of wave-induced vegetation stem breakage and its subsequent effect on the probability of flooding. When stem breakage is applied to the probabilistic model of V. Vuik, the implication of seasonally varying vegetation as well as the effect of different vegetation characteristics is of interest.

Research questions

A. When do stems break in a vegetated foreshore?

- A.1 How can the strength of vegetation stems be quantified using the three-point bending test results from NIOZ?
- A.2 How can the wave load acting on vegetation be quantified?
- A.3 When is the critical point at which the stems break due to wave forcing?

B. How can stem breakage be applied to the wave energy balance?

- B.1 How does the wave energy balance model perform with the implementation of stem breakage?
- B.2 How sensitive is the model to varying wave and vegetation characteristics?

C. What are the possibilities of including stem breakage and varying vegetation characteristics to the stem breakage model? What are the effects and implications?

- C.1 How can vegetation characteristics and the change in vegetation density be incorporated as part of the wave energy dissipation calculations and probabilistic model?
- C.2 How do different scenarios perform in the probabilistic model?
- C.3 How do individual vegetation characteristics influence the model result?

1.3. METHODOLOGY AND APPROACH

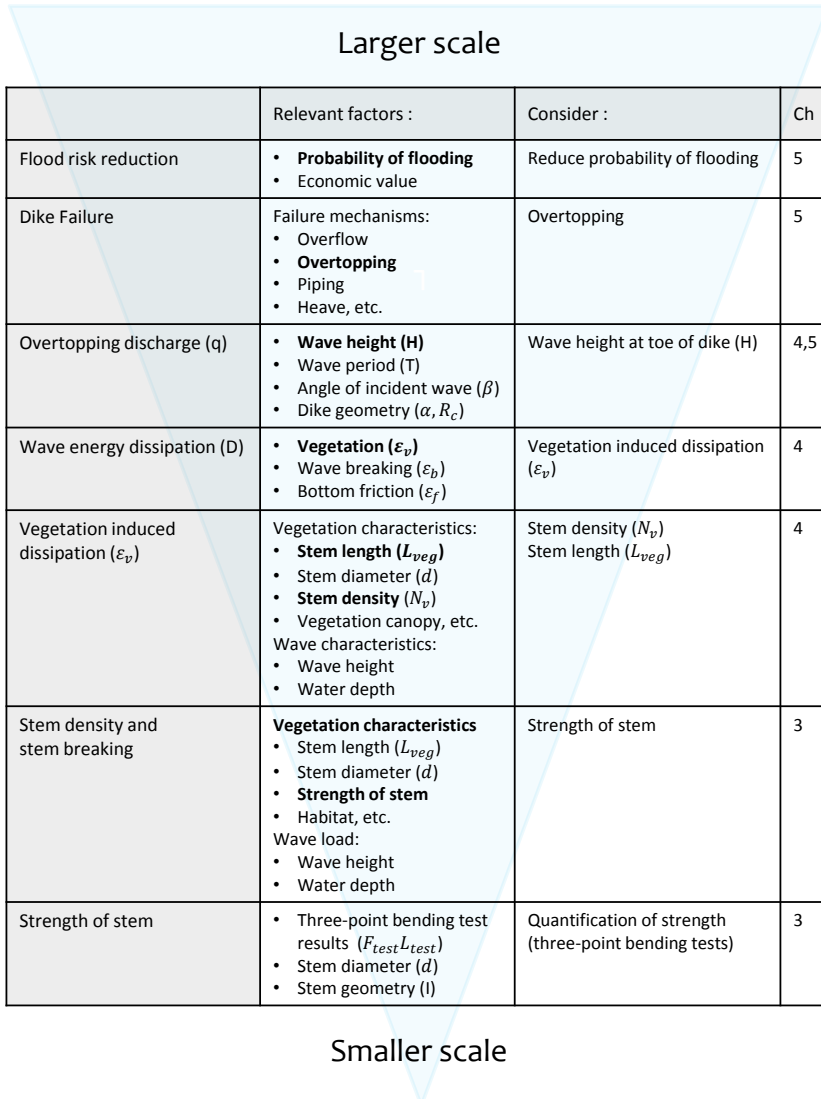


Table 1.1: Schematic of research approach. The order of research starts from the smaller scale vegetation and proceeds in the direction of the larger scale, eventually reaching the probability of overtopping and flooding (indicated in chapters). Also refer to Figure 1.4 for a visual representation.

As a measure for flood risk reduction along the coast, a vegetated foreshore is studied in this research. Of the many different possibilities to reduce the probability of flooding, this research will be focusing on minimizing overtopping discharge, which is the amount of water that spills over the top of the dike. Overtopping discharge is often the main failure mechanism of coastal foreshore dikes, because this overtopping quantity

determines the load acting on the inner (landward) slope which is the weakest part of the dike (Schiereck and Verhagen [2012]). The overtopping discharge is calculated from the probabilistic model developed by V. Vuik which is a function of wave height (H), wave period (T), slope of dike (α), angle of incoming waves (β) and free board (added height of the dike R_c). Of these parameters mentioned, the wave height, slope of dike and free board can be influenced by humans. However, increasing the free board (i.e. heightening the dike) is not considered in this research because it is considered unfavorable for aesthetic and economic reasons. The slope of the dike is also not considered because it cannot be easily modified once the structure is built. The objective of project BE SAFE is assessing the effectiveness of a vegetated foreshore as an alternative measure for flood protection. Therefore the interest lies in how effective the vegetated foreshore is for wave height reduction.

Wave height reduces from various wave energy dissipation factors that act on the waves as they travel towards the shore. This research will be quantifying the variation in wave energy dissipation over the year by evaluating the energy density flux. There are three main mechanisms for wave energy dissipation in a vegetated foreshore, the most common being bottom friction (ϵ_f), depth-induced wave breaking (ϵ_b), and in this case with significant vegetation in the foreshore, also vegetation-induced wave dissipation (ϵ_v). Depth-induced wave breaking may or may not occur depending on the wave conditions and bathymetry of the foreshore, but it has been found that in a vegetated foreshore, the depth-induced wave breaking is significantly reduced and maybe even negligible compared to the dominant dissipation mechanism being vegetation (Vuik et al. [2016]). Refer to Figure 1.3. This figure shows a comparison of a foreshore with and without vegetation. Here, a vegetated foreshore has a more significant reduction of wave height, and also the wave energy dissipation due to vegetation is most significant.

Vegetation induced wave energy dissipation will be one of the main focuses of this re-

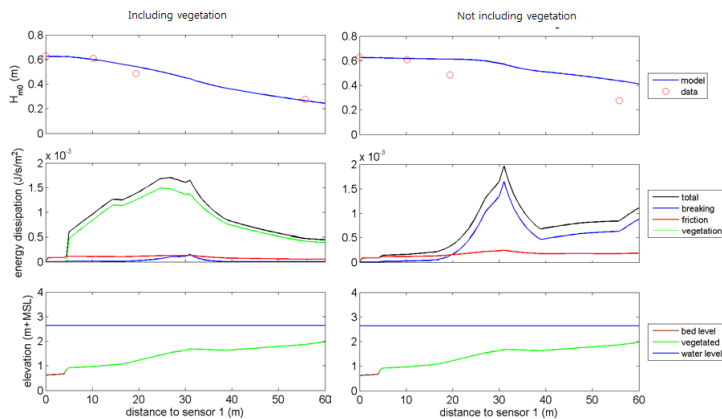


Figure 1.3: Difference in wave energy dissipation of a foreshore with vegetation (left) and without vegetation (right). *Reprinted from Vuik et al. [2016].

search. Wave characteristics such as wave height (H) and water depth (h) influence dissipation due to vegetation, but also several vegetation characteristics are strong factors that influence dissipation. Stem length, diameter, and density are main characteristics that will be analyzed in this research, but this is a vast simplification because in reality, many other factors such as leaves, vegetation canopy, and flexibility are also influential vegetation characteristics for wave dissipation. Among the factors that influence wave energy dissipation, stem density N_v often has a large fluctuation, whereas the stem length and diameter has a smaller variation for a given species. For this reason, the variation in stem density is evaluated in this research. Stem length, which is also found to be an influential factor, is considered as 10cm when broken.

With the periodically fluctuating water (currents, tides, waves) and seasonal/eventful storms, the vegetation stem density in the marsh will change over time. This variation in stem density N_v can be understood by understanding the number of stems that break. Stem breakage is quantified by comparing the strength of the vegetation (resistance) to the wave forcing (load) acting on the stem. When the wave load exceeds the resistance of the stem, the stem will break.

The vegetation species studied in this research, *Spartina anglica* and *Scirpus maritimus*, are relatively stiff stems compared to seaweed which is very flexible. As a result, the strength of the stem can be quantified by a three-point bending test, which are often a testing method for structural beams. The method in which the strength is quantified will be elaborated more in the Section 2.1. This stem strength is determined in terms of maximum flexural stress, and it will be evaluated against the wave-induced stress acting on vegetation. This will be further discussed in Chapter 3, which discusses the analytical approach to stem breakage. Refer to Table 1.1.

Structure of report

The order of research takes place from the smaller scale, taking an analytical approach to define the vegetation strength and wave loading (Chapter 3), and proceeds in the larger scale direction as the data on vegetation characteristics will be evaluated with a deterministic and probabilistic calculation of stem density, wave dissipation, and wave height transformation across the foreshore (Chapter 4). Further analysis will be performed to evaluate the effects of a vegetated foreshore on the probability of flooding by understanding the influence factor of various parameters, with recommendations on how to apply and improve this model for different locations and species (Chapter 5). Refer to Figure 1.4.

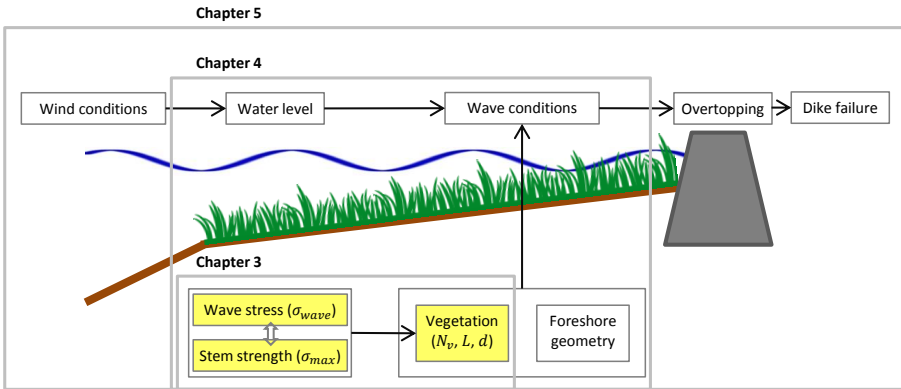


Figure 1.4: Overall schematization of research. Detailed processes are listed in Table 1.1.

2

BACKGROUND

Chapter 2 provides essential information that would facilitate the understanding of this research. Background information on the three-point bending tests of NIOZ, probabilistic model, wave energy balance, effects of vegetation on wave attenuation, quantification of overtopping and dike failure will be discussed in this chapter.

2.1. THREE-POINT BENDING TEST AND MAXIMUM ALLOWABLE LOAD

One of the collaborating parties, NIOZ conducts studies of ecology and provides field measurement data. Field studies and analysis are held in the Western Scheldt of the Netherlands, focusing on two locations: Hellegat and Bath (refer to Figure 1.1 for the map of these two locations). Vegetation samples are taken from the field, and three-point bending tests are performed to quantify the strength of the stem (Section 3.1). This data will be used to assess the strength of vegetation stems against wave-induced stresses, and further how the vegetation stem density reacts to such load. Each measurement location has different types of vegetation: cordgrass (*Spartina anglica*) for saline environment and club rush (*Scirpus maritimus* and *Phragmites australis*) that live in a more brackish environment. Measurement data of vegetation characteristics such as vegetation density, stem length and diameter from these locations are used in this research (information of the samples can be found in Table 3.1).

Various measurements, including the previously mentioned field measurements, have been made by NIOZ which will be utilized for this research. Additional data of interest is the three point bending test, which measurements were done in the laboratory of NIOZ. The objective of this test is to measure the maximum load and flexure stress the stem is able to withstand. Vegetation samples from 2014 December, 2015 April, September, and November are available for species *Spartina anglica* and *Scirpus maritimus*.

As can be seen in Figure 2.1, the portion of the stem is placed on two stands, and a pressure force is gradually applied in the middle of the stem. As the device is lowered into the center of the stem, the amount of force felt by the device is measured and recorded. The measured force increases until a maximum point, afterwards, the force no longer increases but rather reduces despite the continuously moving device further lowering into the stem. The declining force after reaching the maximum load does not indicate the stem has broken, but that the stem has probably folded, and it can no longer carry the amount of load beyond the maximum force measured. This maximum force is the point of interest. When the stem experiences a force exceeding this maximum load, it is considered folded and no longer being able to resist the wave load acting on the stem. This can be explained as skimming (water passing over the stem) and will be further explained in the next section.

With the three-point bending test, the device measures 1) time 2) magnitude of the force 3) flexure extension and 4) flexure stress. These measurement data will subsequently be converted into the maximum allowable moment, force, and stress that the stem experiences. The portion of the stem that is subject to experiment is the bottom 35mm. The reason for performing the test on the bottom part of the stem is that the stem experiences maximum stress near the bottom, and it is where the stem normally breaks as a result.

Information from the NIOZ three-point bending test will provide knowledge of the strength of the stem which will be expressed as a flexure stress, since this is the main mechanism that yields folding and subsequent breakage. The maximum flexure stress (i.e. strength

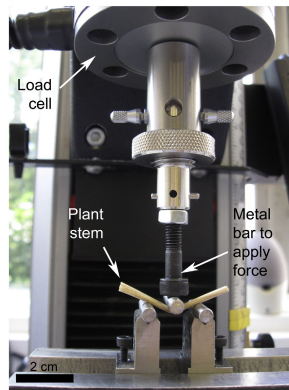


Figure 2.1: Example of the three point bending test measurement device. The three-point bending test by NIOZ has the same configuration. *Reprinted from Rupprecht et al. [2015].

of the stem) is then compared to the wave-induced vegetation stress. Calculation and further explanation of quantifying the wave-induced vegetation stress follows in Section 3.2.

2.2. NIOZ FIELD MEASUREMENTS OF WAVES

At Hellegat and Bath of the Western Scheldt, there are NIOZ wave measurement devices that continuously monitor four locations along the vegetated foreshore. These wave measurement devices are pressure sensors that convert the water and air pressure data into water level fluctuations, taking into account the pressure variation by depth. With the pressure data, there are two possible sets of wave characteristics based on the different conversion methods. The first set includes H_{m0} , T_p , and $T_{m-1,0}$, etc. found from wave spectrum of the Fourier analysis, and the second set includes H_{mean} , T_{mean} , H_s , etc. from the zero-crossing analysis. Measurements are available from November, 2014 to January, 2016 for four locations each in both Bath and Hellegat. Pressure gauges record 5Hz measurements for 7 minutes every 15 minute. In other words, the wave information is measured 5 times per second (=5Hz) for 7 minutes, and then rests for 8 minutes, completing a 15 minute burst cycle. Due to the configuration of pressure sensors, wave data is unavailable for low tides but available for high tides (twice per day for semi-diurnal tides in the Netherlands) and storms with large wave heights.

However, difficulties exist due to the lack of vegetation measurements from the field, since there are only four sets of vegetation data from December 2014 to November 2015. Therefore it is not possible to directly quantify the changes in stem density before and after a large wave condition. Instead, by comparing the wave height reduction with varying seasonal vegetation characteristics, it would be possible to estimate and analyze the effectiveness of vegetation on wave dampening. It is expected that there will be less wave height reduction (i.e. less wave attenuation) after a large storm, since much of the vegetation stems break, and therefore significant reduction in stem density occurs after a large storm. This approach will be further validated with model simulations mentioned in the next section.

2.3. PROBABILISTIC MODEL AND 1-D WAVE ENERGY BALANCE

Wave transformation and the probability of flooding will be calculated using the probabilistic model provided by V. Vuik. This model utilizes the MATLAB computational platform to simulate the 1-D energy balance for wave transformation and First Order Reliability Method (FORM) for calculating the probability of dike failure with overtopping being the dominant failure mechanism.

Varying vegetation characteristics obtained by NIOZ field data will be expressed in terms of stochastic (random) variables, having found the most suitable distribution type and its relevant parameters (e.g. a normal distribution will require an average and standard deviation). These vegetation characteristics will be inputted into the probabilistic model and wave attenuation will be modeled through the 1-D energy balance model.

Mendez and Losada [2004] developed a method for wave damping from vegetation, which is implemented into the 1-D energy balance calculations by means of a vegetation-induced wave energy dissipation term. Based on previous research and field data, this vegetation-induced dissipation term has been validated in numerical modeling by means of wave model SWAN (Simulating WAVes Nearshore) for computing wave height reduction for various hydrodynamic conditions (Suzuki et al. [2012]).

Maximum stress variations exist within the same species, because not all the stems have the same thickness, height and strength. This variability is implemented into the probabilistic model by means of defining the vegetation characteristics such as, thickness, height and strength, as stochastic (random) variables. These characteristics will be used to simulate the percentage of stem breakage and consequent variation in vegetation density that ultimately affects the wave damping behavior in the foreshore. Wave height transformation will take into account the change in vegetation and wave height near the dike. As a result, the probability of overtopping and failure calculated from the model will yield a more comprehensive and well-predicted outcome.

Further complementary measures to improve the probabilistic model include finding the correlation between the vegetation characteristics previously mentioned and implementing this correlation into the probabilistic calculations. For instance correlation among two of the following vegetation characteristics: thickness, height, and strength of stem.

2.4. WAVE DISSIPATION BY VEGETATION

Wave energy dissipation by vegetation is an undeniable phenomenon that multiple researchers have investigated and proved to be true around the globe (Dean and Bender [2006], Fonseca and Cahalan [1992], Mendez and Losada [1999]). Refer to Figure 2.2 of experimental results of wave height reduction due to vegetation. Multiple species of seagrass were observed and analyzed over the years, and wave energy reduced for different combinations of shoot density and water depths. In vegetated foreshores, dissipation of wave energy is a direct function of the percentage of the water column occupied by vegetation (Fonseca and Cahalan [1992]) and Mendez and Losada [1999] modeled the evolution of wave transformation through vegetation, both through regular and irregular waves, in order to evaluate the wave height damping, fluid motion, forces and moments on the vegetation.

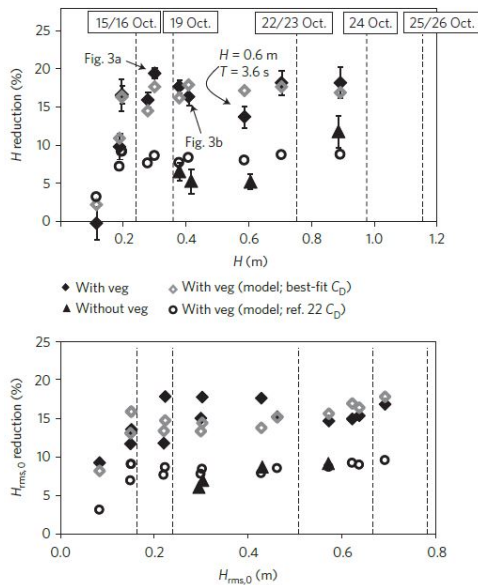


Figure 2.2: Percentage of wave height reduction for regular waves (H ; top) and irregular waves (H_{rms} ; bottom) from experiments with and without vegetation. *Reprinted from Möller et al. [2014].

Research nowadays focuses more on the extent of the effect of vegetation, and the governing mechanisms that are involved. Ecosystem functions such as wave attenuation are highly dynamic and usually change in a non-linear way over time and space (Koch et al. [2009]). This gives researchers and stakeholders all the more reason to study the behavior, in order to have better insight into designing such vegetated foreshores to reduce the risk of dike failure and flooding.

There are many means to protect the coast by decreasing the intensity of the incoming wave energy. Three most dominant mechanisms for wave energy reduction are: 1) energy dissipation due to wave breaking (Battjes and Janssen [1978]); 2) energy dissipation

due to friction; 3) energy reflection in the offshore direction (Duarte et al. [2013], Koch et al. [2009]) energy dissipation due to vegetation. Assuming normally incident waves on a straight and parallel coast, energy conservation yields:

$$\frac{dEc_g}{dx} = -\langle \varepsilon_v \rangle - \langle \varepsilon_b \rangle - \langle \varepsilon_f \rangle \quad (2.1)$$

The energy density flux is expressed by E [$N/m = J/m^2$], energy density; c_g [m/s], group velocity; ε_v [$N/ms = J/m^2s$], energy dissipation induced by vegetation; ε_b , energy dissipation due to wave breaking; and ε_f , energy dissipation due to bottom friction. The energy dissipation is expressed as the average rate per unit area, expressed within the angles brackets $\langle \cdot \rangle$. Wave breaking in shallow water is expressed as a phenomenon, in between a bore and a hydraulic jump (Battjes and Janssen [1978]), and it is expressed in Equation 2.2 below.

$$\varepsilon_b = \frac{1}{4} Q_b \rho g \frac{H_{\max}^2}{T_p} \quad (2.2)$$

Here, H_{\max} is the maximum wave height before breaking, which can be expressed in terms of the breaker parameter, γ as $H_{\max} = \gamma h$. The breaker parameter defines the limit of the wave height, and it widely ranges from approximately 0.4 to 0.88 depending on the wave conditions. Additionally, ρ is the water density [kg/m^3], g is the gravitational acceleration [m/s^2], Q_b is the relative number of broken (irregular) waves.

Among these wave energy dissipation mechanisms, the one due to vegetation (ε_v) has additional benefits. Vegetation is beneficial that it induces less modification of the coastline compared to artificial structures, and it is more adaptive to climate change (Ondiviola et al. [2014]). Over the years, many researchers studied wave dissipation and tried to include the influence of vegetation. The most widely implemented wave dissipation formula for random breaking waves is the research from Mendez and Losada [2004]. Wave energy dissipation from vegetation (ε_v) is the focus of this research, and it is obtained from the following Equation 2.3 of Mendez and Losada [2004].

$$\varepsilon_v = \frac{1}{2\sqrt{\pi}} \rho \tilde{C}_d b_v N_v \left(\frac{kg}{2\omega} \right)^3 \frac{\sinh k\alpha h + 3 \sinh k\alpha h}{3k \cosh^3 kh} H^3 \quad (2.3)$$

where \tilde{C}_d is the bulk drag coefficient [-], b_v is the stem thickness [m], N_v is the vegetation density (number of plants per square meter) [m^{-2}], k is the wave number [m^{-1}], ω is the wave angular frequency [s^{-1}], α is the relative vegetation height h_v/h (where $\alpha \leq 1$), h is the water depth [m] and H_{rms} is the mean wave height [m].

This vegetation-induced wave energy dissipation formula from Mendez and Losada [2004] is a step forward from the theory of Dalrymple et al. [1984] for vegetation-induced wave damping for non-breaking regular waves and horizontal bottom. The new model from Mendez and Losada includes the randomness of waves, vegetation, and breaking dissipation. A bulk drag coefficient (\tilde{C}_d) is incorporated as part of a simplification of the

model, accounting for the many unknowns into a single empirical value (Dalrymple et al. [1984], Mendez and Losada [2004]). This drag coefficient is determined empirically and is vegetation- and site-specific. Mendez and Losada [1999] found that the drag coefficient not only depends on vegetation properties, but it also depends on wave height and wave period. The drag coefficient has been calibrated for this model by Vuik et al. (2016) through field experimental data as well as model simulations.

Research over the years found that there are many factors that contribute to vegetation-induced wave damping. Paul and Amos [2011] found that there is a minimum shoot density that is necessary in order for vegetation to actually have an effect on wave damping. This threshold of minimum shoot density was found to vary with wave period. Refer to figure 2.3.

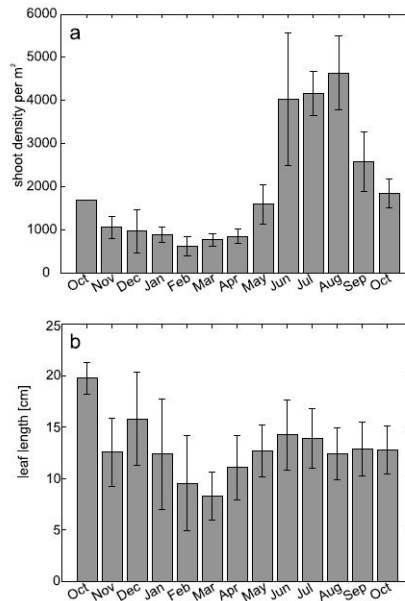


Figure 2.3: Monthly variation of (a) shoot density per m^2 and (b) leaf length of sea grass-*Zostera noltii*
 *Reprinted from Paul and Amos [2011].

2.5. PROPERTIES OF VEGETATION AND ITS EFFECTS ON WAVE ATTENUATION

Wave attenuation is found to be highly related to combinations of vegetation characteristics such as marsh size, biomass, vegetation density and stem stiffness. These findings are repeated over several researches (Bouma et al. [2010, 2005], Möller et al. [2014], Ondiviela et al. [2014], Paul and Amos [2011], Ysebaert et al. [2011]) and confirmed through recent meta-analysis by Shepard et al. [2011]. Refer to figure 2.4 for a quick view of relevant factors affecting wave attenuation in a salt marsh, quantified by number of studies.

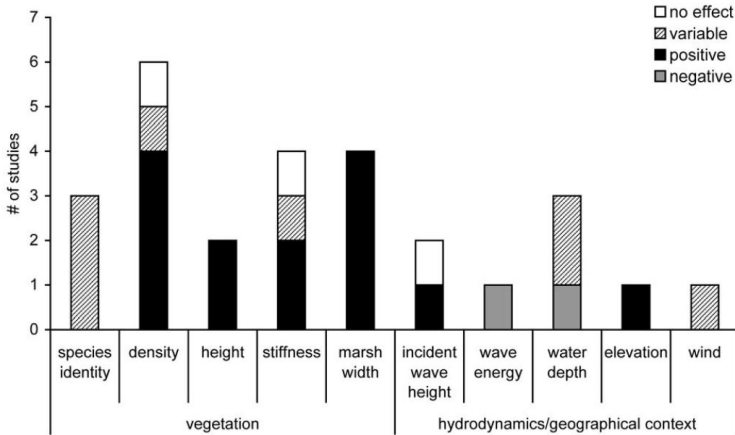


Figure 2.4: Most commonly quoted important factors for wave attenuation in salt marsh vegetation. *Reprinted from Shepard et al. [2011]

Vegetation along the coast acts as a hindrance for waves heading towards the shore, and therefore dampens the waves. However, the rate at which wave attenuation occurs varies depending on the situation. There are multiple factors that reduce the rate of wave damping especially during storm conditions. Under these severe conditions with large waves, Möller et al. [2014] found the vegetation stems bend more than 50 degrees during forward motion. Consequently, rather than traveling through the vegetation field which would retain energy and dissipate waves, the waves would instead skim over the vegetation. Furthermore, the bending motion led to a higher tendency for stem fracture and loss of biomass.

Two main mechanisms for avoiding breakage are: 1) leaning (tilting towards the flow of water) and 2) tolerance (resistance against the flow of water, by means of strength and stiffness). However, for a certain vegetation type, these two mechanisms were found to be negatively correlated (Puijalón et al. [2011]). This is understandable since the stem would not lean as easily if the stem is rigid and strong, and vice versa. Leaning stems are less effective for wave attenuation due to increased skimming that occurs above the height of the vegetation. Therefore, for wave damping due to vegetation, it is more favorable if the dominant mechanism for avoiding breakage is tolerance rather than leaning.

As mentioned previously, most wave damping from vegetation occurs when waves flow through the vegetation field.

Wave characteristics such as the incident wave height and period are undeniably an important factor in the rate of wave attenuation Möller et al. [2011], Yang et al. [2012], Ysebaert et al. [2011]), yet it is not in the control of humans to be able to regulate this parameter. Therefore it is important to quantify the influence of vegetation on wave attenuation in order to fully understand the behavior of waves in a certain type of vegetated foreshore, and how it can be implemented for protection against flooding. The coastal ecosystem as a coastal defense strategy has been understudied (Bouma et al. [2014], Shepard et al. [2011]), and it is important to build enough knowledge in order to provide more general application tactics for varying situations.

In figure 2.5, the seasonal differences in wave height reduction is shown by comparing results from measurement devices located at water depths less than 1m for varying months of the year. The decrease in wave height is greatest for July measurements which has the highest sea grass density (Paul and Amos [2011]). Other deployments showed a wave height reduction of less than 10%, indicating that the vegetation density is one of the key factors in influencing wave attenuation. Stem density and biomass reduction may occur from various reasons, but the main mechanisms are uprooting and breakage. Uprooting is a factor of wave characteristics as well as its root length (Liffen et al. [2013]), whereas stem breakage may be influenced by multiple factors which will be further investigated during this research.

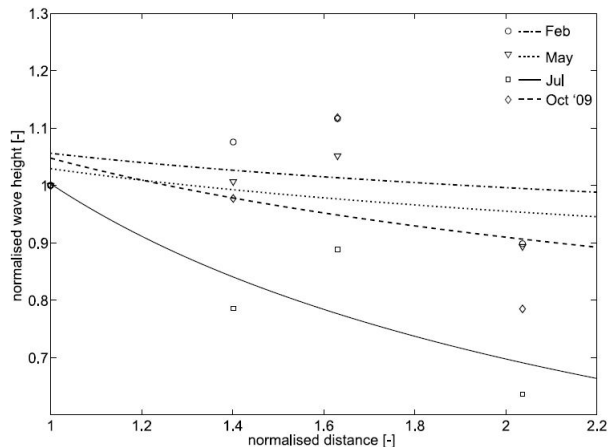


Figure 2.5: Mean normalized significant wave height in water depths <1m for seasonal variations. Normalized wave height and distance H/H_{s0} and x/x_0 where 0 denotes the values at the outermost station.*Reprinted from Paul and Amos [2011].

As one of the strategies to find a more generally applicable basis for wave attenuation by vegetation, vegetation characteristics such as density, biomass, and stem stiffness (strength) and its sensitivity and susceptibility to wave characteristics is studied.

2.6. RISK OF FLOODING AND DIKE FAILURE

Flood defenses for coastal safety in the Netherlands largely depend on dunes and dikes. Assuming that the dunes and dikes are built according to the Dutch standards and are regularly maintained as required, erosion and failure probability of dunes are considered minor compared to the failure probability of dikes (Vuik et al. [2015]). Further, vegetation in the foreshore stabilizes the sediment and shoreline (Fonseca and Cahalan [1992], Ondiviela et al. [2014], Shepard et al. [2011]), and therefore lowers the probability of dune failure even more. As a result, dike failure is the dominant mode of failure in the Netherlands.

Focusing on dike failure, there are many possible failure mechanisms, such as overflow, wave overtopping, piping, heave, instability of outer slope armoring, macro-instability of the inner or outer slope, etc. (Allsop et al. [2007]). Among these mechanisms, overtopping due to waves is considered most critical for sea dikes in the Netherlands, due to the shorter time scale of hydraulic loads on coastal dikes (Vuik et al. [2015]). Therefore, the probabilistic model used in this research will be based on the most conservative approach in the Netherlands: overtopping on the dike.

A probabilistic modeling is found to be a very practical and comprehensive approach because it is possible to include the variations in multiple input parameters. A fully probabilistic assessment with the probabilistic level II, FORM (first-order reliability method, more in Appendix B) solves the solution through an iterative correcting process. A limit state function ($Z=R-S$) is defined based on a critical failure situation, with R being the resistance (strength e.g. dike) and S being the load (e.g. hydraulic load, overtopping). The system is considered to have failed when $Z < 0$ which is equivalent to a situation in which the load (S) has exceeded the resistance (R).

In the probabilistic model used in this research, the limit state function for overtopping is defined by the following equation.

$$Z = m_{qc}q_c - m_qq \quad (2.4)$$

Here, m_{qc} and m_q are model factors accounting for the uncertainty of the critical overtopping discharge and computed actual overtopping discharge, respectively. Similarly, q_c is the critical overtopping discharge and q is the actual overtopping discharge in units of [m^3/s] per m width, as calculated with the highest 2% wave run-up height ($R_{u,2\%}$). The overtopping formulas of Van der Meer et al. [1994] (also in Equation 5.8 of EurOtop et al. [2007] manual) will be used to calculate the time averaged overtopping discharge. These formulas are related to the breaker parameter ($\xi_{m-1,0}$) also known as the Iribarren number, a function of the bathymetry slope ($\tan\alpha$), significant wave height (H_{m0}), and deep water wave length (L_0) as can be seen in Equation 2.5

$$\xi_{m-1,0} = \frac{\tan\alpha}{\sqrt{H_{m0}/L_0}} \quad (2.5)$$

When the breaker parameter is $\xi_{m-1,0} < 5$, the minimum of q_A and q_B is the overtopping

discharge (q). The values for q_A and q_B are calculated in equations 2.6 and 2.7.

$$q_A = \frac{2}{3} \sqrt{\frac{gH_{m0}^3}{\tan\alpha}} y_b \xi e^{-\frac{C_1 R_c}{\xi H_{m0} y_b y_f y \beta y_v}} \quad (2.6)$$

$$q_B = 0.2 \sqrt{gH_{m0}^3} e^{-\frac{R_c}{H_{m0} y_f y \beta}} \quad (2.7)$$

$$q = \text{minimum}(q_A, q_B) \quad (2.8)$$

Overtopping discharge for a breaker parameter $\xi_{m-1,0} > 7$ is also included in the EurO-top et al. [2007] manual, and for the values in between, $5 < \xi_{m-1,0} < 7$, the overtopping discharge is linearly interpolated. These conditions are written as part of the MATLAB code for the probabilistic model of overtopping discharge. More information regarding the probabilistic model are included in Section 5.1.

3

MECHANICAL ANALYSIS OF STEM BREAKAGE

THE smaller scale interaction between vegetation stems and wave load is formulated and discussed in Chapter 3 to determine when stems break due to wave load. First, the strength of the stem is quantified as maximum allowable stress (σ_{max}) with results of the three-point bending tests by NIOZ (Section 3.1). In the following section (3.2), the wave load is formulated as wave-induced stress (σ_{wave}) which is comparable to the stem strength σ_{max} . Stem breakage is defined as the point at which the wave load σ_{wave} exceeds the resistance of the stem, σ_{max} . Further, actual wave and vegetation measurement data is applied to this mechanical approach to verify whether the theory is applicable to real data with a reasonable order of magnitude (Section 3.4 and 3.3).

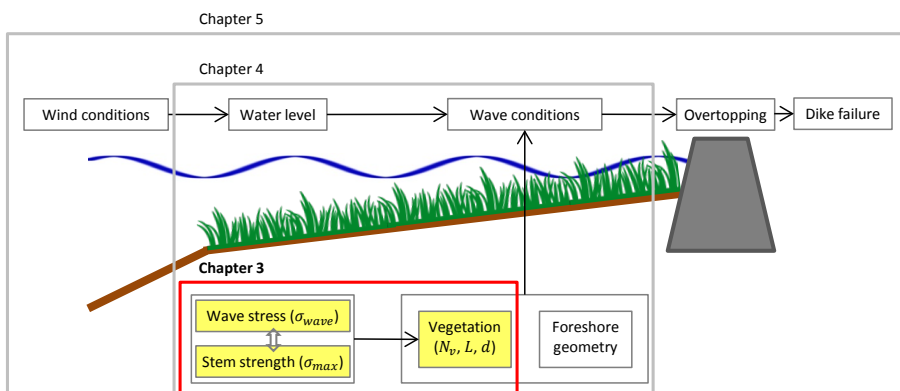


Figure 3.1: Chapter 3 in overall schematization.

Elasticity measurement

A general application of the three-point bending test is to determine the material property, Young's modulus (E , ratio of stress to strain) of the beam which is constant for small deformations. The Young's modulus is a measure of how swiftly the material returns to its original position after a force has been applied (elasticity). As a measure of elasticity, the Young's modulus E , combined with the area moment of inertia I , becomes a measure of flexural rigidity (EI). This material property (EI) is widely used in structural engineering to evaluate the characteristics of relatively stiff materials. Also in the field of ecology, many researchers including Dijkstra and Uittenbogaard [2010], Rupprecht et al. [2015], Usherwood et al. [1997], and others used this property to analyze the elasticity and movement of vegetation stems. This approach only applies to smaller forces, during which the force and displacement show a linear behavior (Refer to Figure 3.2).

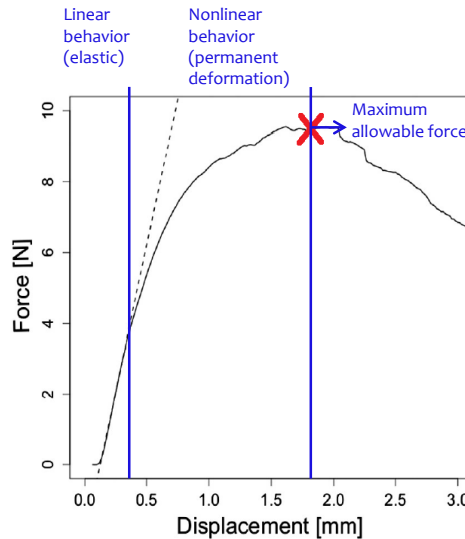


Figure 3.2: Example of a force to displacement curve (solid line) from a three-point bending test. Young's modulus (E) and flexural rigidity (EI) are calculated from the slope of the initial linear part (dotted line). The curve shape is representative for many vegetation species including *Spartina anglica* and *Scirpus maritimus*. *Reprinted from Rupprecht et al. [2015].

In this research however, an unconventional approach is taken for evaluating the strength of vegetation stems. Rather than considering the movement and resilience of the flexible stems, the extreme situation in which the stems break is of interest. Instead of the stem's initial elastic phase, the maximum allowable force is more relevant. In other words, when applying force to the stem, the force continuously increases until the stem is no longer elastic, and the force to displacement curve starts to act in a nonlinear way. At this point, the material experiences permanent deformation and does not return to its original position. In Figure 3.2, the maximum allowable force which is indicated as a red cross (stem folding or breaking) will be used in this research to compute the maximum allowable flexural stress of the stem.

3.1. MAXIMUM ALLOWABLE STRESS OF VEGETATION STEM

The previously discussed three-point bending test from NIOZ is used to calculate the maximum allowable stress a vegetation stem can withstand before breaking. The three point bending test can be simplified and expressed as a beam with two supports near the ends with a steady force applied at the center, in between the two supports. A schematic is provided below as Figure 3.3.

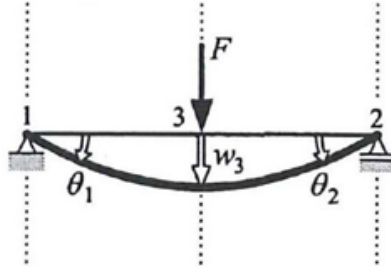


Figure 3.3: Schematic of three-point bending test: simply supported beam at both ends with load at center. *Reprinted from Vrijling et al. [2015].

Here F is equivalent to the testing force, F_{test} which is the load applied by the three-point bending test device. The distance between the two supports 1 and 2 in figure 3.3 is L_{test} , and I is the second moment of area which is also known as the area moment of inertia. The area moment of inertia I , is a measure of the cross-sectional resistance to bending. The beam experiences maximum flexure stress at the center where the greatest curvature and deflection occur. A general formula for calculating the flexure stress follows in equation 3.1, and this formula is also applicable to the situation for maximum loading (Vrijling et al. [2015]).

$$\sigma_{\text{max}} = \frac{M_{\text{max}}y}{I} \quad (3.1)$$

The maximum flexure stress is expressed as σ_{max} , the maximum moment is M_{max} , and y is the distance from the center of the specimen (beam) to the convex surface (i.e. the radius or half the width of the beam as shown in Figure 3.4), and I is again the area moment of inertia.

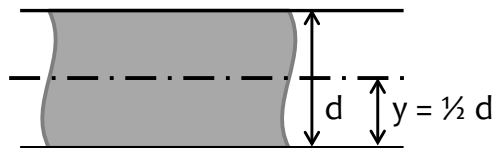


Figure 3.4: Side view of the specimen (or beam) of the three point bending test. The variable y is equivalent to the radius or $1/2$ of the thickness d for circular stems.

For the statically determined case three point bending test mentioned above, the maximum flexure stress at the center of the beam can be calculated with the following calculations of maximum moment M_{\max} and distance y .

$$M_{\max} = \frac{1}{4}F_{\text{test}}L_{\text{test}} \quad (3.2)$$

and

Of which, d is the thickness of the beam. From the equation 3.1 mentioned above, this yields a maximum flexure stress of:

$$\sigma_{\max} = \left(\frac{1}{4}F_{\text{test}}L_{\text{test}} \right) \left(\frac{1}{2}d \right) / I = \frac{F_{\text{test}}L_{\text{test}}d}{8I} \quad (3.3)$$

The calculations so far are invariable of the shape of the stem because the area moment of inertia I is not yet expressed per stem geometry. Vegetation stems do not have the same shape, and therefore the correct geometry must be used for the respective species. *Spartina anglica* in Hellegat has a hollow and circular stem with an inner and outer diameter, each noted by a subscript in the Equation 3.4. The species *Scirpus maritimus* in Bath has a stem with a solid (filled) triangular cross-section. Refer to Figure 3.5 below. The average width (d) of the three sides (d_{ave}) was determined, and this value is used for calculations of the area moment of inertia (I) of an equilateral triangle (Equation 3.5). The distance y (from the center of the beam to the convex surface) is considered half the height of an equilateral triangle as can be seen in Figure 3.5. The area moment of inertia (I) does have a significant impact on calculating the stem strength. For instance, *Spartina anglica* has a smaller area moment of inertia (I) than that of *Scirpus maritimus*, and due to such difference, *Spartina anglica* is more flexible, and resistant to breaking than *Scirpus maritimus*.

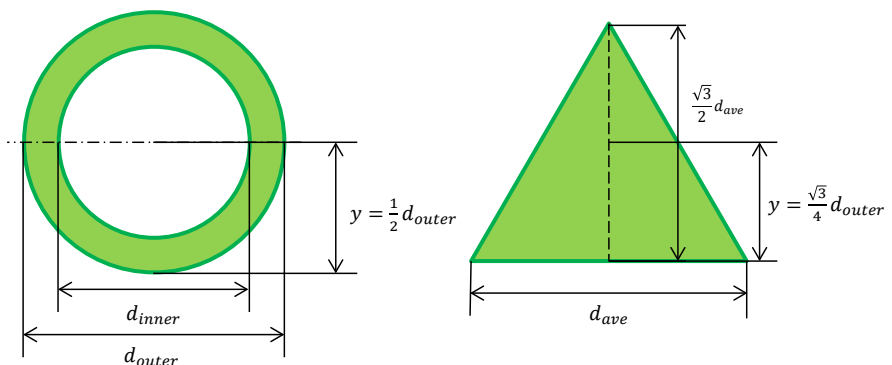


Figure 3.5: Cross-section of vegetation stems. *Spartina anglica* has a hollow circular stem (left), whereas *Scirpus maritimus* has a solid triangular stem, which is assumed to be equilateral (right).

$$I_{\text{Spartina}} = \frac{1}{4}\pi(r_{\text{out}}^4 - r_{\text{in}}^4) = \frac{1}{64}\pi(d_{\text{out}}^4 - d_{\text{in}}^4) \quad (3.4)$$

$$I_{\text{Scirpus}} = \frac{1}{36} \frac{3\sqrt{3}}{8} d_{\text{ave}}^4 \quad (3.5)$$

From Equation 3.3, the maximum flexure stress of the stem is representative of the strength of the stem. The value of σ_{max} would indicate the maximum allowable stress that the stem can withstand before folding or breaking. This maximum stress σ_{max} is a function of material strength ($F_{\text{test}}L_{\text{test}}$), diameter (d), and area moment of inertia (I , based on stem geometry). As can be seen in equations 3.4 and 3.5, the area moment of inertia is a function of diameter d , and as a result the respective equations for the maximum stress is presented as follows.

$$\sigma_{\text{max,Spartina}} = \frac{8F_{\text{test}}L_{\text{test}}}{\pi} \left(\frac{d_{\text{out}}}{d_{\text{out}}^4 - d_{\text{in}}^4} \right) \quad (3.6a)$$

$$\sigma_{\text{max,Scirpus}} = \frac{12F_{\text{test}}L_{\text{test}}}{\sqrt{3}} \left(\frac{1}{d_{\text{ave}}^3} \right) \quad (3.6b)$$

In the next section, stem strength will be further compared to the wave induced stress acting on the vegetation stems.

3.2. WAVE-INDUCED STRESS ON VEGETATION

Now, the real situation with a vegetated foreshore is considered. Vegetation in water is schematized as a situation as a cantilevering beam attached to a fixed bottom with uniform loading applied along the entire length of the beam (Figure 3.6).

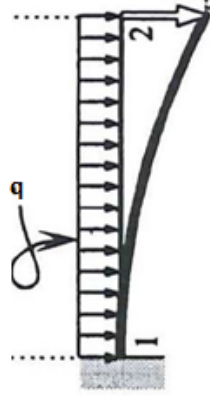


Figure 3.6: Schematic of vegetation stem experiencing wave load: fixed support with uniform loading. *Reprinted from Vrijling et al. [2015].

In this case the uniform load q [N/m] is a depth-constant wave load. The uniform wave load is a simplification of the actual phenomena, but it is applicable in this situation since shallow water conditions are valid, and the horizontal orbital velocity may be considered uniform over the entire depth. Refer to Appendix A.1 for background information on linear wave theory. To find the flexure stress that the vegetation experiences, the same equation 3.1 for flexure stress is applied. The general formula for maximum moment in the case of uniform loading can be found as follows.

$$M_{\max} = \frac{1}{2} F_{\max} L_{\max} = \frac{(qL_{\text{veg}})L_{\text{veg}}}{2} = \frac{qL_{\text{veg}}^2}{2} \quad (3.7)$$

Then the maximum flexure stress due to waves, in [Nm^{-2}] can be calculated as:

$$\sigma_{\text{wave}} = \frac{M_{\max} y}{I} = \left(\frac{qL_{\text{veg}}^2}{2} \right) \left(\frac{1}{2} d \right) / I = \frac{qL_{\text{veg}}^2 d}{4I} \quad (3.8)$$

Here, L_{veg} is the height of vegetation which is equivalent to the distance from 1 to 2 in Figure 3.6. The height of vegetation (L_{veg}) is not equivalent to the testing length (L_{test}) previously discussed in Section 3.1. The height of vegetation is the length of the entire stem, whereas the testing length (usually a few centimeters) is the bottom portion of the stem which is cut for three point bending tests.

In order to quantify this maximum stress, the vegetation height L_{veg} and diameter d are

available from field measurements of NIOZ. However, the uniform wave load q is yet to be determined. Neglecting plant swaying motion and inertial force, the Morison-type equation used by Dalrymple et al. [1984], Kobayashi et al. [1993] is implemented into this equation. The consequences for neglecting swaying motion of plants will be discussed later in this chapter. The equation for horizontal force per unit area per unit height [Nm^{-3}] acting on vegetation is given by:

$$F_x = \frac{1}{2} \rho C_d b_v N u |u| \quad (3.9)$$

Here ρ is the density of the fluid; C_d is the drag coefficient; b_v is plant area per unit height (i.e. approximately the width or diameter of the stem); N is the number of stems per unit area, and u is the relative horizontal orbital velocity in the vegetation region. Since F_x is given as the horizontal force per unit (land) area per unit height of vegetation [$Nm^{-2}m^{-1}$] (Figure 3.7), dividing F_x by N [m^{-2}] would yield the horizontal force per unit height of each stem [Nm^{-1}].

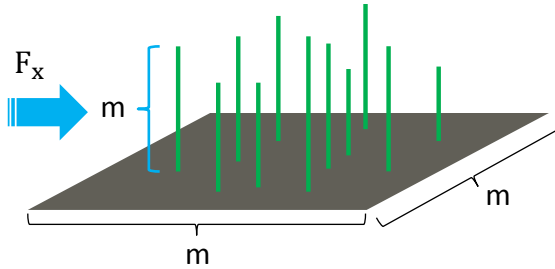


Figure 3.7: Horizontal wave force F_x acting on vegetation. Force [N] per unit area [m^{-2}] per unit height [m^{-1}]

This value of F_x/N can be seen as the equivalent to uniform wave load experienced by the vegetation stem, and thus can be substituted as $q=F_x/N$ in Equation 3.8. Doing so would lead to the following result:

$$q = \frac{F_x}{N} = \frac{1}{2} \rho C_d b_v u |u| \quad (3.10)$$

and consequently

$$\sigma_{\text{wave}} = \left(\frac{1}{2} \rho C_d b_v u |u| \right) \frac{L_{\text{veg}}^2 d}{4I} \quad (3.11)$$

Further simplification is possible as the plant area per unit height (b_v), can be assumed to be equal as the stem diameter (d), and the horizontal orbital velocity (u) is expressed below in Equation 3.12 for shallow water. For more explanation on horizontal orbital velocity and the linear wave theory, refer to the Appendix A.1. In an ideal situation for

more accurate quantification, the relative velocity between the plant and the water motion should be used (Dalrymple et al. [1984]), but because the swaying velocity of the plant relative to the water is too difficult to quantify, a simplification is used. Plant is considered rigid without any swaying or bending motion which will lead to a relative velocity equal to the horizontal orbital velocity ($u_{\text{relative}} = u$). This is one reason the wave induced force is overestimated and this will be further discussed in Section 3.4.3.

$$u = \frac{H}{2} \sqrt{\frac{g}{h}} \quad (3.12)$$

As a result, the wave-induced stress acting on the vegetation stem can be determined by the following equation 3.13.

$$\sigma_{\text{wave}} = \frac{1}{32} \rho g C_d \left(\frac{L_{\text{veg}}^2 d^2}{I} \right) \left(\frac{H^2}{h} \right) \quad (3.13)$$

Here, the area moment of inertia (I) is fully dependent on stem diameter (d), as discussed in Section 3.1. Therefore this Equation 3.13 for σ_{wave} indicates that vegetation characteristics (L_{veg} and d) as well as wave conditions (H and h) are influential parameters for the wave-induced vegetation stress. For longer, thicker vegetation and larger wave heights the vegetation experiences greater stress. This is easily understood since a longer, thicker stem would induce greater bending moment and subsequent flexure stress as can be verified from equations 3.7 and 3.8 of the bending test. Also larger wave heights indicate larger horizontal orbital velocities and a greater force acting on the vegetation. On the contrary, greater water depth (h) will reduce the stress working on the vegetation because larger water depths reduce the influence of high waves as seen from the Equation 3.12 for shallow water horizontal orbital velocity. Later discussed in Section 3.3, the influence of area moment of inertia (I) will become irrelevant, being cancelled out when comparing the strength of the stem (maximum allowable stress σ_{max}) to the wave induced stress (σ_{wave}).

With the stem's maximum allowable stress (σ_{max}) calculated from Equation 3.3 of Section 3.1, this value can be compared to the wave-induced vegetation stress (σ_{wave}) of Equation 3.13. Considering the stem as a rigid beam, the vegetation will only be able to withstand a stress of σ_{max} , and for situations of which the wave load induces a large σ_{wave} that exceeds σ_{max} , the vegetation is assumed to break or fold.

As previously acknowledged, the mechanical analysis in this research simplifies many aspects of the interaction between wave and vegetation. Waves affect the stems, but also the stems affect the waves through dissipating wave energy, but also by changing the wave field. This aspect is not dealt in this research, but it is also a possibility for further research. Also refer to Chapter 6, Discussion.

3.3. WAVE DATA ANALYSIS AND VEGETATION

3.3.1. THRESHOLD WAVE HEIGHT OF STEM BREAKAGE

Based on the mechanical approach, the wave height at which the stems break (threshold wave height) can be used for preliminary analysis at which the stems may start to break. The threshold wave height is determined by equating the maximum flexure stress to the wave-induced stress acting on vegetation both determined with the analytical approach in previous sections. The threshold wave height at which the stems break can be seen as the point where the load acting on the stem (wave-induced stress) exceeds the strength of the stress, which is measured from the NIOZ three-point bending tests.

Setting the two equations for maximum allowable stress (Equation 3.3) and wave-induced vegetation stress (Equation 3.13) equal, yields:

$$\frac{8F_{\text{test}}L_{\text{test}}d}{I} = \frac{1}{32}\rho g C_d \left(\frac{L_{\text{veg}}^2 d^2}{I} \right) \left(\frac{H^2}{h} \right) \quad (3.14)$$

Using the equation 3.14 above to solve for wave height H ,

$$H_{\text{threshold}} = \frac{2}{L_{\text{veg}}} \sqrt{\frac{F_{\text{test}}L_{\text{test}}h}{\rho g C_d d}} \quad (3.15)$$

Excluding the constants, the threshold wave height is a function of vegetation length L_{veg} , stem diameter d , maximum force from tests F_{test} , span of testing device L_{test} , and water depth h . This is a combination of vegetation characteristics as well as water depth.

$$H_{\text{threshold}} \propto \frac{1}{L_{\text{veg}}} \sqrt{\frac{F_{\text{test}}L_{\text{test}}h}{d}} \quad (3.16)$$

As can be seen from the Equation 3.16, the height of the vegetation (L_{veg}) has the greatest order of influence compared to the other variables, but also the variation in L_{veg} is greatest among differing seasons. Average vegetation height of *Spartina anglica* varied in the range of 33cm in December to 56cm in September. The difference in vegetation height which amounts to nearly 170% turns out to be the most dominant factor influencing the threshold wave height. This difference in vegetation height is even greater for *Scirpus maritimus* ranging from 44cm in April to 100cm in September.

The ratio between ($F_{\text{test}}L_{\text{test}}$) and diameter (d) is fairly constant because the two characteristics are relatively proportional: larger diameter requires greater force to break the stem during the three point bending test. The water depth (h) has some variation per season, but the difference is in the range of 10% ($\pm 5\%$) depending on the location of the measurement device. Furthermore, the square root of water depth results in an even smaller effect to the threshold wave height.

3.3.2. VARIATION IN WAVE HEIGHT ATTENUATION

The wave height variation is evaluated in Hellegat, in order to assess the wave dampening effect due to vegetation by changing season. Wave measurement is recorded from the beginning of the vegetated marsh (S1) to 50m into the marsh (S4). In Figure 3.8, in order to neglect the effects due to depth, the wave measurements are discretized by depth increments, and is evaluated for incident wave heights between 0.10 and 0.20m.

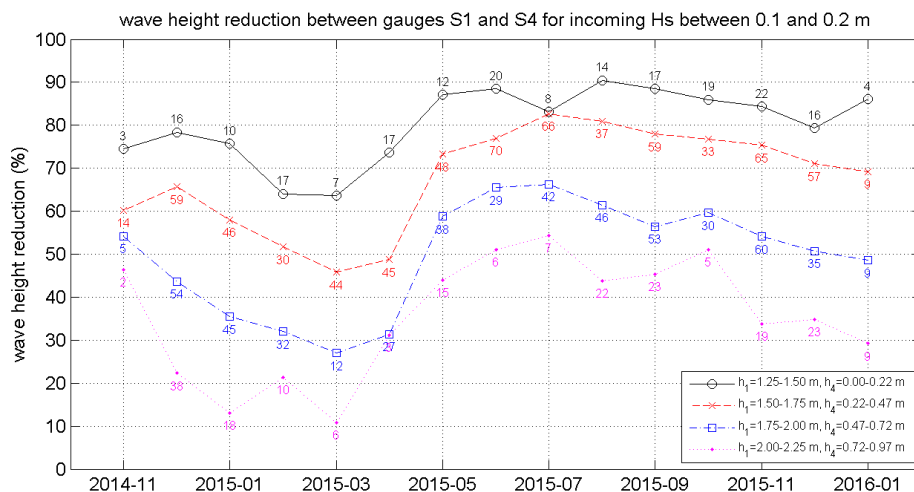


Figure 3.8: Percentage of wave height reduction for an incident wave height between 0.1m and 0.2m. Received from V. Vuik.

In Figure 3.8, given the same conditions, it can be seen that the wave height reduction (%) is higher from May to September 2015, and then gradually starts decreasing. This difference can be expected due to the variation in vegetation characteristics by season. In Hellegat, the *Spartina anglica* flourishes from May to September, and then steadily withers over the months (personal communication with Z. Zhu - ecologist at NIOZ, 10/06/2016). With the species-specific characteristic of *Spartina anglica* that does not easily break, the wave height reduction is observed quite strong even after September 2015. Also, the yearly vegetation difference between November 2014 and the following year November 2015 can also be observed by the amount of wave height reduction.

From field measurement data of vegetation, it is observed that indeed in November 2014 the vegetation length and diameter is significantly lower than in the same time 2015 for *Spartina anglica*. Refer to Figure 4.6 for vegetation measurement statistics. Even without calculations involving vegetation characteristics, a clear relation can be seen from the behavior of wave height reduction to the trend in vegetation characteristics.

3.4. REAL DATA APPLICATION OF MECHANICAL ANALYSIS

The mechanical approach is applied to real wave measurement data and vegetation statistics, as a preliminary check of whether the results are within reasonable order of magnitude. NIOZ wave data measurements are available from November 2014 to January 2016, and three-point bending tests were performed for four sample sets of vegetation from periods: 2014 December, 2015 April, September, and November of the species *Spartina anglica* and *Scirpus maritimus* (photo of the two species are in Figure 3.9). Also refer to Table 3.1 for the number of vegetation data available.



Figure 3.9: The species *Spartina anglica* (left) and *Scirpus maritimus* (right) are studied in this research. Photograph by Z. Zhu taken 14/09/2015 in Rilland (Western Scheldt), the Netherlands.

	2014 Dec	2015 Apr	2015 Sep	2015 Nov
<i>Spartina anglica</i>	55	51	50	40
<i>Scirpus maritimus</i>	31	41	42	40

Table 3.1: Number of vegetation samples during the respective measurement period.

With this vegetation data, the average values from each measurement period for stem length (L_{veg}), diameter (d), test results ($F_{test}L_{test}$) are used to calculate stem strength σ_{max} with Equation 3.6. Similarly, the wave-induced stress σ_{wave} is calculated based on the Equation 3.13. However, the vegetation characteristics (L and d) used to calculate wave-induced stress (σ_{wave}) is based on the average value from all measurement periods of each species. This ensures that the variation in wave-induced stress represents the wave conditions rather than the different vegetation characteristics.

Figure 3.10 and 3.11 show the comparison in magnitude of σ_{max} and σ_{wave} for different measurement periods as well as for the two different species. The boxplots indicate the variation in maximum allowable flexure stress (σ_{max}) of the stems per measurement period, whereas the dotted lines are the wave-induced vegetation stress (σ_{wave}). Figures show that whenever the dotted line exceeds the boxplot that the wave-induced stress

exceeded the stem strength, and the stems would break.

3.4.1. SPARTINA ANGLICA

In figure 3.10, the black line indicates that wave-induced stress acting on vegetation most often exceeds the stem strength (box plots) in September and November. This can be seen when much of the stems are expected to fold or break, and the vegetation density reduces. The larger waves and storm conditions start to occur in September in the Netherlands, as well as a significant reduction in wave height is observed (Figure 3.8). At first glance, it is counter-intuitive that the strength is lowest in September (directly after the summer growing season) and highest in December measurements. However, this can be interpreted as: from September to December, the majority of weaker stems steadily break over the months, and therefore the remaining standing vegetation in December must be those with much stronger stems which have been able to withstand the previous extreme wave conditions and high load of wave stresses.

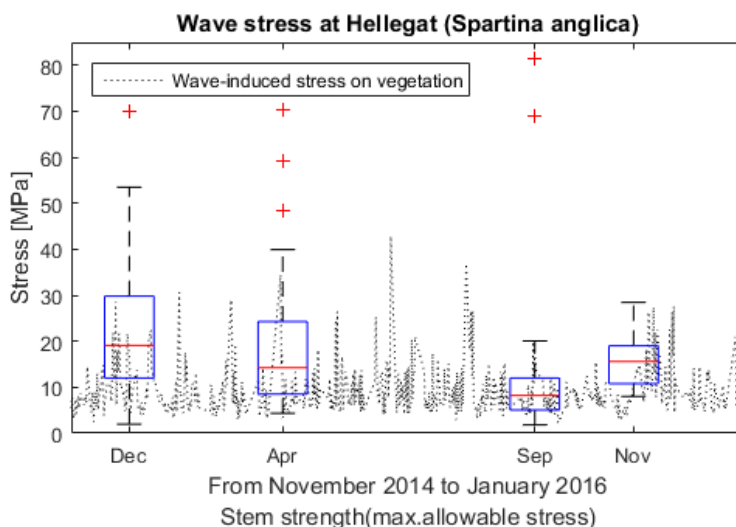


Figure 3.10: Wave-induced stress in Hellegat (dotted line) versus the stem strength (box plots). Wave height used in the wave-induced stress calculations are based on the highest 10% waves ($H_{10\%}$).

3.4.2. SCIRPUS MARITIMUS

From Figure 3.11 vegetation in Bath (*Scirpus maritimus*) behave differently from that at Hellegat (*Spartina anglica*). The dominant vegetation species in Bath (*Scirpus maritimus*) are much weaker than *Spartina anglica* in Hellegat and susceptible to breaking for even relatively lower waves. The strength of vegetation stems are most often exceeded by the wave stress in November and December.

Based on the real data application and preliminary calculations of stem strength (σ_{max})

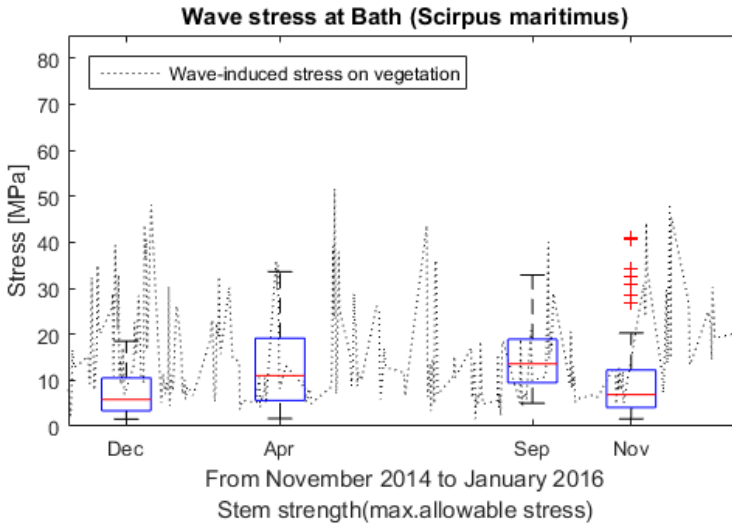


Figure 3.11: Wave-induced stress in Bath (dotted line) versus the stem strength (box plots). Wave height used in the wave-induced stress calculations are based on the highest 10% waves ($H_{10\%}$).

and wave-induced stress (σ_{wave}), both *Spartina anglica* and *Scirpus maritimus* would break quite easily under the highest 10% waves ($H_{10\%}$). Although the highest 10% waves ($H_{10\%}$) are stronger than normal conditions, it is possible that the wave-induced stresses are overestimated in figures 3.10 and 3.11. This possible overestimation is taken into account later in Chapter 4, and as a result, a correction factor will be introduced in Section 4.2.2.

Comparing the difference between the two vegetation species, *Spartina anglica* has relatively stronger stems than *Scirpus maritimus*. As a result, this would indicate less breaking of *Spartina anglica* stems than *Scirpus maritimus* in the field, and therefore more consistent wave dampening effects over the seasons.

3.4.3. LIMITATIONS OF MECHANICAL APPROACH

The preliminary results cannot be seen as a comprehensive result of the variations in months. As previously mentioned, the vegetation characteristics are based on only four sample sets of NIOZ field measurements from April, September, November, and December, and therefore the variation in between these four months are not accounted for in the results. Also the large dependence on vegetation length indicates that there could be uncertainty in this quantification due to insufficient data. Further analysis and application of the change in vegetation characteristics for varying months will be necessary for more accurate quantification.

The analytical approach discussed so far neglects the effects of the plant swaying motion and consequent fatigue that accumulates from the continuous back and forth wave load.

The swaying motion results in a smaller relative wave velocity (u) since the plant's motion is in phase with the water motion and therefore also reducing the horizontal force F_x from Equation 3.9. Additionally, the plant will be leaning in the direction of the flow of water, and therefore reducing the bending moment, since the distance of horizontal force application will be reduced. Further limitations are discussed in Chapter 6.

4

APPLICATION OF STEM BREAKAGE TO WAVE ENERGY BALANCE

IN this chapter, the mechanical analysis of stem breakage (discussed in Chapter 3) will be applied to the wave energy balance formulas. After implementing stem breakage to the wave energy balance model, the performance and effect of this new implementation will be evaluated. A correction factor is added to the quantification of wave-induced stress in order to account for the overestimation of wave load due to the leaning of stems, and a sensitivity analysis is performed based on varying wave heights and vegetation data per measurement period.

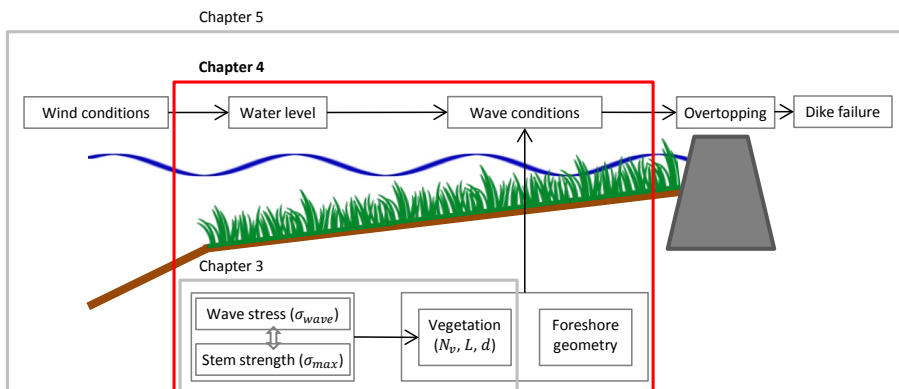


Figure 4.1: Chapter 4 in overall schematization.

4.1. WAVE ENERGY BALANCE

The wave energy balance, as discussed in Section 2.4 (Wave dissipation by vegetation), accounts for the change in wave energy due to vegetation (ϵ_v), wave breaking (ϵ_b), and bottom friction (ϵ_f) as the waves propagate towards the shore (Equation 2.1). Applying vegetation stem breakage to the wave energy balance will allow more accurate calculation of the wave energy dissipation due to vegetation (ϵ_v : which is a function of stem density N_v , as well as other vegetation and wave characteristics) and consequently better modeling of the wave height transformation along the foreshore. Until now, the wave energy dissipation due to vegetation (ϵ_v) was modeled with a non-varying initial value for stem density (N_v) throughout the entire marsh. However, by implementing stem breakage to the wave energy balance, wave dissipation from vegetation (ϵ_v) will vary with the change in stem density along the foreshore. Further, this will prove that stem breakage can be successfully implemented to the overall probabilistic model of wave overtopping and dike failure.

4

The underlying theory of the wave energy balance is the conservation of energy along the foreshore. The foreshore is discretized into equidistant cells that each have a certain amount of energy that is conserved. The energy density flux (i.e. the change in energy), is expressed in Equation 2.1 with the three different dissipations terms, ϵ_v , ϵ_b , ϵ_f each representing wave energy dissipation due to vegetation, wave breaking, and bottom friction, respectively (equations 2.2 to 2.3). With conservation of energy, the wave energy is balanced for each cell by calculating all three dissipation terms, and re-calculating the reduced wave energy based on the wave energy flux. Consequently the wave height is updated, since wave energy is a function of wave height ($E = \frac{1}{8}\rho g H^2$). The newly calculated wave energy and wave height are used as values in the next cell, and this process is repeated for all the cells along the foreshore as a process of wave transformation. The results will lead to a visualization of the wave height transformation as the wave approaches shore.

A summary of the main vegetation related equations for the wave energy balance are provided in Table 4.1. From the left, the first two equations for σ_{\max} and σ_{wave} determine whether the stems break or not (break when: $\sigma_{\max} < \sigma_{\text{wave}}$), whereas ϵ_v is a quantification of how much wave energy dissipates due to vegetation. The last row excludes all the constants from the equations, and indicates what variables are influential to the respective equation.

Note: The variable L is equivalent to the height of vegetation L_{veg} , but simply L will be used for simplification of notations. The other variable L_{test} is not the stem length, but represents the span length between two supports of the three-point bending test device.

The appropriate wave height (H) used for each calculation is listed in Table 4.2. The model input is based on the significant wave height H_{s0} which is the average of the highest 1/3 of waves. The significant wave height has practical significance compared to the average wave height because it is approximately equivalent to the visual estimates of experienced sea observers (Bosboom and Stive [2015]). The root mean square wave height H_{rms} is used for the calculations of the wave energy balance because the wave

Strength of stem (σ_{\max})	Wave induced stress (σ_{wave})	Dissipation due to vegetation (ϵ_v)
$\sigma_{\max} = \frac{F_{\text{test}}L_{\text{test}}d}{8I}$	$\sigma_{\text{wave}} = \frac{1}{32}\rho g C_D \left(\frac{L^2 d^2}{I}\right) \left(\frac{H^2}{h}\right)$	$\epsilon_v = \frac{1}{2\sqrt{\pi}}\rho \widetilde{C}_D d N_v \left(\frac{\text{kg}}{2\omega}\right)^3 \frac{\sinh kah + 3 \sinh kah}{3k\cosh^3 kh} H^3$
Proportional to:		
$\sigma_{\max} \propto \frac{F_{\text{test}}L_{\text{test}}d}{I}$	$\sigma_{\text{wave}} \propto \left(\frac{L^2 d^2}{I}\right) \left(\frac{H^2}{h}\right)$	$\epsilon_v \propto d N_v (\alpha h) \left(\frac{k}{\omega}\right)^3 H^3 = d N_v (\alpha h) \left(\frac{H}{\sqrt{h}}\right)^3$

Table 4.1: Equations most relevant to stresses of vegetation stem breakage (first and second column) and vegetation-induced wave energy dissipation (third column). This is a summary of equations: 3.3, 3.13, and 2.3 (starting from the first column, respectively) previously discussed in Chapters 2 and 3. Also note, $L_{\text{veg}} = L$ for simplification of notations. Explanations for the submerged stem length ($\alpha h = \alpha_r h$) can be found in Equation 4.1 and Figure 4.2.

energy is related to the wave height squared (mentioned previously in Section 4.1 that $E = \frac{1}{8}\rho g H_{\text{rms}}^2$). For the calculation of wave-induced stress that breaks the stem, the highest 10% of waves $H_{10\%}$ is used to determine the high waves that would more likely break the stems.

	Relation to H_{m0}	Use
H_{m0}	1	Model input
H_{rms}	$H_{m0} / \sqrt{2}$	Wave energy balance
$H_{10\%}$	$H_{m0} \times 1.27$	Wave-induced stress σ_{wave} (for stem breakage)

Table 4.2: Appropriate uses of wave height. H_{m0} , H_{rms} and $H_{10\%}$ each indicate the significant wave height, root-mean square wave height, and highest 10% wave height, respectively.

Dissipation due to vegetation (ϵ_v) in the third column of Table 4.1, is a resistance term (decreases wave energy and consequently also reduces wave height), and it is a function of αh . Here, α is not the same as the influence factor α (later discussed in Chapter 5), but it is the ratio of stem length to water depth (L/h). For better distinction between the two α 's, the ratio of stem length to depth will be differentiated as α_r . The $\alpha_r h$ is therefore the submerged stem length, which is equivalent to the stem length (L) for completely submerged stems, and $\alpha_r h = h$ when the stem protrudes out of the water. Refer to Equation 4.1 and Figure 4.2.

$$\alpha_r h = \begin{cases} L, & \text{if } L \leq h \\ h, & \text{if } L > h \end{cases} \tag{4.1}$$

The submerged stem length ($\alpha_r h$) included in the calculation of ϵ_v implies that wave energy dissipation occurs only along the submerged proportion of the stem.

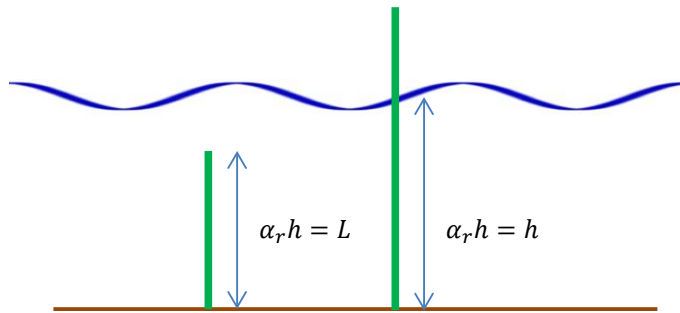


Figure 4.2: Schematic of submerged length of the vegetation stem, which is expressed as the ratio of stem length to water depth (α_r) multiplied by water depth (h).

4.2. IMPLEMENTATION OF STEM BREAKAGE

4.2.1. MODEL SETUP

The wave energy balance model is one part of the probabilistic model by V. Vuik, and it will be used in this chapter to test the behavior of stem breakage implemented in the wave energy balance. A simplified foreshore was used in this model with two types of bathymetries. Both bathymetries have a 150m foreshore length, of which 50m is before the marsh with 1:20 bottom slope, followed by the 100m vegetated marsh with a slope of 1:40. A schematization is provided in Figure 4.3 below. The bathymetry with a slope of 1:40 allows the effects of depth-induced wave breaking.

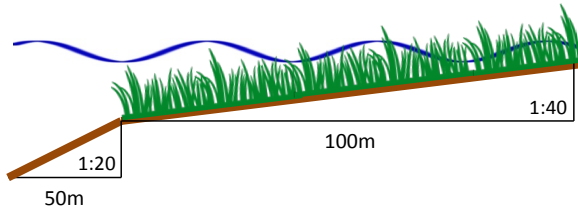


Figure 4.3: Schematization of the model bathymetry for computing the wave energy balance. Not to scale.

The initial conditions at the boundary are defined with a significant wave height (H_{m0}) of 0.8m and peak period (T_p) of 3.2 seconds (consequent deep water wave length, $L_0 = 16m$). The depth is approximately 2.5m at the start of the marsh. These initial values and boundary conditions are based on actual observations of winter (severe wave) conditions in the field as well as considering a reasonable wave steepness (H/L_0) as 0.05.

Stem breakage is modeled using the mechanical analysis previously discussed in Chapter 3. Stems are determined broken when the wave-induced vegetation stress (σ_{wave} : load) exceeds the maximum allowable stress of the stem (σ_{max} : strength, resistance). Vegetation measurement data from NIOZ are inputted into the model, and for the analysis of implementing stem breakage, average values are used for the stem's maximum stress (σ_{max}), height, and thickness. With this setup there are limitations in evaluating the performance because only one single averaged value is used for the vegetation characteristics, whereas in reality there is a wider range of strengths, height, and thicknesses. Although the data is not comprehensive of the real situation, it is sufficient as a preliminary analysis of evaluating the validity of including stem breakage in the wave energy balance model. More detailed statistical descriptions of the vegetation characteristics will be later included in Chapter 5, Overtopping discharge and probability of flooding.

There are two approaches to quantifying stem breakage, and a summary is provided in Table 4.3.

1. **Binary (all/none) stem breakage approach:** Based on these average vegetation characteristic values, the wave-induced vegetation stress (σ_{wave}) is calculated every 1m, corresponding to a spatial cell along the foreshore. For every 1m cell within

the vegetated marsh, a constant initial stem density N_{v0} is defined. If σ_{max} (stem strength) is greater than σ_{wave} (wave load), none of the stems break, and the initial stem density N_{v0} is conserved. On the other hand, if σ_{max} (stem strength) is smaller than σ_{wave} (stem load), all of the stems are considered broken, and a new stem density $N_{vbr} = 0$ is assigned to the cell. The updated (or conserved) stem density will be used in calculating the wave energy dissipation due to vegetation.

2. **Percentage stem breakage approach:** From the NIOZ measurement data of vegetation characteristics, the mean and standard deviation of the stem strength (maximum allowable stem stress σ_{max}) is calculated prior to inputting them in the wave energy balance model (Section 3.4). A normal cumulative distribution function (CDF) of the stem strength σ_{max} is defined within the model, and the wave-induced vegetation stress σ_{wave} is evaluated within this σ_{max} distribution. The normal CDF of σ_{wave} (P_{br}), which is between 0 and 1 would indicate the percentage of broken stems, whereas the complement of the normal CDF ($1 - P_{br}$) would be the percentage of remaining stems.

4

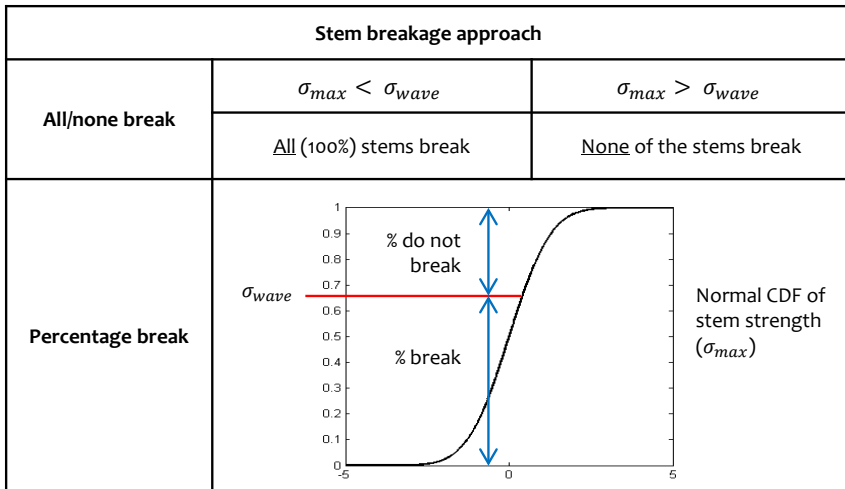


Table 4.3: Two approaches for stem breakage modeling.

Wave energy dissipation due to vegetation is a function of several constants as well as the vegetation characteristics (stem density N_v , height L , diameter d , strength σ_{max}) and wave characteristics (wave number k , angular frequency ω , water depth h , and wave height H), as can be verified from Table 4.1 and Equation 2.3 in Section 2.4. The wave height is updated from the energy balance calculations mentioned previously, whereas the vegetation density N_v will be updated through quantifying the amount of remaining vegetation stems after wave propagation and stem breakage. These computations are repeated for every 1m cell as the wave approaches shore, and as a result the stem density, wave energy, and wave height are updated.

4.2.2. OVERESTIMATE OF WAVE-INDUCED STRESS

With the model setup introduced in Section 4.2.1, the change in stem density, wave energy, and wave height transformation are computed along the entire foreshore. The first results showed that the vegetation stems indeed break for such strong (winter) wave conditions imposed as initial boundary conditions. It is true that the stem breakage model considers breaking under strong wave conditions, but many of the model results showed that the amount of stem breakage was much greater than what would be expected from visual field observations.

In Figure 4.4, the results for the first binary approach of quantifying stem breakage (all/none of the stems break) in November, 2015. The wave energy was modeled with an initial stem density of $1000/\text{m}^2$ and $500/\text{m}^2$ for *Spartina anglica* and *Scirpus maritimus*, respectively (approximation based on stem density measurements, Table 4.4). For both species, it can be observed that the wave energy balance model resulted in complete stem breakage for the first 75m of the vegetated marsh. Although the incoming wave conditions are considered quite strong, a single strong wave would not necessarily break so many stems as seen in this figure.

This result cannot be a comprehensive representation of the vegetated foreshore because only one average value from the vegetation data set is used, and this average value is assumed to represent all the stems in the marsh (i.e. all the stems have the same aver-

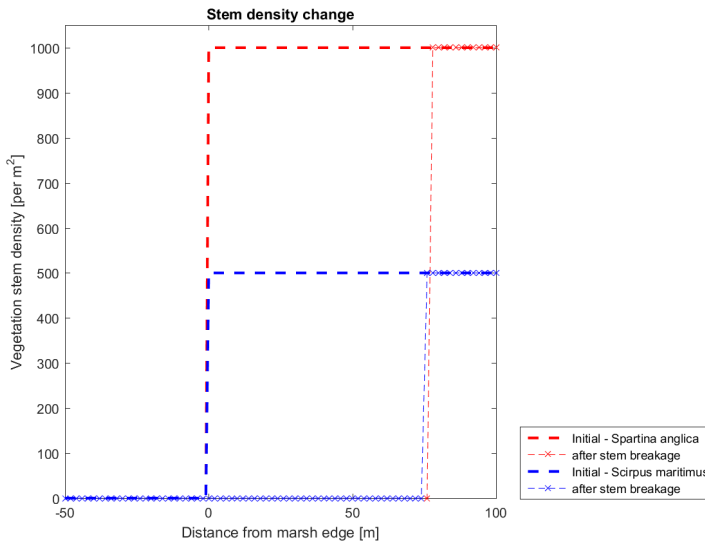


Figure 4.4: Binary stem breakage approach (all/none of stems break). Stem breakage modeling for an initial stem density of $1000/\text{m}^2$ and $500/\text{m}^2$ for *Spartina anglica* and *Scirpus maritimus*, respectively, along a vegetated marsh of 1:40 slope. Wave conditions (Section 4.2.1): significant wave height $H_{m0}=0.8\text{m}$ (equivalent $H_{10\%} = 0.99\text{m}$), peak period $T_p=3.2$ seconds, consequent deep water wave length $L_0 = 16\text{m}$, depth=2.5m at the start of the marsh. This example uses vegetation data from November, 2015.

age stem strength and break at the same threshold). Referring back to Table 4.1, the last row shows only the relevant variables, excluding all constants in the equations. Stem breakage is determined by comparing stem strength (σ_{\max}) and wave-induced stress (σ_{wave}). Here, wave-induced stress (σ_{wave}) only varies depending on wave height (H) and water depth (h) because all the other vegetation characteristics (L , d and I) are constant average values. This binary stem breakage approach does not take into account that vegetation characteristics vary per stem. That is why the second approach (percentage stem breakage) is also considered.

The results of the percent stem breakage approach is shown in Figure 4.5. The same wave and boundary conditions are applied to the percent breakage approach, and the only difference between the two is the type of stem breakage approach that quantifies the variation in stem density. Although the change in stem density is more gradual with the percent stem breakage than it is in the binary stem breakage approach, the number of stems that break is still quite larger than what is expected from visual field observations.

Table 4.4 are stem densities recorded by NIOZ from each measurement period. In this table, the labels “High” and “Low” indicate approximate locations relative to each other along the bathymetry profile. There is no record of how high and low in the bathymetry profile the stem density measurements were taken, nor is there any record of how far away the two locations are from each other. Although the locations of these stem den-

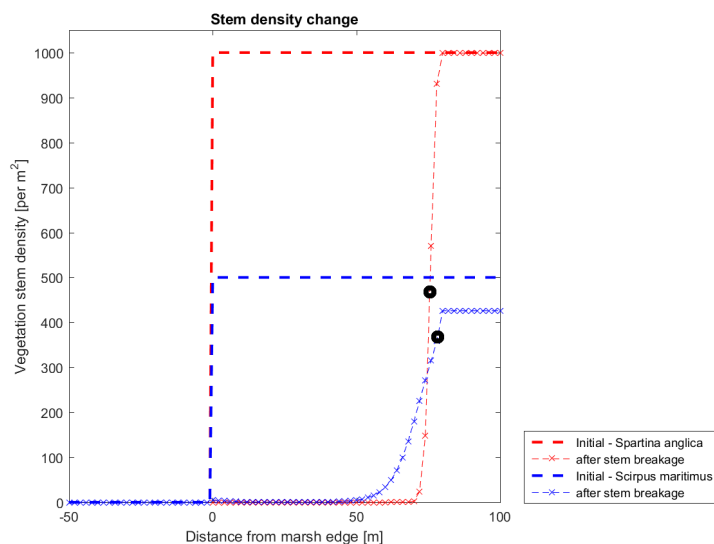


Figure 4.5: Percentage stem breakage approach. Stem breakage modeling for an initial stem density of $1000/\text{m}^2$ and $500/\text{m}^2$ for *Spartina anglica* and *Scirpus maritimus*, respectively, along a vegetated marsh of 1:40 slope. Wave conditions (Section 4.2.1): significant wave height $H_{m0}=0.8\text{m}$ (equivalent $H_{10\%} = 0.99\text{m}$), peak period $T_p=3.2$ seconds, consequent deep water wave length $L_0 = 16\text{m}$, depth=2.5m at the start of the marsh. Black circles represent the ratio of stem density reduction based on measurement data from Table 4.4. This example uses vegetation data from November, 2015.

sity measurements are not documented, the information will serve as an approximate comparison to how the model behaves.

The stem density difference for November 2015, which is the example data set used in this section, is highlighted in red (Table 4.4). From this data, it can be seen that the vegetation stem density reduces approximately 52% and 14% for *Spartina anglica* and *Scirpus maritimus*, respectively. Such variation in density cannot be represented in the binary stem breakage approach (Figure 4.4) because the stem density can only be 0 or N_{v0} (initial stem density), and it cannot be any other value in between. The percent stem breakage approach could possibly show the variation in stem density, but as seen in Figure 4.5, the change in stem density is very steep. Assuming that the stem density at the shore is the “High” location, the expected stem density difference based on 52% and 14% for each species, is marked as a black circle in the Figure 4.4.

In both stem breakage scenarios, the stem density reduction seems to be much steeper and greater than what is expected. The reason for the overestimation of stem density reduction (too many stems breaking from the model) can be due to two possibilities: 1) an overestimate of wave-induced vegetation stress (σ_{wave}) or, 2) an underestimate of maximum allowable vegetation stress (=stem strength, σ_{max}). The first possibility of an overestimate of the wave-induced load, σ_{wave} is reasonable because the simplified approach in Section 3.2 neglects the leaning and bending of the stem, which would reduce the amount of force and consequent moment that the stem experiences. The second possibility of an underestimate of σ_{max} is also possible because the mechanical approach does not consider the flexibility of the stem. In reality, the stem is more resilient to wave forces as it is able to change shape and orientation according to the direction of the waves. These two possibilities leads to the possibility of including a correction factor, which will be discussed next.

		2014	2015	2015	2015
		Dec	Apr	Sep	Nov
Spartina anglica	High	1920	1088	1027	928
	Low	1168	928	842	448
	% difference	39	15	18	52
Scirpus maritimus	High	384	384	371	352
	Low	384	192	355	304
	% difference	0	50	4	14

Table 4.4: Stem density difference along a foreshore transect. “High” and “Low” indicate relative locations to each other along the bathymetry profile. Measurements for species *Spartina anglica* and *Scirpus maritimus* were measured in Rilland and Hellegat, the Netherlands.

4.2.3. CORRECTION FACTOR

In order to take into account the overestimation of stem breakage, a correction factor should be included in the calculations of stresses. Of the two possibilities that lead to an overestimate of stem breakage, the first possibility of an overestimate of wave-induced stress σ_{wave} due to stem leaning will be considered as the more dominant factor. The second possibility (underestimate of stem strength σ_{max}) will be neglected because it can be considered as partially included in the first possibility which includes stem leaning, both reasoning taking into account the flexibility of the stem and resilience to wave induced forces.

Equation 3.13 for the quantification of wave-induced stress (σ_{wave}) already includes a drag coefficient C_D , which is a factor that encompasses pressure differences and drag due to skin friction, but also many other processes such as plant swaying, attenuation of orbital motion by the vegetation canopy, and interaction between individual wakes in dense vegetation fields (Vuik et al. [2016]). These are influential processes that are not captured in the physical model, and therefore they are included in the drag coefficient. In a similar sense, an additional correction factor will be multiplied to the wave-induced vegetation stress σ_{wave} , in order to capture the influences of vegetation stem leaning.

Stem leaning is justified by considering a simplified model, in which the stem is assumed to be a rigid stick that does not bend, but simply leans. Refer to Figure 4.6. In reality the stems do bend which results in leaning stems, however for simplicity, the calculations for bending will be assumed included in the leaning angle.

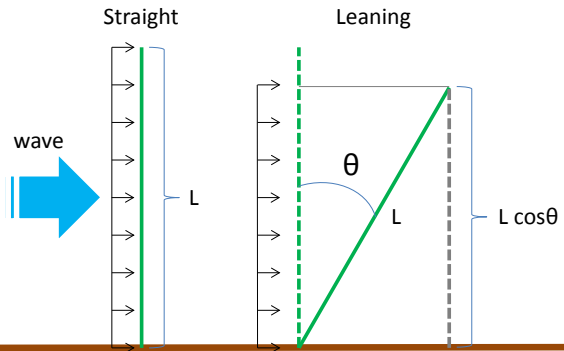


Figure 4.6: Schematization of a straight up (left) stem and leaning (right) stem. The stem standing straight up on the left represents the original case where the entire length of the stem experiences the uniform horizontal wave loading, as depicted in Section 3.2, Figure 3.6. The stem leaning on the right represents the more realistic case, with a leaning angle θ which experiences a smaller horizontal wave load along a length of $L \cos \theta$.

Two species *Spartina anglica* and *Scirpus maritimus* are evaluated in this research, and the amount to which they lean also vary. *Spartina anglica* is considered more elastic and hard to break (or even difficult to cut by scissors), comparatively *Scirpus maritimus* is more stiff, brittle and can easily break, even by hands (personal communication with Z. Zhu - ecologist at NIOZ, 10/06/2016). Silinski et al. [2015] studied the bending be-

havior of vegetation, especially for the species *Scirpus maritimus*, in which on average a bending angle of more than 30° was observed for adult vegetation at high waters that may apply to extreme storm conditions. The research also acknowledges that the final bending angle could be an indicator for the overall plant survival or failure, as this angle may determine whether or not the stem topples (=folds/breaks). Taken from the results of this research, a maximum leaning angle of 30° will be used as the correction factor for *Scirpus maritimus*.

Although there is no research directly related to the maximum bending angle of *Spartina anglica*, data from the three-point bending tests provides quantification of the flexural rigidity (EI), which is a measure of the resistance to bending forces. Based on this information, the smaller flexural rigidity (i.e. smaller resistance to bending forces) of *Spartina anglica* than that of *Scirpus maritimus* signifies greater flexibility and larger bending angles. Further, based on field observations (video of *Spartina anglica* affected by ship waves, received from V. Vuik 2015) and personal communication with Z. Zhu (ecologist at NIOZ, 10/06/2016) who has observed this plant species for several years, it is reasonable to conclude that *Spartina anglica* has a larger bending angle than *Scirpus maritimus*. As a result, the bending angle of *Spartina anglica* will be assumed to be 45° . This is still a conservative choice of leaning angle which could be further calibrated and researched in future research.

As seen in calculations for σ_{wave} (Equation 3.13 or Table 4.1), the height of vegetation is taken to the power two ($=L_{\text{veg}}^2 = L^2$), and therefore the reduction of horizontal force $\cos\theta$, must also be squared ($=\cos^2\theta$). Refer to Table 4.5 below.

	max. bending angle (θ)	$L\cos\theta$	$L^2\cos^2\theta$	correction factor
<i>Spartina anglica</i>	45	0.71L	$0.5L^2$	0.5
<i>Scirpus maritimus</i>	30	0.87L	$0.75L^2$	0.75

Table 4.5: The leaning angle and correction factor of species *Spartina anglica* and *Scirpus maritimus*.

After including the correction factor in the wave energy balance calculations, the variation in stem density is shown in Figure 4.7. Here, the blue lines show the results without a correction factor, and the red lines are the results after applying the correction factor. The difference in the case of November 2015 is not very large, but the variation differs per vegetation data. Also refer to Figure 4.8 for another example of stem density variation for percent stem breakage approach from vegetation data of December, 2014. Binary stem breakage approach is not shown for this period because the behavior is almost similar to that of the November 2015 results shown in Figure 4.7. It is logical that results from *Spartina anglica* have a bigger difference before and after applying the correction factor, because a stronger leaning factor ($=0.5$) is applied than that of *Scirpus maritimus* ($=0.75$).

Since the stem density data currently available is not sufficient enough to match the results, calibration of the correction factor would be a possible topic for future research. Refer to Chapter 6, Discussion.

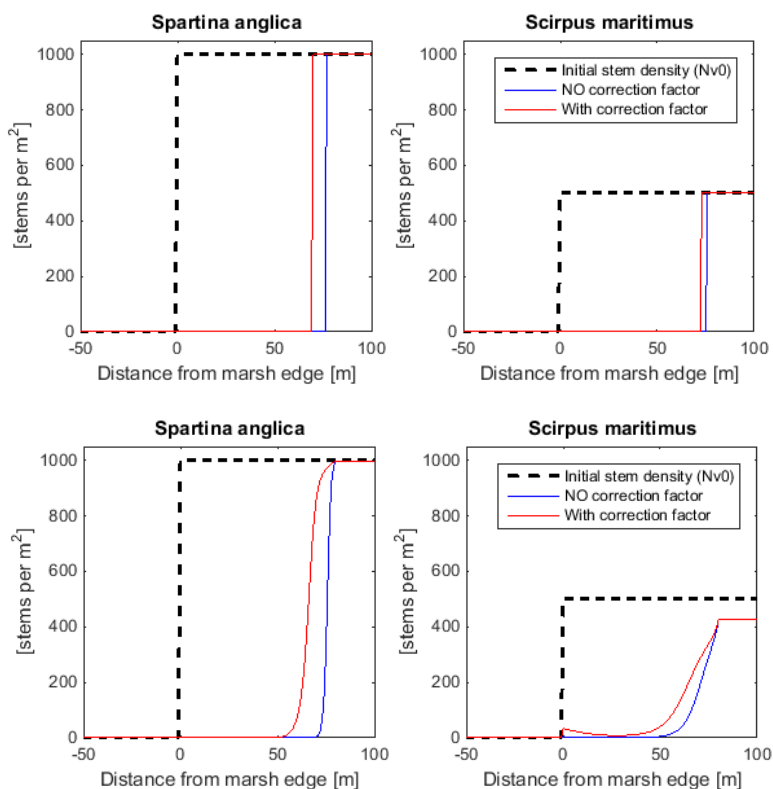


Figure 4.7: Stem density variation before and after applying the correction factor. The two figures on top are results from the binary stem breakage approach, and the two figures on the bottom are from the percent stem breakage approach. This example uses vegetation data from November, 2015.

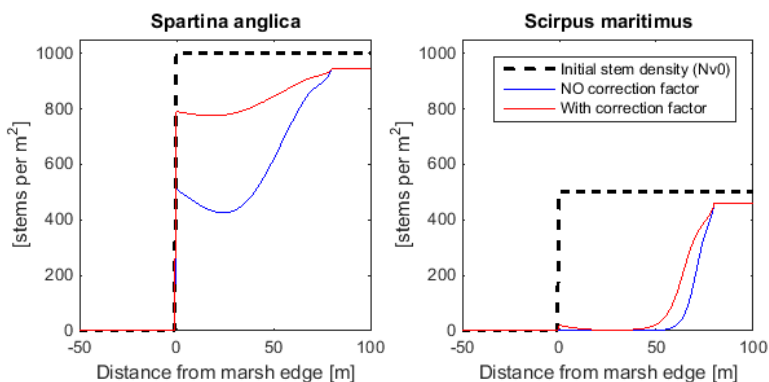


Figure 4.8: Stem density variation before and after applying the correction factor. The results from the percent stem breakage approach from vegetation data of December, 2014.

4.3. MODEL APPLICATION

Based on the sloping bathymetry model setup and correction factor discussed in Section 4.2, implementation of stem breakage to the wave energy balance model is evaluated in this section based on two different criteria. The first criteria is analyzing the sensitivity to the wave height, and the second is an analysis to the sensitivity by varying seasons.

In order to represent reality better, a stem density of $1000/\text{m}^2$ will be used for *Spartina anglica*, and $500/\text{m}^2$ for *Scirpus maritimus*. The sensitivity of the model will be assessed based on two criteria.

1. Wave height (Load) : Model results based on varying wave heights will be analyzed. The wave heights are influential in computing the wave-induced vegetation stress, and therefore can be considered as the load parameter.
2. Seasonality - varying vegetation characteristics (Resistance) : Varying seasons have different vegetation characteristics, which are influential to the strength of the stems. The seasonality thus is influential in assessing how much the resistance of the vegetation stems vary, and how they influence the results in wave height transformation.

4.3.1. SENSITIVITY TO WAVE HEIGHT

Various incident wave heights are tested in the model, varying from an initial wave height of 0.8m (winter conditions) to 1.8m (extreme conditions) on a 1:40 sloping bathymetry. For both species studied, the change in stem density varies depending on the incident wave height. The water depth at the beginning of the marsh is 2.5m regardless of the initial wave conditions. Figure 4.9 clearly shows the variation in stem density change depending on the incident wave height at the boundary. There is less stem breakage for smaller wave heights and a gradual increase of stem breakage can be noted as the wave height increases in 0.2m increments. The incident wave height increases by 0.2m, but the amount of increase in stem breakage is smaller each time. It can be deduced that the influence of a increasing wave height is less for higher waves.

The reasoning for decreasing influence of higher waves can be attributed to the depth-induced wave breaking. With higher wave heights, the waves start breaking earlier and closer to the beginning of the marsh. More depth-induced wave breaking would indicate greater wave energy dissipation due to wave breaking (ϵ_b), in effect, the wave height will decrease more rapidly. With the rapid decrease in wave height, the wave-induced vegetation stress acting on the stems will be smaller, thus the wave load will not be strong enough to break the stems.

The figure of the wave height variation, located below the stem density figure, shows that the location at which the stems do not break align with the point at which wave height shows a more abrupt decrease in wave height reduction. This is logical since the presence of vegetation will incur much more wave energy dissipation and resulting in smaller wave heights.

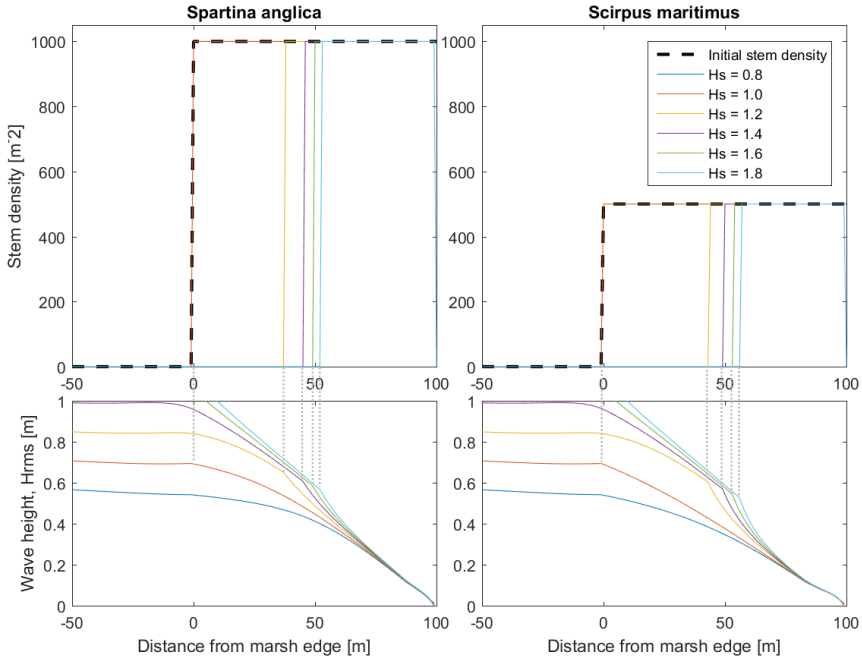


Figure 4.9: Stem density change (top) and wave height transformation (bottom) plotted for different incident wave heights along a vegetated marsh of 1:40 slope with vegetation characteristics from April, 2015. Initial stem density of $1000/\text{m}^2$ for *Spartina anglica* and $500/\text{m}^2$ for *Scirpus maritimus*.

The ratio of wave height reduction is plotted in Figure 4.10 for both species. This ratio of wave height reduction is calculated by dividing the wave height at 25m from the shore (i.e. 75m of wave energy dissipation including vegetation) by the wave height at the start of the vegetated marsh ($H_{\text{shore}}/H_{\text{startMarsh}}$). In Figure 4.10, *Spartina anglica* (red line) indicates a clear reduction in relative wave height reduction. The trend of ratio reduction is nearly linear until the incident wave height reaches 1.6 to 1.8m, at which the ratio barely reduces. This figure supports the reasoning above that with the increase in incident wave height the influence of wave height reduction reduces due to depth-induced wave breaking in higher waves.

Scirpus maritimus (blue line) shows a similar trend in decreasing wave height reduction. However, there is more wave height reduction for *Scirpus maritimus* than that of *Spartina anglica*, which can be attributed to the species specific characteristics of *Scirpus maritimus* which induces greater wave energy dissipation. This may be due to the thicker and longer stems of *Scirpus maritimus* ($\epsilon_v \propto N_v, d, \alpha h, H_{\text{rms}}^3$). Even with the initial stem density being half of *Spartina anglica* ($N_{v0, \text{Spartina}} = 1000/\text{m}^2$, $N_{v0, \text{Scirpus}} = 500/\text{m}^2$), the wave energy dissipation in *Scirpus maritimus* was found to be greater than that of *Spartina anglica*. This is a good indicator that not only the stem density but also the vegetation characteristics strongly do influence the amount of wave energy dissipation in the vegetated foreshore.

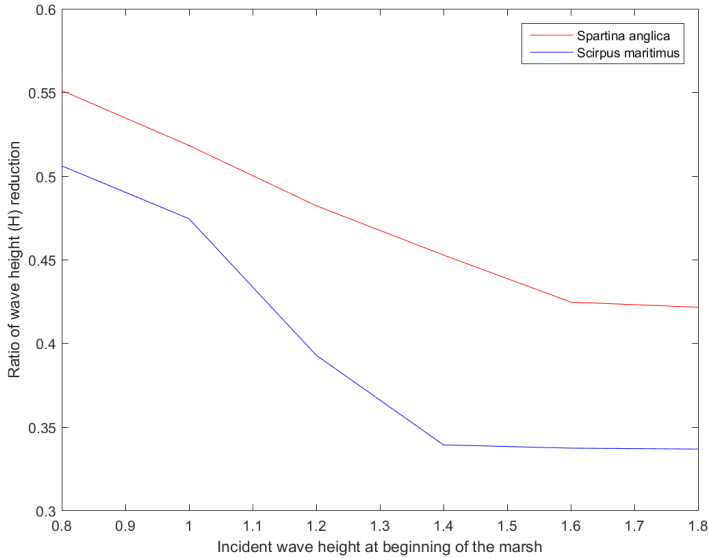


Figure 4.10: Ratio of wave height reduction plotted for different incident wave heights along a vegetated marsh of 1:40 slope with vegetation characteristics from April, 2015. Ratio is calculated as: wave height at shore (H_{shore}) divided by wave height at beginning of marsh ($H_{startMarsh}$). i.e. $H_{shore}/H_{startMarsh}$.

The same initial and boundary conditions were modeled with the second, percentage stem breakage approach with varying fractions of stems breaking based on the normal CDF of maximum allowable stress distribution of stems σ_{max} and wave-induced stress σ_{wave} within the distribution. The results are included in Figures 4.11 and 4.12), and it can be seen that the results are similar to that of the binary approach of which all or none of the stems break in each cell along the vegetated marsh. However, in this percentage stem breaking approach, the change in stem density is gradual and also the wave height reduction shows a more gradual reduction since the change in vegetation stem density is not so abrupt as the first approach.

From the sensitivity analysis of wave heights, it can be concluded that the vegetation stem density and wave height reduction is indeed influenced by the incident wave height. There is more vegetation stem breakage and wave height reduction with increasing wave height, but at a declining rate. The declining influence of incident wave height can be attributed to increased depth-induced wave breaking along the sloping foreshore, and thus incurring greater wave energy dissipation due to wave breaking (ϵ_b).

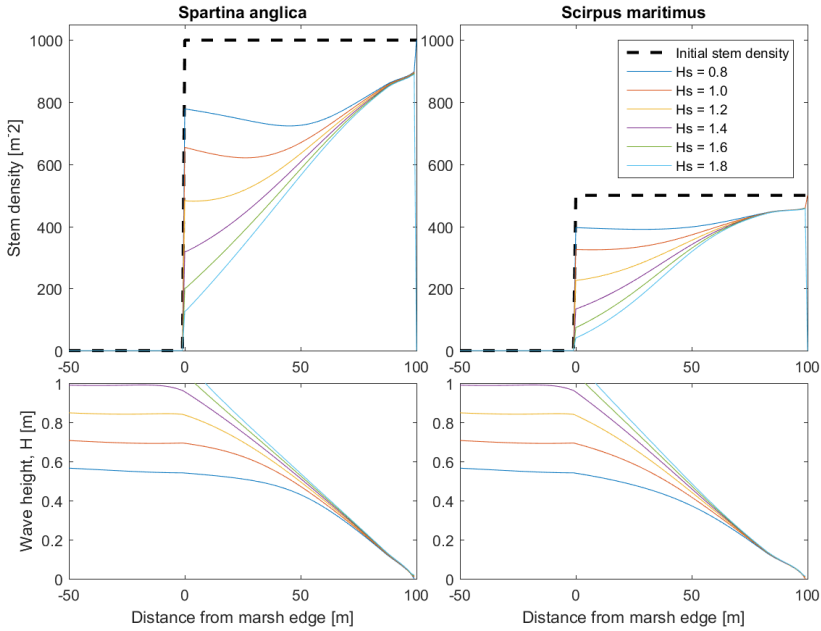


Figure 4.11: Stem density change (top) and wave height transformation (bottom) plotted for different incident wave heights along a vegetated marsh of 1:40 slope with vegetation characteristics from April, 2015. Initial stem density of 1000/m² for *Spartina anglica* and 500/m² for *Scirpus maritimus*.

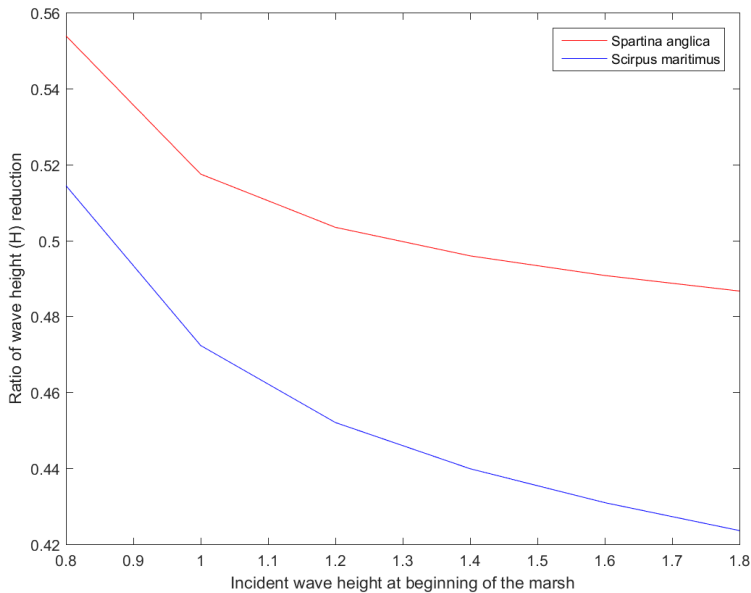


Figure 4.12: Ratio of wave height reduction plotted for different incident wave heights along a vegetated marsh of 1:40 slope with vegetation characteristics from April, 2015. Ratio is calculated as: wave height at shore (H_{shore}) divided by wave height at beginning of marsh ($H_{startMarsh}$). i.e. $H_{shore}/H_{startMarsh}$.

4.3.2. SENSITIVITY BY SEASON

Seasonal changes are observed all around the world, and the varying season is most likely accompanied with growth and decay of vegetation. In the Western Scheldt of the Netherlands where the field measurements were held for this research, the vegetation starts growing in March to June depending on the species, and starts withering as early as September (*Scirpus maritimus*) and others as late as in December (*Spartina anglica*) - from personal communication with Z. Zhu - ecologist at NIOZ, 10/06/2016. The field location is located at approximately 50° latitude in the northern hemisphere, therefore spring and summer is considered as march to August, on the other hand autumn and winter is considered as September to February. Prior to analysis, given the same wave conditions, it would be expected that growing and strong vegetation in the spring and summer would less likely break, whereas decaying and weak vegetation in the winter would more easily break.

In this section, the performance of stem breakage included in the wave energy balance model will be analyzed with seasonally varying vegetation characteristics. As previously mentioned, the average values from each measurement period are used as inputs for the model. The specific values from each measurement period can be found in Table 4.6.

For analysis, the vegetated marsh starts at a 2.5m depth, and an incoming wave height of 1.2m is applied as a severe winter condition. Figure 4.13 clearly illustrates that depending on the seasonal vegetation characteristics (stem height L , width d , and strength σ_{\max}), the number of stems breaking varies along the foreshore. At first glance, the two figures on the left for *Spartina anglica* show that 2014 December vegetation break the least, followed by 2015 April, September and November. *Scirpus maritimus* plotted on the two figures on the right, show that 2015 April vegetation break the least followed by 2014 December, 2015 November and September vegetation.

This behavior can be understood by evaluating the contributing parameters in Table 4.1.

Species	Measurement period	L_{ave}	L_{std}	d_{ave}	d_{std}	$\sigma_{\max, \text{ave}}$	$\sigma_{\max, \text{std}}$
<i>Spartina anglica</i>	2014 Dec	349	144	2,7	0,5	22	14
	2015 Apr	330	106	2,7	0,7	18	14
	2015 Sep	567	140	4,1	0,9	11	14
	2015 Nov	545	115	3,4	0,6	16	5
	All	440	168	3,2	0,9	17	13
<i>Scirpus maritimus</i>	2014 Dec	660	430	7,9	2,1	8	5
	2015 Apr	441	266	8,0	2,7	13	9
	2015 Sep	999	363	7,0	1,8	15	7
	2015 Nov	693	401	6,4	1,8	12	11
	All	699	416	7,3	2,2	12	9

Table 4.6: Distribution parameters for each measurement period, the subscripts 'ave' and 'std' are the mean and standard deviation of the measurement data of the respective period. The stem height (L) and width (d) are in units of [mm]; and strength parameter (σ_{\max}) are in units of [MPa].

Vegetation break when wave-induced stress σ_{wave} exceeds stem strength σ_{max} . An average value of L , d , and σ_{max} is assumed representative for the entire measurement period. Since one value of stem strength σ_{max} is compared to σ_{wave} , the value of σ_{wave} determines whether the stems break or not. In Table 4.1, wave-induced stress σ_{wave} is proportional to:

$$\sigma_{\text{wave}} \propto \left(\frac{L^2 d^2}{I} \right) \left(\frac{H^2}{h} \right) \quad (4.2)$$

Every simulation has the same wave conditions (H , h), therefore the combination of average stem height L , width d , and area moment of inertia I (Equations 3.4 and 3.5 in Section 3.1) influence the magnitude of σ_{wave} . Refer to Table 4.7 for a summary of the relative influence due to vegetation ($L^2 d^2 / I$) for all the measurement periods. From this table, it can be seen that the wave-induced stress is smallest in 2015 April which shows that most of the stems did not break. *Spartina anglica* (left figures) show that 2014 December showed even less stem breakage, which could be attributed to the exceptionally

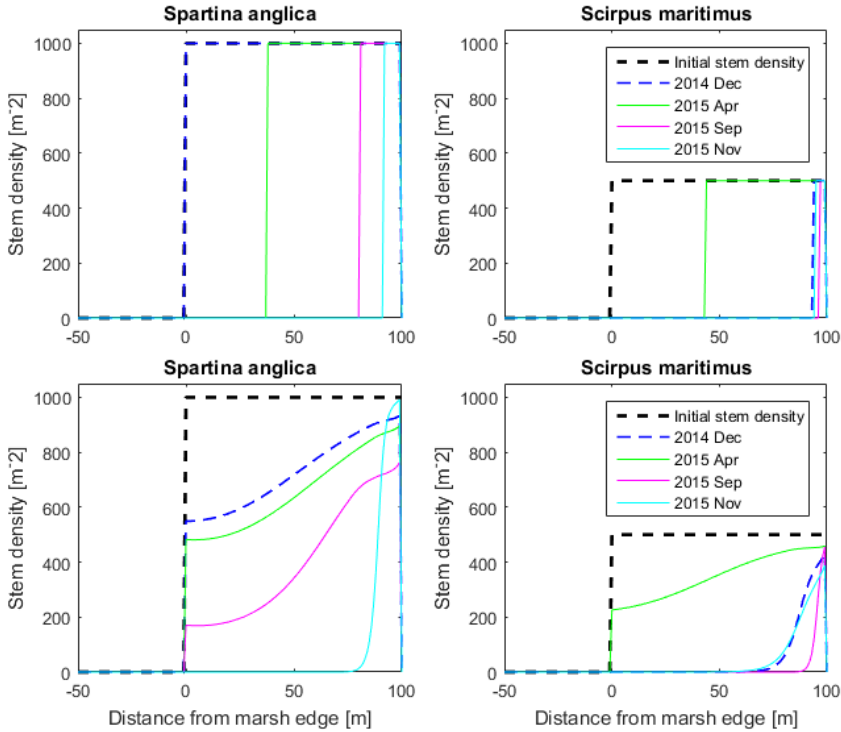


Figure 4.13: Stem density variation with first binary approach (above) that either all or none of the stems break in each spatial cell along the vegetated marsh. The second approach (below) models a percentage of stems breaking depending on wave-induced stress (σ_{wave}) evaluated on the normal CDF of stem strength (σ_{max}). Measurement data for species *Spartina anglica* (left) and *Scirpus maritimus* (right) are used, and modeled for 1.2m incoming wave height and 2m depth at the beginning of the marsh.

strong stems as can be seen from the high σ_{\max} in Table 4.7. *Scirpus maritimus* (figures on the right) show that 2015 April has the least stem density reduction, since the wave load σ_{wave} acting on the stems are the weakest, whereas the stem strength is relatively high.

Stem breakage and consequent stem density reduction is greatest 2015 November for *Spartina anglica* and September for *Scirpus maritimus*. Again, this can be attributed to the relatively strong wave load acting on the stems during the respective period.

Wave-induced stress σ_{wave} is strongly dependent on the stem height (L), since the order of magnitude at which the stem height varies (up to 220%) is much greater than the variation in stem width (approximately 50 to 70%). From the model results presented, *Scirpus maritimus* break relatively early (in September), whereas *Spartina anglica* break later (in November). These results are similar to what is observed in the field, as *Scirpus maritimus* have an earlier growth period from March to June, and *Spartina anglica* grow from May to November (from personal communication with Z. Zhu - ecologist at NIOZ, 10/06/2016). Further, a large number of *Scirpus maritimus* are reported already broken in late September, contrary to *Spartina anglica* that is still observed strong and unbroken during the same period of time.

The amount of wave energy dissipation is plotted in Figure 4.14 for the second percent stem breakage approach. Here, the solid lines are the total wave energy dissipation including dissipation due to 1) vegetation, 2) wave breaking, and 3) bottom friction. The dotted lines are wave energy dissipation due to vegetation, which show reasonable results according to how much stem breakage occurred in the foreshore. *Spartina anglica* has greater wave energy dissipation due to vegetation than *Scirpus maritimus*, not only because of the larger stem density, but also because the stems are more flexible and resilient to the wave load, as could be verified in Figure 4.13. *Scirpus maritimus* also dissipates a significant amount of wave energy, but since vegetation stems break more easily, other than in 2015 April, the most dominant means for wave energy dissipation is wave breaking.

Species	Measurement period	$\sigma_{\text{wave}} \propto$	$\sigma_{\text{max,ave}}$
<i>Spartina anglica</i>	2014 Dec	3,60 E+05	22
	2015 Apr	3,41 E+05	18
	2015 Sep	4,43 E+05	11
	2015 Nov	10,57 E+05	16
<i>Scirpus maritimus</i>	2014 Dec	3,82 E+05	8
	2015 Apr	1,66 E+05	13
	2015 Sep	11,39 E+05	15
	2015 Nov	6,44 E+05	12

Table 4.7: Summary of relative influence of vegetation on wave-induced stress, $\sigma_{\text{wave}} \propto (L^2 d^2 / I)$ [-] per measurement period. This is representative of the relative wave load acting on the vegetation stem. The column to the right labeled ($\sigma_{\text{max,ave}}$) [MPa] are the average strength of the stem per measurement period.

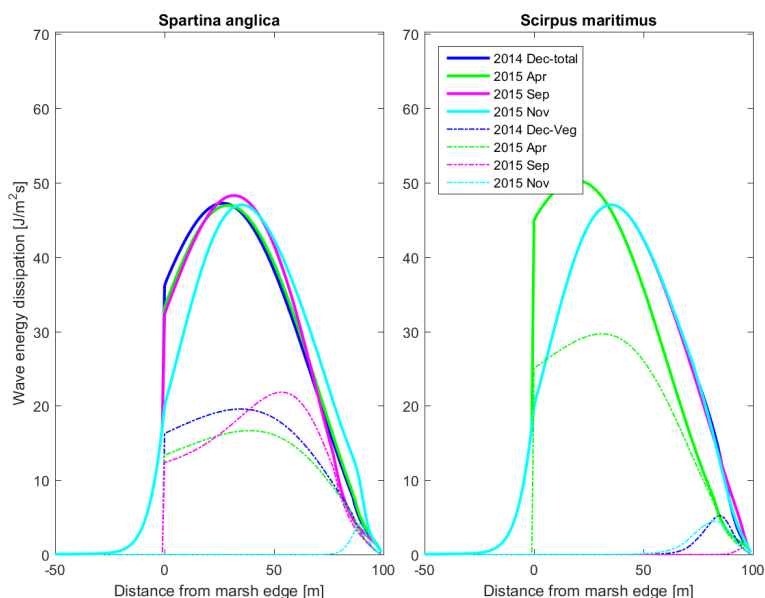


Figure 4.14: Wave energy dissipation for the percentage of stem breakage approach, of both species. Incoming wave height: 1.2m, depth at beginning of marsh: 2m.

The first binary approach of stem breakage which modeled all/none of the stems breaking in each cell, also showed reasonable results for wave energy dissipation, but the behavior was more abrupt at the boundaries at which the stems did not break. The wave energy dissipation starts more abruptly in this approach since the transition between all of the stems breaking and none of the stems breaking initiates a large difference in wave energy dissipation due to vegetation (ϵ_v).

There are some limitations to this analysis, since 1) the average value of measurements may not be representative of the vegetation during that season, and 2) in reality, not only the vegetation characteristics, but also the wave conditions (wave height H and water depth h) vary by season. As can be seen from the example of 2014 December measurements of *Spartina anglica*, based on the average data, the model performs as if the vegetation during this period is the strongest. However, comparing to 2015 November measurements, which is around the same time of the year in 2015, it has significantly different vegetation characteristics (Table 4.6). The differences may result from yearly variation in ecological growth patterns, or possible errors due to human measurements. The reasoning for this difference cannot be immediately answered, but could be studied with more vegetation data accumulated over several years.

Summary

The stem breakage model shows to perform reasonably well with the wave energy balance calculations. This was verified by varying the incoming wave height and vegetation

characteristics, followed by an analysis of the results. The variation in stem density, wave height, and also wave energy dissipation all show reasonable behavior along the entire foreshore.

5

PROBABILITY OF FLOODING AND INFLUENCE OF VEGETATION

A mechanical analysis of stem breakage and its implementation to the wave energy balance was found effective in modeling wave height behavior (Chapters 3 and 4). More detailed vegetation characteristics and sophisticated interaction between stems and waves are implemented to the probabilistic model (by V. Vuik) to calculate the probability of overtopping. The implication of including detailed vegetation data and stem breakage in the model is assessed in this chapter.

The probabilistic model of flooding is explained in Section 5.1, followed by a description of the vegetation scenarios (Section 5.2) and correlation scenarios (Section 5.3). Model results and its implications are discussed in Section 5.4. Further, a recommendation on

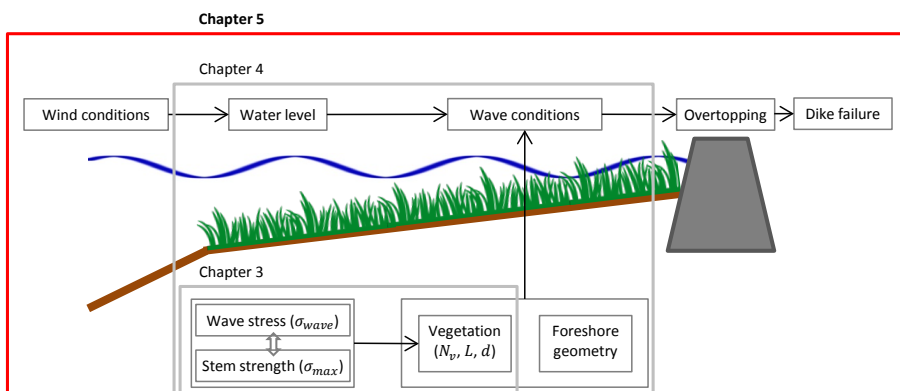


Figure 5.1: Chapter 5 in overall schematization.

how to use stem breakage in the probabilistic model and future possibilities for research will conclude this chapter in Section 5.5.

5.1. PROBABILISTIC MODEL FOR DIKE FAILURE

The probabilistic model runs in MATLAB with the use of Open Earth Tools (OET, open source Deltares [2016]) for calculating the probability of dike failure with the first-order reliability method (FORM). Background information on FORM is included in the Appendix B.1. In the model, each parameter is defined as a deterministic or stochastic variable with a specific distribution and its characteristic values (e.g. mean and standard deviation, Table 5.4). Correlation coefficients are defined for variables that show a clear statistical correlation (further discussed in the Section 5.3), further wind and wave data from the Wadden Sea (The Netherlands) is input into the model.

Based on these input parameters, FORM calculations are performed with a pre-defined limit state function (Z) for overtopping. Note: instead of FORM, a Monte Carlo simulation is also possible, but in this case FORM calculations are found to be more useful, as a sensitivity analysis per variable is possible with the model results. In either case, the same limit state function (Equation 2.4: $Z = m_{qc}q_c - m_qq$) for overtopping and dike failure is defined and input into the model. In this equation, the two model factors m_{qc} , m_q , and the critical discharge q_c are defined earlier either as a stochastic or an average variable. The overtopping discharge q needs to be calculated a priori of calculating Z .

The overtopping discharge q is a function of wave characteristics and dike geometry (Section 2.6). Input wave characteristics (H_{m0} , L_0) are dependent on the wave height (H) transformation which is a result of the wave energy balance in the foreshore, as discussed in Chapter 4. The wave energy balance is affected by the incoming wave height at the boundary, as well as the foreshore geometry, and how much the wave energy dissipates as it travels towards the coast. In the case of a vegetated foreshore, vegetation is often the dominating mechanism for wave energy dissipation and wave height reduction. As a result, the wave height at the dike is calculated by considering the consequent wave conditions, foreshore geometry, vegetation characteristics (stem length L , diameter d , and density N_v), and two different ways to quantify stem breakage (same as in Section 4.2.1).

For broken stems, instead of assuming that stems break at the absolute bottom (bed level), the stems are assumed to break 10cm from the ground. In other words, regardless of the species (*Spartina anglica* or *Scirpus maritimus*), the broken stems will still have a 10cm stem length. This would be a better representation of what happens in reality (personal communication with Z. Zhu - ecologist at NIOZ, 10/06/2016), because the remaining broken stems also contribute to the dissipation of wave energy.

An overview of the different vegetation and correlation scenarios implemented are presented in the next sections, 5.2 and 5.3.

5.2. VEGETATION SCENARIOS

Multiple different scenarios were considered in order to analyze the effectiveness of vegetation stem breakage in the probabilistic model. The same initial and boundary condition are applied to all scenarios. A summary of the scenarios is included in Table 5.1.

Scenarios 1 and 2 are the *existing baseline scenarios* in the probabilistic model of V. Vuik.

Scenario 1 (No vegetation) is the most conservative model because it does not include any vegetation. There is no wave energy dissipation due to vegetation (ϵ_v) in the foreshore, which would result in the least wave height attenuation. Overtopping discharge is expected to be most severe in this situation, leading to a high probability of dike failure.

Scenario 2 (Strong vegetation) is the most optimistic model with strong vegetation. Strong vegetation indicates that there is no stem breaking along the foreshore, and in other words, the initial stem density (N_{v0}) is conserved throughout the vegetated foreshore. Wave energy dissipation due to vegetation (ϵ_v) is strongest in this model, and there will be strong wave height attenuation. Subsequent calculations of the probability of failure are expected to be the lowest in this model.

Scenarios 3 to 5 include the *new implementation of vegetation stem breakage*. The probability of failure from these scenarios (3 to 5) are expected to range between Scenarios 1 and 2 because the implementation includes vegetation with the possibility of stem breaking along the vegetated foreshore. There is wave energy dissipation due to vegetation (ϵ_v), but possibly at a smaller magnitude than in Scenario 2 (strong vegetation with no stem breaking). The scenarios vary depending on the two types of stem breakage applications (Section 4.2.1, refer to Table 4.3) and the average/stochastic input of vegetation related variables (L , d , σ_{\max} , and coefficients from characteristic relations).

Scenario 3 (Average vegetation, binary stem breakage) takes a single average value for each vegetation characteristic (stem length L , diameter d , and strength σ_{\max}) from every measurement period and species. Vegetation stems break along the foreshore based on the binary stem breakage approach, (previously discussed in Section 4.2.1). At each spatial computation cell along the foreshore, the wave-induced vegetation stress (σ_{wave}) is calculated and compared to stem strength σ_{\max} . All stems at that cell are considered to have the same vegetation characteristics, and therefore all or none of the stems break

Scenario	Vegetation-related variables	Stem breakage type (per grid cell)
1 No vegetation	-	-
2 Strong vegetation	Average value	Stems do not break
3 Average vegetation	Average value	Binary (all/none) break
4 Binary stem breakage	Stochastic	Binary (all/none) break
5 Percent stem breakage	Stochastic	Percentage break

Table 5.1: Scenarios of varying probabilistic runs. The vegetation-related variables indicate the stem length (L), diameter (d), strength (σ_{\max}), and coefficients from characteristic relations.

depending on which stress (σ_{wave} or σ_{max}) is greater. Stem density will be either be zero ($N_v = 0$) or equivalent to the initial stem density ($N_v = N_{v0}$).

The vegetation-related variables in Scenarios 4 and 5 are input as *stochastic variables*. As a result, these two scenarios have an important added value: with the first-order reliability method (FORM), the influence factor (α) is calculated for vegetation-related variables. The influence factor provides a good indicator of how much the stochastic variable's standard deviation contributes to uncertainty of the model result. More information on the influence factor (α) is included in Appendix B.1.

Scenario 4 (Stochastic vegetation, binary stem breakage) is similar to Scenario 3 in that the same stem breakage type is used. In both scenarios, the stems either completely break ($N_v = 0$) or do not break at all ($N_v = N_{v0}$). The difference between the two scenarios is how the vegetation characteristics (L , d) and strength (σ_{max}) are input into the model. Scenario 4 now introduces a probabilistic aspect by including the vegetation related variables (L , d and σ_{max}) as stochastic variables. The statistical distribution of each variable is defined as a log normal distribution with its mean and standard deviation from measurement data. The probabilistic model randomly selects one value from each distribution and uses it as the input value. Stem breakage occurs when the randomly chosen strength (σ_{max}) is less than the wave-induced stress (σ_{max}) at that cell.

Scenario 5 (Stochastic vegetation, percent stem breakage) uses the second, percent stem breakage approach from Section 4.2.1 and Table 4.3. The percentage of broken stems is determined by evaluating wave-induced stress σ_{wave} to the normal CDF of stem strength σ_{max} . The normal CDF of stem strength σ_{max} is defined by its mean and standard deviation, included in the probabilistic model as two deterministic variables. This approach is a more realistic quantification of stem breakage, but on the other hand, it does not compute an influence factor α for stem strength (σ_{max}) because it is not defined as a stochastic variable in this approach. Instead, the normal CDF of stem strength (σ_{max}) is used, determined by its mean and standard deviation.

5.3. CORRELATION SCENARIOS

Correlation is a way of expressing the dependence of one characteristic to another. For instance, the height of a tree is positively correlated to its age, since the tree grows taller with increasing age (both characteristics increase or decrease relative to each other: positive correlation). A different case is a negative correlation. For example, the length of a pencil to the amount of usage is negatively correlated because the length of the pencil decreases with increased use (one characteristic decreases as another increases, and vice versa: negative correlation).

Certain vegetation characteristics (stem length L , diameter d , and strength σ_{\max}) are correlated to each another, and implementing correlations in the probabilistic model will allow a more realistic combination of a vegetation characteristics. Three different correlation approaches are implemented.

1. **No correlation:** Does not include any correlation of vegetation characteristics.
2. **Correlation coefficient:** Pearson correlation coefficient is calculated for different vegetation characteristics (stem length L , diameter d , and strength σ_{\max}) based on measurement data, and they are included in a correlation matrix that is input into the probabilistic calculations.
3. **Characteristic relation:** The equation for calculating stress (3.3), as well as a fitted line through the measurement data is defined as characteristic relations of vegetation characteristics. The coefficients in these equations are input in the probabilistic model as stochastic variables, including a mean and standard deviation.

1. No correlation

The baseline configuration for the probabilistic model does not include any correlation between vegetation characteristics.

2. Correlation coefficient

In the calculations of FORM, it is optional to include a matrix of correlation coefficients (correlation matrix). A correlation coefficient is a measure of how one variable changes according to the variation of another variable. A correlation coefficient ranges from -1 and 1, with 0 indicating there is not a distinct relationship between the two variables. If the correlation coefficient is closer to positive 1, variable A increases with an increase of variable B (positively correlated), whereas with a correlation coefficient closer to negative 1 (-1), would mean that variable A decreases with an increase of variable B (negatively correlated). For instance, when both the wind speed U and water level h are stochastic variables, a higher wind speed would induce higher water levels. And therefore, in this model the correlation between U and h is 1, indicating fully positive dependence. The Pearson correlation coefficient (ρ) for two variables Z_1 and Z_2 is calculated with the following Equation 5.1.

$$\rho_{z_1 z_2} = \frac{\text{Cov}(Z_1 Z_2)}{\sigma_1 \sigma_2} \quad (5.1)$$

Here ρ is the correlation coefficient for variables Z_1 and Z_2 , $\text{Cov}(Z_1Z_2)$ is the covariance of the two variables, and the two σ are the standard deviations of the respective variable.

If there are distinct correlations between two variables, it is recommended to include the correlation because it will strengthen the model performance. The correlation coefficient will influence the selection of stochastic variables according to their relationship. In other words, the probabilistic model will be inclined to choose a combination of two variables that are more reasonable and likely to occur.

The Pearson correlation between each variable is listed in Table 5.2. The correlation coefficient was found among the vegetation characteristics: stem length (L), diameter (d), and strength (σ_{\max}). The correlation per measurement period, as well as all the seasons combined (denoted "All") was calculated for both species, *Spartina anglica* and *Scirpus maritimus*.

Length (L) and diameter (d): The correlation between stem length (L) and diameter(d) show differing behavior depending on the species. *Spartina anglica* appears to have a significantly positive correlation, whereas *Scirpus maritimus* shows a weak, but generally negative correlation. Referring to the vegetation measurement data in Appendix C, figures C.1, C.4 and C.5 show that indeed the correlation calculated is representative of the measurement data. In Figure C.1, *Spartina anglica* shows a fairly normal distribution of the stem length, and *Scirpus maritimus* has a wide and fairly uniform distribution. This can be attributed to the weak stems of *Scirpus maritimus* as previously mentioned. *Scirpus maritimus* more easily breaks, and therefore the stem length also shows a wide distribution since the stems break at different lengths over time.

Length (L) and strength (σ_{\max}): Stem length and its strength generally have a positive correlation for both species, but shows a stronger and more distinct correlation for *Scirpus maritimus* than it does for *Spartina anglica*. Refer to Table 5.2, figures C.7 to C.9 in the appendix. This is representative of the measurement data as well as the reasoning that stronger stems generally have longer stems because they do not easily break.

Species	Measurement period	correlation of L, d	correlation of L, σ_{\max}	correlation of d, σ_{\max}
<i>Spartina anglica</i>	2014 Dec	-0,09	0,37	-0,75
	2015 Apr	0,13	0,19	-0,48
	2015 Sep	0,25	0,08	-0,26
	2015 Nov	0,43	0,43	0,17
	All	0,49	0,00	-0,47
<i>Scirpus maritimus</i>	2014 Dec	-0,25	0,55	-0,62
	2015 Apr	-0,25	0,52	-0,68
	2015 Sep	0,19	0,29	-0,62
	2015 Nov	-0,33	0,65	-0,34
	All	-0,22	0,46	-0,52

Table 5.2: Pearson correlation coefficients calculated for vegetation characteristics (stem length L, diameter d, and strength σ_{\max}).

Note: For *Spartina anglica*, when the correlation for length (L) and strength (σ_{\max}) is calculated per measurement period, there is generally a positive correlation. Measurements from 2014 December and 2015 November (winter measurements) show higher positive correlation, whereas 2015 April and September measurements show a small correlation. However, when the data is combined (“All”), the correlation is calculated as nearly zero, indicating there is no significant correlation between the two variables. To verify whether this is the case even when excluding five outliers (neglecting five stems with largest strength values σ_{\max} , Figure C.7), the correlation was re-calculated. However, the newly calculated correlation did not show a big difference ($\rho_{\text{new}} = 0.01$). Therefore the correlation between length (L) and strength (σ_{\max}) for *Spartina anglica* was taken as zero.

Diameter (d) and strength (σ_{\max}): As can be seen in the last column of Table 5.2, stem diameter (d) and strength (σ_{\max}) clearly show a strong negative correlation. The clearly negative correlation can be attributed to the characteristic relation which was discussed in the calculation of stem strength σ_{\max} (Section 3.1, Equation 3.6). Strength σ_{\max} is inversely proportional to d to the third power. Also refer to Figure C.12 of Appendix C. This is often observed in the field where thicker stems more easily break whereas the thinner stems are more elastic, and therefore are harder to break (personal communication with Z. Zhu - ecologist at NIOZ, 10/06/2016).

Correlation coefficients for the combined measurement data labeled “All” in Table 5.2 is input into the probabilistic model as part of the correlation matrix. For calculation of correlations, the combined data from all measurement periods better represents the vegetation data and respective behavior because the larger sample size allows smoothing out of the extreme values (possibly outliers) of the data.

Although correlation coefficients are useful for a more realistic selection of stochastic variables, the disadvantage of using a correlation matrix is that it is harder to analyze the influence factor α because the variables influence each other through the correlation coefficient. Each stochastic variable has an influence factor indicating how much relative uncertainty is due to that variable. However, with the correlation coefficient influencing the selection of stochastic variables, it becomes harder to assess the influence factor, as it is not exactly clear from where the uncertainty is originating. In order to reduce the ambiguity due to correlation coefficients, characteristic relations may be an alternative approach.

3. Characteristic relation

Instead of a correlation coefficient which defines the relation between two variables with a single number, the characteristic relation may be a more straightforward and comprehensive method for incorporating the relation between two variables. In this approach two characteristic relations are included.

1. diameter (d) and strength (σ_{\max})
2. diameter (d) and stem length (L)

For the **first characteristic relation** between diameter (d) and strength (σ_{\max}), the Equation 3.3 (repeated below) is directly included in the model, and the coefficients ($F_{\text{test}}L_{\text{test}}/8$) is defined as a single stochastic variable (recap: I is the area moment of inertia, a function of d). This way, the relation between diameter d and strength σ_{\max} is clearer, and further the influence factor of the coefficient can also be assessed.

$$\sigma_{\max} = \frac{F_{\text{test}}L_{\text{test}}}{8} \left(\frac{d}{I} \right) \quad (3.3)$$

The **second characteristic relation** is defined between the diameter (d) and stem length (L), based on a fitted line through the measurement data (Figure C.6). The characteristic relation is defined in Equation 5.2, and the coefficients (a and b) are defined as stochastic variables with an inverse log normal distribution. The mean and standard deviation of these variables are listed in Table 5.3 for species *Spartina anglica* and *Scirpus maritimus*.

$$d = aL + b \quad (5.2)$$

From Table 5.3, *Spartina anglica* has a positive (+) sign for the slope a_{ave} , and *Scirpus maritimus* has a negative (-) sign of a_{ave} . This is in agreement with the correlation analysis previously discussed for length L and diameter d (Table 5.2), as a positive correlation is observed for *Spartina anglica* and a negative correlation for *Scirpus maritimus*.

	a_{ave}	b_{ave}	a_{std}	b_{std}
<i>Spartina anglica</i>	2.568 E-3	2.062	3.248 E-4	0.15
<i>Scirpus maritimus</i>	-1.236 E-3	8.206	4.289 E-4	0.35

Table 5.3: Average (ave) and standard deviation (std) of the coefficients (a and b) for the characteristic relation between stem length L and diameter d in Equation 5.2.

In summary, the characteristic relation scenario does not include stem diameter (d) as a stochastic variable, instead it is calculated based on the second characteristic relation (Equation 5.2) with coefficients a and b defined as stochastic variables based on Table 5.3. Also, in place of the stem strength (σ_{\max}) as a stochastic variable, now three-point bending test results ($F_{\text{test}}L_{\text{test}}/8$) of Equation 3.3 is a stochastic variable that is used to

calculate the stem strength σ_{\max} . Table 5.6 summarizes the vegetation-related stochastic variables per correlation scenario.

With these two characteristic relations defined in the probabilistic model, it is no longer necessary to define another relation between stem length L and strength σ_{\max} because the two characteristic relations (σ_{\max} vs. d , and d vs. L) provide a sufficient link between stem length L and strength σ_{\max} .

5.4. RESULT ANALYSIS

The probabilistic model is ran based on the various scenarios mentioned in Sections 5.2 and 5.3. In brief, there are **5 vegetation scenarios**:

1. *No vegetation* (conservative)
2. *Strong vegetation* (optimistic): stems do not break
3. *Average vegetation*, with binary stem breakage approach (all/none break)
4. *Binary stem breakage*, stochastic vegetation variables with binary stem breakage approach
5. *Percent stem breakage*, stochastic vegetation variables with percent stem breakage approach (% break based on normal CDF of σ_{\max})

And for each vegetation scenario, there are **3 correlation scenarios** that differ by:

1. No correlation
2. Correlation coefficients
3. Characteristic relations with coefficients input as stochastic variables

In total there are 150 runs which are from 5 vegetation scenarios, 3 correlation scenarios, and 10 vegetation data sets (2 species from 5 periods of April, September, November, December, and all combined), which yields $5 \times 3 \times 10 = 150$.

The first-order reliability method (FORM) is used to calculate the probability of failure, which is defined by a limit state function as the point at which the overtopping discharge exceeds the critical overtopping discharge. The model performance of the various correlation and vegetation scenarios are assessed by analyzing the probability of failure and influence factors α of the vegetation characteristics. In cases where the model results did not yet converge after 25 iterations, the last three reliability indices (β) were evaluated, and if the difference between one to another was less than 0.2, the result is considered to have converged. Refer to Section 2.6 and Appendix B.1 for more background information.

The input values for the boundary conditions (equivalent in all scenarios) and the design values from one of the model runs (“characteristic relation” and “percent stem breakage” scenario of *Scirpus maritimus* in December, 2014) are included in Table 5.4. The Wadden Sea data from the Netherlands (Gautier and Groeneweg [2012]) is used for the respective wind speed (U) and water level (h). The design values lie on the failure plane ($Z=0$) of the limit state function where failure is most likely to occur (refer to Appendix B.1). One set of example design values for wind speed (U) and water level (h) are expressed in Table 5.5 for the “characteristic relation” scenario of *Scirpus maritimus* in December 2014.

FORM calculates the design value as the condition in which failure most likely occurs. As shown in Table 5.5, in cases of no vegetation, failure occurs at a lower wind speed and water level. On the other hand, for strong vegetation, a higher wind speed and water level is necessary for failure to occur. The three other vegetation scenarios that involve vegetation stem breakage lie in between these two scenarios. Although the design point cannot

always be an accurate way to evaluate the performance of the probabilistic model, it can still be used as a preliminary assessment of whether the model results are reasonable.

The last three rows in Table 5.5 show that wave height reduction is smallest for no vegetation, and largest for strong vegetation. The other vegetation scenarios including stem breakage showed values in between these two extreme vegetation scenarios. The design values and wave height are in line with the results of probability of failure which will be discussed in the next section (5.4.1).

Variable	Type	Input		Design value	Unit
Wind speed (U)	Table	Data file		29.05	m/s
Water level (h)	Table	Data file		4.47	m
Critical overtopping discharge (q_c)	Deterministic	10 ⁻³		-	m ³ /s
Wind direction	Deterministic	340		-	°
Foreshore slope	Deterministic	1/100		-	-
Nikuradse roughness length scale (kN)	Deterministic	0.02		-	m
		Mean	Std.dev		
Crest height	Normal	6	0.1	5.98	m
Dike slope	Normal	0.25	0.0125	0.25	-
Coefficient (C1)	Normal	4.75	0.5	4.59	-
Coefficient (C2)	Normal	2.6	0.35	2.60	-
Coefficient (C3)	Normal	-0.92	0.24	-0.92	-
Bed level	Normal	1.5	0.2	1.47	m
Model factor of q_0 (m_q)	Log normal	1	0.5	0.99	-
Model factor of q_c (m_{qc})	Log normal	1	0.5	0.81	-
Foreshore width	Log normal	400	100	372.07	m
Drag coefficient (C_d)	Log normal	0.4	0.1	0.37	-
Breaker parameter (γ)	Log normal	0.63	0.1	0.64	-

Table 5.4: Input for stochastic variables of the probabilistic model and an example design point from the “characteristic relation” and “percent stem breakage” scenario of *Scirpus maritimus* in December, 2014. Wind speed (U) and water level (h) takes the Wadden Sea data (Gautier and Groeneweg [2012]), in the Netherlands.

	No veg.	Ave veg.	Binary breakage	Percent breakage	Strong veg.	unit
Wind speed (U)	28.0	29.1	29.1	28.5	32.6	m/s
Water level (h)	4.3	4.5	4.5	4.4	5.2	m
Wave height offshore (H_{in})	1.15	1.25	1.25	1.21	1.56	m
Wave height at dike (H_{end})	0.94	0.72	0.73	0.70	0.40	m
H reduction ($H_{in} - H_{end}$)	0.21	0.53	0.52	0.51	1.16	-

Table 5.5: Probabilistic model results from “characteristic relation” of *Scirpus maritimus* in December 2015: design value of wind speed (U), water level (h), offshore wave height (incoming wave height at the beginning of marsh, H_{in}), wave height at dike (H_{end}), and the wave height reduction from incoming to the dike ($H_{in} - H_{end}$) for varying vegetation scenarios.

5.4.1. VEGETATION SCENARIOS AND PROBABILITY OF FAILURE

Figure 5.2 provides an overview of the probability of failure for the different scenarios based on vegetation data of four measurement periods (x-axis), and “all” indicates the data set combining all four measurement periods. These results are useful for assessing the effect of differing the vegetation scenarios. There are 30 results per vegetation scenario (3 correlation scenarios \times 10 vegetation data sets).

In this figure, it is clear that the black diamonds for the **no vegetation** scenario has the highest probability of failure regardless of the correlation scenario or vegetation data. The probability of failure results are equivalent in all “no vegetation” cases, since the varying scenarios are relevant to the input of vegetation which is not present in these runs. The probability of failure is highest because of the absence of wave energy dissipation due to vegetation, which is often one of the dominating wave energy dissipation mechanisms. Consequently, the wave height reduction in the foreshore is the smallest, resulting in a larger amount of overtopping discharge than other vegetation scenarios.

The failure probability of the dike in the “no vegetation” case is 0.0017, with a return period of approximately 1/588 years. Under Dutch safety standards, this is often unsatisfactory. Inland and rural areas occasionally have lower safety requirements for dikes of approximately 1/300, but most coastal and urban areas are obligated to meet higher safety standards of approximately 1/10,000 and even up to 1/100,000 (van der Doef et al. [2014]).

The green circles in this Figure 5.2 represent the model results for **strong vegetation**, assuming the vegetation stems do not break even under extreme wave conditions. This is the most optimistic scenario which yields the lowest probability of failure. In reality, stems do break from extreme wave conditions which can be verified from field observations, and using such strong vegetation would not be representative of the interaction between waves and vegetation.

The three other vegetation scenarios, average vegetation and the two probabilistic models, range in between the “no vegetation” and “strong vegetation” scenarios. The three models include vegetation, as well as a certain stem breakage model.

The **average vegetation** scenario and **binary breakage** scenario (labeled in Figure 5.2 as: Probabilistic 1) use the same stem breakage approach of which all/none of the stems break, but the two differ in which vegetation characteristics are used as input. The average vegetation scenario uses a single set of average values from the respective measurement period, whereas the binary probabilistic approach takes randomly selected vegetation characteristics from the pre-defined statistical distribution (log normal with mean and standard deviation).

As can be seen in Figure 5.2, the probability of failure of “binary stem breakage” and “Average vegetation” are generally very close or even overlapping each other. The instances when the two results are farther apart (example: *Spartina anglica* in September and combined “all”), the standard deviation of the stem length (L) is large relative to the mean value (can be verified from vegetation measurement statistics in Table 4.6). Stem length as mentioned previously, is dominant in determining the amount of wave-induced stress

σ_{wave} (Section 3.3 and Table 4.1).

The similar results of the average vegetation and binary probabilistic scenario is understandable because when the standard deviation is small, it is more likely that the randomly chosen values in the binary stem breakage approach are closer to the average values. This is why in most cases, the probability of failure results of the two scenarios are similar. In contrast, noticeable differences only occurred in cases when the standard deviation of stem length (L) was relatively large compared to the mean value. This would most likely lead to a selection of stem length (L) farther away from the mean (possibly higher) and consequently greater wave induced stress and probability of failure.

Results of the **binary stem breakage** scenario are quite sensitive to the magnitude of

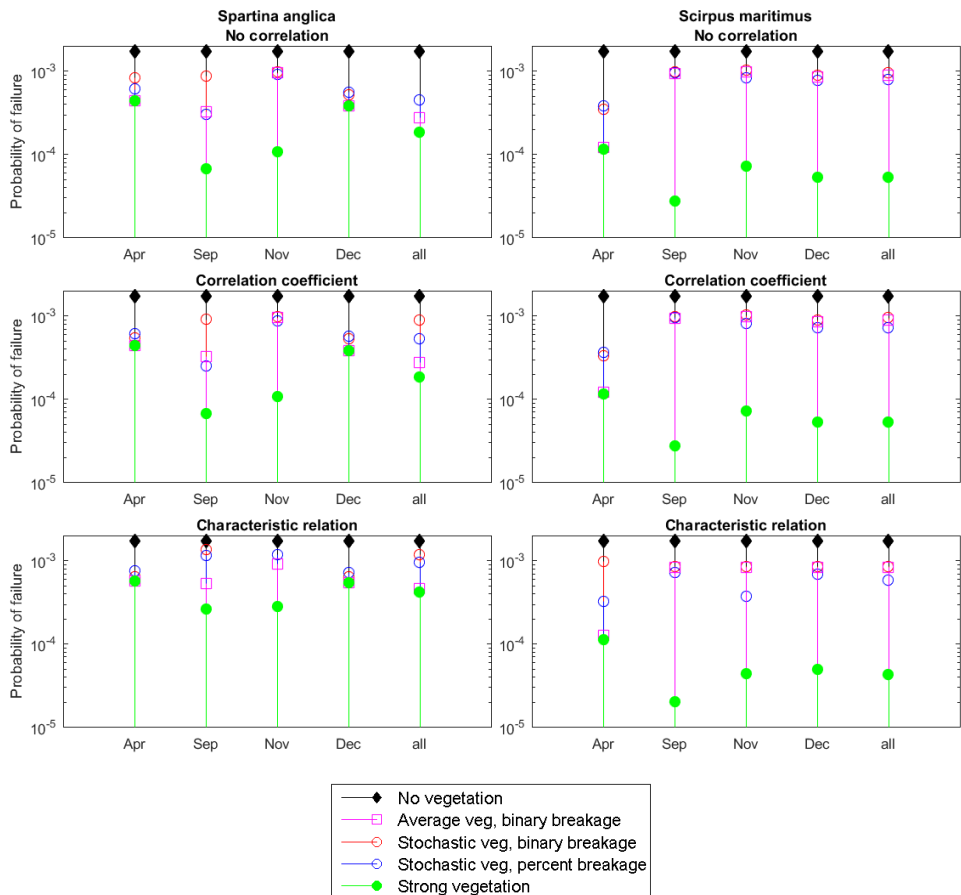


Figure 5.2: Probability of failure results from the first-order reliability method (FORM), for different correlation and vegetation scenarios. Vegetation data are from four different measurement periods of the species *Spartina anglica* (left) and *Scirpus maritimus* (right). The label “all” indicates the combined data from all four measurement periods.

stem strength because only one randomly selected stem strength is compared to the wave load. In reality, the stem strength would vary per stem, which in general there are 500 to 3000 stems per square meter. In this approach, all stems are considered to have the same strength. Therefore it is most likely that, depending on the single stem strength selected, the entire marsh is either completely wiped out or completely undamaged. In other words, rarely was there any variation along the marsh. Figure 5.3 compares wave-induced stress (σ_{wave}) to stem strength (σ_{max}). The title of each plot shows the different possibilities of stem breakage along the vegetated foreshore. With the binary stem breakage approach, the left most situation in Figure 5.3 (which all stems break throughout the marsh), most often occurred (20 of 30 results in Figure 5.2).

In the binary and percent stem breakage scenario (labeled in Figure 5.2 as: stochastic veg, 0/1 breakage and % breakage), vegetation characteristics (stem length L and diameter d) are randomly selected as stochastic variables in both cases, but the percent breakage scenario uses a different stem breakage approach. Previously explained in Section 4.2.1 and Table 4.3, the **percent stem breakage** approach calculates the probability of broken stems by evaluating the wave-induced stress σ_{wave} to the normal cumulative distribution function (CDF) of stem strength σ_{max} . In this case, rather than all/none of the stems breaking, a percentage of stems break and the remaining stems are able to withstand the wave load.

Compared to the binary breakage scenario, the percent breakage scenario showed a generally lower probability of failure (23 of 30 results in Figure 5.2). This behavior can be understood by the differences in quantifying stem breakage. In the binary stem breakage

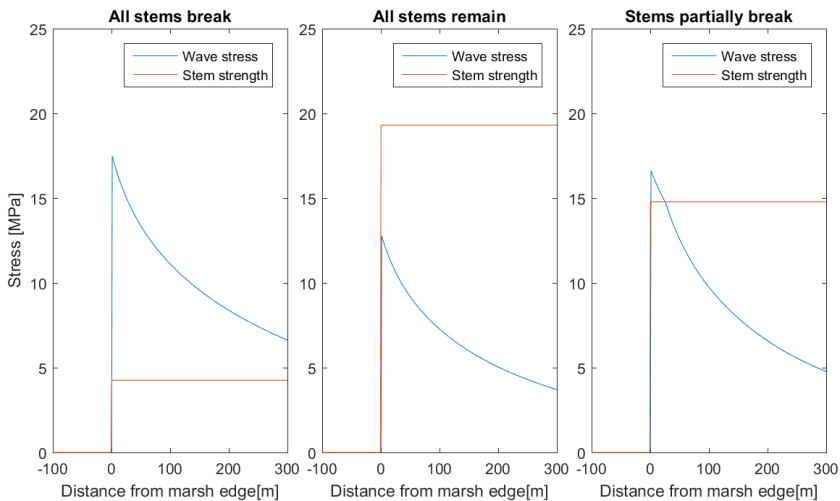


Figure 5.3: Wave-induced stress (σ_{wave}) versus stem strength (σ_{max}). Stems break when the wave load exceeds the stem strength. Examples are from the 'correlation coefficient' and 'binary stem breakage' scenario, for vegetation data from the left: September, December, and April of *Spartina anglica*.

approach, even when the wave-induced stress slightly exceeded the stem strength, the stems were considered all broken. However, in the percent stem breakage approach, the intermediate percentage (between 0 and 100%) of breaking allows for a more gradual change in stem density variation along the vegetated foreshore. As a result, the difference between broken stems and standing stems is not as extreme as the binary breakage approach, and therefore leads to a more gradual dampening of wave height and lower failure probability.

In summary, the probability of failure results were useful indicators of the behavior of vegetation scenarios. The “no vegetation” and “strong vegetation” scenarios are the most conservative and optimistic situation, respectively. In between the results of these two extreme scenarios, the “average”, “binary stem breakage” and “percent stem breakage” scenarios better represent the behavior of vegetation by implementing stem breakage. The “average” vegetation scenario has its limitation by only taking one average value for each vegetation characteristic, and that is why in the two different stem breakage approaches the vegetation is selected as stochastic variables.

5

The two stem breakage approaches quantify vegetation stem breakage in two different ways. The binary stem breakage approach yields a result that either all or none of the stems break per grid cell, whereas the percent stem breakage approach quantifies the percentage of stems breaking based on evaluating the wave-induced stress to the normal CDF of stem strength. The percent stem breakage approach is more realistic in quantifying the number of broken stems because the variation in stem strength is taken into account. However, with this approach in FORM calculations, it is not possible to quantify the amount of uncertainty (influence factor α) of the stem strength contributing to the model results. In contrast, the influence factor of stem strength is calculated in the binary breakage approach, and this will be further discussed in the next section.

5.4.2. CORRELATION SCENARIOS AND INFLUENCE FACTORS

In the process of calculating the design point and probability of failure with FORM, the uncertainty measure (influence factor α) is calculated for each stochastic variable. The influence factor quantifies the relative uncertainty that each stochastic variable brings to the model. In very simplistic terms, a wider standard deviation of stochastic variable X would lead to a higher influence factor because there is a wider variation in possible values for X . Additionally, if the variable X is used to a higher power (e.g. X^2 , X^3 , or higher), the influence factor would also increase due to its increased weight to the results. Also in more complex limit state functions involving multiple equations (as in the probabilistic model in this research), the interaction between variables and how they relate also affects the magnitude of the influence factor.

For every limit state function, the squared sum of all influence factors equals 1 as in Equation 5.3. Here, n is the number of stochastic variables.

$$\alpha_1^2 + \alpha_2^2 + \alpha_3^2 \dots \alpha_n^2 = 1 \quad (5.3)$$

The influence factor (α) of resistance generally has a positive (+) sign and load parameter generally has a negative (-) sign, but when the influence factor is squared (α^2), the (+/-) sign is no longer relevant because it becomes positive in either case. As such, the magnitude of the influence factor is more important because it represents the relative contribution to the total uncertainty of the model.

Analyzing the influence factors, the wind speed (U) is undeniably the most critical parameter, as the squared value ranges from 0.88 to as high as 0.97. It is clear that the wind speed contributes most to the uncertainty of the model, which is reasonable since the wind speed directly relates to the water level leading to overtopping of the dike. However, the uncertainty of wind speed is unavoidable, as it is part of the unpredictability of nature. Such types of uncertainty are categorized as inherent uncertainty in time (Van Gelder [2000]), and it may not significantly reduce due to more data or research. Since the high influence factor of wind speed (U) cannot be easily controlled, in order to improve the model performance, it is important to reduce the uncertainty due to vegetation.

In this research, the input boundary and wave conditions are the same in all scenarios, and the scenarios only differ by vegetation-related parameters and calculations. Stated differently, the uncertainty due to boundary and wave conditions are equivalent in all scenarios, but the relevant influence due to vegetation varies by scenario. This is why in Sections 5.4.2 and 5.4.3, the implications of different scenarios and vegetation characteristics will be discussed by analyzing its influence factors.

For this research, the unavoidable uncertainty of wind speed, offshore wave climate and its consequent water level will not be assessed. Instead, other vegetation-related influence factors are analyzed. In particular, the newly added stochastic variables related to vegetation will be assessed. In order to assess this influence, the only two vegetation scenarios that use stem-related parameters as stochastic variables are the binary and percent breakage approach (refer to Table 5.1). Thus, for each of the 3 correlation scenarios, there are 20 model results that include vegetation characteristics as stochastic variables: 2 from the previously mentioned vegetation scenarios and 10 measurement data sets from different periods. In total, these 60 results (3 correlation scenarios \times 20 = 60) will be used to assess the effect of correlation scenarios as well as to compare the influence of vegetation characteristics with each other.

The influence factor of vegetation characteristics (stem length L, diameter d, density N_v , σ_{\max} , and coefficients of characteristic relations) are assessed separately, by taking the sum of squared influence factors as in Equation 5.4. Here, the subscripts z1 to zn represent the vegetation-related characteristics.

$$\alpha_{z1}^2 + \alpha_{z2}^2 + \dots + \alpha_{zn}^2 = A_{\text{veg}} \quad (5.4)$$

Considering the high influence factor due to wind speed (U), the combined influence of vegetation A_{veg} is small. However, it is still a good indication of how much uncertainty is due to vegetation, given that all other conditions are equivalent for every model run (e.g. wind, wave and boundary conditions). Combining the results per correlation scenario

(20 results each), the outcome can be seen in Figure 5.4. List of stochastic variables can be found in Table 5.6.

In Figure 5.4, from the first “**no correlation**” scenario to the “**correlation coefficient**” scenario, the uncertainty trend is almost similar but could also be seen to have slightly increased. Including correlation coefficients may not necessarily be beneficial unless the two variables have a clear and distinct correlation. As previously seen in Table 5.2, the correlations between L , d , and σ_{\max} did not always show a consistent trend, even switching between a positive (+) and negative (-) correlation for different data sets. The correlation coefficients may help the model in selecting a more realistic set of variables, but at the same time, they add more uncertainty towards the model results since the correlation itself may not always be fully reliable. Further, including correlation coefficients makes it more difficult to analyze the individual variable’s influence factor because it is not clear how much the correlation coefficient played a role in selecting the stochastic variable.

The scenario with “**characteristic relations**” shows the lowest amount of uncertainty due to vegetation. As a recap of the two different characteristic relations previously defined, they are listed below (Section 5.3, Equations 3.3 and 5.2).

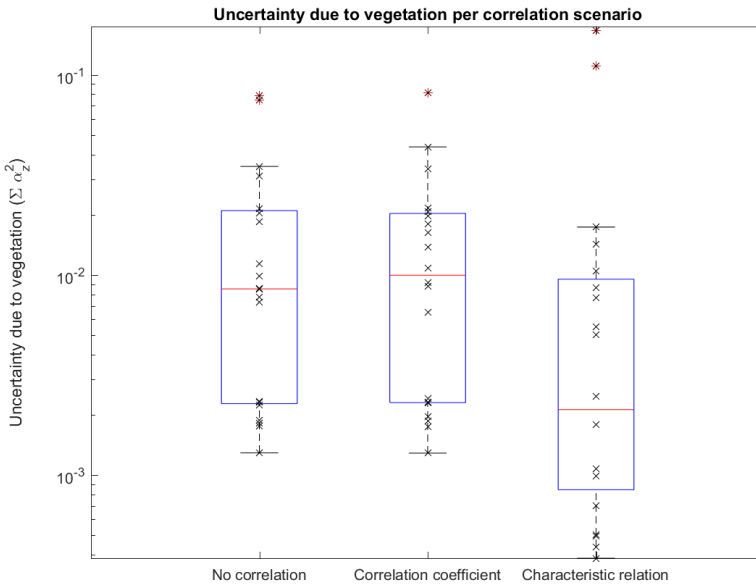


Figure 5.4: The uncertainty due to vegetation is quantified as A_{veg} (Equation 5.4) from 20 results per correlation scenario. A_{veg} is the sum of squared influence factors ($\Sigma \alpha_{zi}^2$) for vegetation-related variables z_i (e.g. stem length, diameter, strength, density, and relevant coefficients). A list of relevant variables per scenario is included as Table 5.6. The ‘x’ marks are the individual values of A_{veg} , and the second and third quartile is expressed as a box plot.

$$\sigma_{\max} = \frac{F_{\text{test}}L_{\text{test}}}{8} \left(\frac{d}{I} \right) \quad (3.3)$$

$$d = aL + b \quad (5.2)$$

The two characteristic relations show a much clearer relationship with better defined coefficients. In Equation 3.3, $F_{\text{test}}L_{\text{test}}/8$ is the coefficient for the relation between σ_{\max} and stem diameter d (area moment of inertia (I) is a function of d), and in Equation 5.2, a and b are coefficients for the relation between stem length L and diameter d . These coefficients are included as stochastic variables in the probabilistic model, and they directly come from three-point bending test data (for $F_{\text{test}}L_{\text{test}}/8$) and field measurement data (for a and b , Figure C.6).

The characteristic relation scenario has well-defined equations for the different vegetation characteristics (σ_{\max} and d), as well as better specified distribution of coefficients. As a result, this scenario has the least amount of uncertainty which was discussed and verified from Figure 5.4.

5.4.3. INFLUENCE OF INDIVIDUAL VEGETATION CHARACTERISTICS

The individual vegetation characteristics have different contributions to the uncertainty of the probabilistic model. This is assessed by considering the individual vegetation characteristics for all vegetation and correlation scenarios. Influence factor α of vegetation-related variables is only available for models which include vegetation characteristics as stochastic variables (Table 5.1), which are scenarios 4 and 5, binary and percent stem breakage scenario, respectively. The results are shown in Figure 5.5 which illustrates the variation of influence factor α and its squared value α^2 for each vegetation characteristic.

Each vegetation-related variable has a different number of results, due to the differences in the setup of correlation and vegetation scenarios. Refer to Table 5.6, of which the number within the parenthesis represents the number of results. For each correlation scenario, there are in general 20 results as previously mentioned (2 vegetation scenarios and 10 vegetation data sets, $2 \times 10 = 20$). However, the variables related to stem strength (σ_{\max} and $F_{\text{test}}L_{\text{test}}/8$), are not included in both stem breakage approaches, but only apply to the binary stem breakage, Scenario 4.

From Figure 5.5, it is clear that the uncertainty due to **stem diameter (d)** is greatest. As previously seen in Table 4.1 that summarizes three of the most relevant equations to vegetation (stresses σ_{\max} , σ_{wave} , and dissipation ε_v), stem diameter (d) is included in all three equations with varying orders of magnitude. When taking into account the area moment of inertia I as a function of stem diameter ($\propto d^4$), each vegetation-related equation is a function of stem diameter (d) approximately to the power -3, -2, and +1, respectively. This is reflected in the Figure 5.5, that the selection of diameter most significantly influence the model results than other vegetation-related variables.

Further, by comparing the influence factors of d (stem diameter), a and b (coefficients

	Equivalent	Difference	
No correlation (20)	L, N _v (60)	d (40)	σ_{\max} (20)
Correlation coefficient (20)			
Characteristic relation (20)		a, b (20)	$F_{\text{test}}L_{\text{test}}/8$ (10)

Table 5.6: List of vegetation-related stochastic variables per correlation scenario. The “Characteristic relation” scenario differs from the other two scenarios by including a characteristic relation between stem length L and diameter d (with coefficients a, b) as well as a relation for σ_{\max} and stem diameter d (with three-point bending test results of $F_{\text{test}}L_{\text{test}}/8$). The number within the parenthesis () indicates the number of model results available for analysis. There are 20 results per correlation scenario from: 2 stem breakage scenarios (Scenario 4 and 5, binary and percent stem breakage) and 10 vegetation data sets.

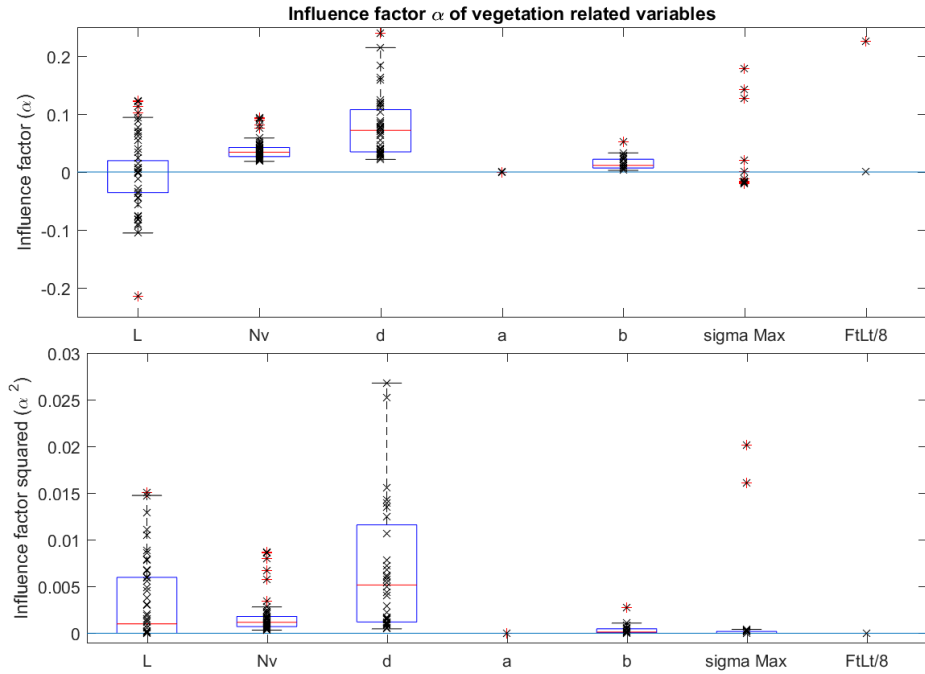


Figure 5.5: Influence factors of the individual vegetation characteristics from the probabilistic model results of FORM. Influence factor α are represented in the upper figure, whereas the squared values α^2 are included below. From the left, each variable represents: stem length (L), stem density (N_v), diameter (d), coefficients to define d (a and b, Equation 5.2), stem strength ($\text{sigma Max} = \sigma_{\max}$), and coefficient for defining stem strength σ_{\max} ($FtLU/8 = F_{\text{test}}L_{\text{test}}/8$, Equation 3.3). For better illustration of the results, a few of the highest α and α^2 values for stem length (L) and diameter (d) are not represented in this figure, but all α for stem length are presented in Figure 5.6.

of the characteristic relation between d and L, it can be seen that it is a better choice to use characteristic relations instead of correlation scenarios. Refer back to Table 5.6, as a reminder of which stochastic variables were used for each correlation scenario. In the third correlation scenario with “characteristic relations”, stochastic variables a, b, and

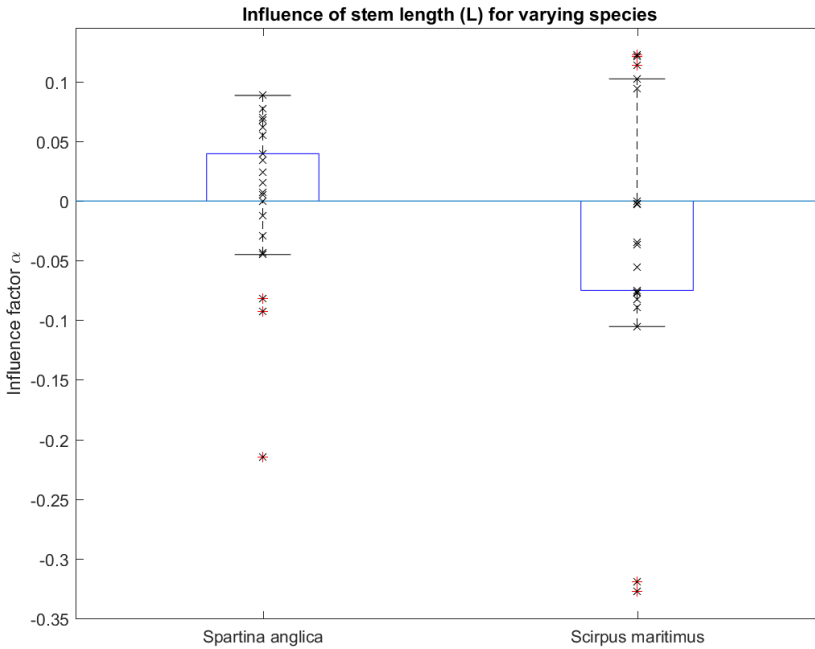


Figure 5.6: Influence factor α of stem length for two different species, *Spartina anglica* and *Scirpus maritimus* (30 results each).

$F_{\text{test}}L_{\text{test}}/8$ are used in place of d and $\sigma_{\text{Max}} (= \sigma_{\text{max}})$. Figure 5.5 shows that the uncertainty due to the stem diameter (d) and stem strength ($\sigma_{\text{Max}} = \sigma_{\text{max}}$) has significantly decreased by using characteristic relations. Also, including stem strength ($\sigma_{\text{Max}} = \sigma_{\text{max}}$) as a stochastic variable did not necessarily contribute towards reducing the influence factor. On the other hand, the stochastic variable $F_{\text{test}}L_{\text{test}}/8$ in the characteristic relation scenario was found to reduce the influence factor, as well as better represent the stem strength (σ_{max}) as a function of the stem diameter (as in Equation 3.3).

The (+) or (-) sign of the influence factors from FORM calculations are often representative of whether the variable acts as the resistance ($+\alpha$) or load ($-\alpha$). However, although the sign is *often* representative of the resistance or load, it is not always a definitive indicator, and therefore conclusions should not be drawn from the signs.

In order to get a better idea of how the variables act in general, the signs of the stochastic variables will be assessed. Of the various vegetation-related variables in Figure 5.5, **stem length (L)** is the only variable that shows a distinct positive (+) and negative (-) distribution of influence factors. The difference in signs are not distinguishable from the varying vegetation or correlation scenarios, but rather from the differing species. Refer to Figure 5.6.

In this figure, it can be seen that the influence factor of stem length (L) of *Spartina anglica* generally has a positive (+) sign, whereas that of *Scirpus maritimus* more often has a negative (-) sign. The reason for the different signs of the influence factor α can be assessed by evaluating Table 4.1. Of the three vegetation-related equations in this table, the wave-induced stress (σ_{wave}) and dissipation due to vegetation (ε_v) are functions of stem length (L). For both species *Spartina anglica* and *Scirpus maritimus*, the stem length is considered submerged, and therefore dissipation due to vegetation (ε_v) is a function of stem length (L) to the first power, whereas wave-induced stress (σ_{wave}) is a function of stem length (L) to the second power ($\propto L^2$). A summary is provided in Table 5.7.

	Resistance $\varepsilon_v \propto L$	Load $\sigma_{\text{wave}} \propto L^2$
<i>Spartina anglica</i>	dominant	-
<i>Scirpus maritimus</i>	-	dominant

Table 5.7: Vegetation-related equations that are a function of stem length (L).

5

Dissipation due to vegetation (ε_v) contributes towards the resistance because it reduces the wave energy and consequently decreases the wave height and overtopping discharge. On the other hand, wave-induced stress (σ_{wave}) is a load factor because a higher wave-induced stress indicates more stem breakage ($\sigma_{\text{wave}} > \sigma_{\text{max}}$) and therefore less wave energy dissipation due to vegetation.

The differing stem length of *Spartina anglica* and *Scirpus maritimus* seems to influence the dominance between resistance and load. In general, the stem length (L) of *Scirpus maritimus* is greater than *Spartina anglica* by approximately 150% to 180% (refer to Table 4.6 and Figure C.1 of Appendix C). There are many other variables that also influence these two parameters (ε_v and σ_{wave}), which is why for lower stem lengths in *Spartina anglica* the resistance may dominate, whereas for higher stem lengths in *Scirpus maritimus*, the second power of stem length (L^2) in σ_{wave} starts to have a greater effect.

The length of the stem (L) is effective for wave energy dissipation, but at the same time, a longer stem is more vulnerable to breaking. The positive and negative influence of stem length could be assessed by the two species with differing stem lengths. In future research, it may be useful to find a threshold stem length at which the influence of stem length changes from a resistance to a load.

Returning to Figure 5.5, the influence of **stem density** (N_v) seems to be significant, but with a smaller magnitude and variation than the stem diameter (d) and stem length (L). The relatively small influence and variation of stem density may be the result of its small standard deviation input in the probabilistic model. Stem density strongly depends on its location, and there is not much information about its variation within a single field. As a result, the standard deviation of the stem density was defined as 20% of its initial stem density (N_{v0}). For instance, for *Spartina anglica* the initial stem density is 1000/m² and the standard deviation is 200/m². With more field measurement and research, if the variation of stem density is found to be larger, it may be possible that the influence

factor and uncertainty due to stem density may increase. Furthermore, the stem density directly affects the magnitude at which wave energy dissipation occurs, and therefore it may be very influential to the overall result. In summary, the influence of stem density is quite significant, and it may be subject to change with more available data.

5.5. RECOMMENDATIONS

The result analysis in the previous Section 5.4, leads to a few important recommendations when including stem breakage in the probabilistic model of overtopping and dike failure.

Recommendation for the users and modelers of probability of flooding

Vegetation scenario 5 (stochastic vegetation variables, and percent stem breakage approach) returned the most reasonable results (Section 5.4.1). The results in this scenario are most representative of reality because it takes into account the variation in stem strength, rather than considering one single average value for all the stems in the foreshore (as does in Scenario 4, stochastic vegetation and binary stem breakage).

Among the different correlation scenarios, the characteristic relation scenario is the most preferable because it minimizes the amount of uncertainty in the model results. However, a possibility to improve the probabilistic model would be to better define the characteristic relations between variables. This could be done by gathering more data as well as studying the sophisticated relationship between variables. The characteristic relation used in this research for stem length (L) and diameter (d) is one of the most simplistic linear relations, but it is possible that using different relationships could better represent the behavior between two variables.

Recommendation for researchers

Currently the vegetation stem density data from field measurements is scarce, and it is not very detailed nor well-documented. It would be useful to have more detailed field measurement data for stem density, particularly along a transect of the foreshore with the locations of measurements specified. This way, the stem density variation along the foreshore can be better understood, and the correction factor mentioned in Section 4.2.3 could be calibrated to better represent stem breakage phenomena.

Also, it would be useful to record stem density at shorter time and space intervals. This will provide information almost directly before and after an extreme storm event as well as the variation of stem density along the transect of a foreshore. In effect, the stem breakage model could be analyzed and verified for the response to extreme events, as well as how it affects the stem density over space.

6

DISCUSSION

MODELING wave-induced stem breakage in a vegetated foreshore is found to be effective in representing the stem density difference over the foreshore and the consequent wave height transformation and probability of overtopping. However, there are still limitations and possibilities for improvement which will be discussed in this chapter.

Simplification of vegetation

The mechanical analysis taken in this research simplifies the behavior of the stem by considering the stem simply as a stiff beam that leans with the flow of water. This simplification neglects many other features of vegetation such as the flexibility, canopy (branches and leaves), and fatigue due to the repeated wave load. These features may all contribute in some way to the interaction between stem and wave.

1. Overestimate of stem breakage

For instance, the flexibility of the stem may serve as a mechanism to avoid stem breaking. Flexibility allows the plant to adjust the position of its stem according to the orbital motion of waves, and therefore neglecting the weakest point along the stem from being directly exposed to the largest wave force. Furthermore, the flexibility and bending motion of the stem enables the stem to reduce the surface area exposed to wave forcing, even more than the leaning situation as was assumed in this research (Section 4.2.3). With a shorter length exposed to the wave forcing, the maximum moment acting on the stem will further reduce than in Equation 3.7. Flexibility of the stem may be an important factor adding to the resilience of the stem as well as reducing wave-induced stress (σ_{wave}). Calibration of the correction factor may be an important subject for future research.

2. Underestimate of stem breakage

Wave-induced vegetation stem breakage may not only be overestimated, but there is a

possibility that it is also underestimated by neglecting the canopy and effects of stem fatigue.

Vegetation canopy refers to the part that extends out of the stem, such as the branch, leaf, flower, and possibly fruit. In general, the canopy spreads out from the upper part of the stem which is often subject to greater wave loading than near the bottom. It is possible that the large canopy containing more biomass may significantly influence the amount of wave loading that the stem experiences.

Another possible factor that contributes to an underestimate of stem breakage is fatigue and the cumulative effect of wave loading. Waves in the sea continuously affect vegetation, and it is possible that even without an extreme storm event, the stems may weaken and break due to the continuous and accumulated wave load.

Limited data available

Currently the stem density measurements available are used for ecological research, and as a result, there are not sufficient spatial information recorded. Also the stem density is only measured every 3-4 months, which makes it difficult to understand the short term variation and effects of extreme events. With more frequent stem density measurements and accurate recordings of its location, the effect of stem breakage and density variation along the foreshore could be better understood. If more well-recorded data are available, it will be possible to calibrate the correction factor and understand whether the stem density changes gradually over time or abruptly after a storm. In effect, wave attenuation and probability of flooding could also be more accurately modeled and provide better guidelines to building a vegetated foreshore.

Choice of wave condition

The choice of wave height in this research is the highest 10% ($H_{10\%}$) that is assumed to break the stems. However, this selection of the wave height could be subject to change if more data is available. Also, the horizontal wave velocity is assumed to be uniform over the length of the stem, but in reality, the horizontal wave load may be higher near the water surface and lower at the bottom, both because of the linear wave theory but also due to the presence of stems.

There are yet more possibilities for further specification and calibration of the stem breakage model and its effect on stem density variation in the vegetated foreshore. Further study may serve to better represent the phenomena in a vegetated foreshore, as well as to provide more accurate predictions for the probability of flooding.

7

CONCLUSION

The objective of this research is to understand the mechanism of wave-induced vegetation stem breakage and its implication to the probability of flooding. The interaction between waves and vegetation stems is studied by comparing its strengths, and the threshold of stem breakage is defined. Stem breakage is then implemented to the wave energy balance formulas by varying the stem density along the foreshore. As a result of wave energy balance (including dissipation), the wave height reduces in front of a coastal dike. Further, this stem breakage formulation is applied to the probabilistic model of V.Vuik, and the implication on the model results is analyzed. Conclusions from this research are included in this chapter.

Stems break when wave load exceeds the strength of stems.

Stem breakage can be seen as a simplistic limit state function (Z) of which the stem strength is the resistance and wave force is the load. The basic idea is that stems break when wave force exceeds the strength of the stem. The strength of the stem is quantified by analyzing three-point bending test results from NIOZ (Royal Netherlands Institute for Sea Research), which measures the maximum allowable force by treating the stem as a structural beam. With the measurements of maximum force and geometry of the stem, the maximum allowable stem stress (σ_{\max}) is calculated and compared to the wave load. Two vegetation species are studied in this research: *Spartina anglica* and *Scirpus maritimus*.

The wave load is considered as a uniform force acting along the entire length of the stem, and it is converted into a wave stress (σ_{wave}) which is comparable to the stem strength previously mentioned. The stem is schematized as a cantilevering beam with a uniform wave load applied along its length. The stems are assumed to break near the bottom where the flexure stress is maximum. The horizontal force acting on vegetation is determined by using the equation of Dalrymple et al. [1984].

With the two stress expressions for stem strength (σ_{\max}) and wave load (σ_{wave}), the point

at which stems break can be determined. Further, the critical point (when $\sigma_{\max} = \sigma_{\text{wave}}$) allows for an expression of the threshold wave height at which stems break. Real wave measurement data from Hellegat and Bath in the Netherlands were used to verify whether this approach is within reasonable order of magnitude (Chapter 3).

Correction factor is necessary to account for the overestimation of stem breakage.

The results from the wave energy balance showed that the number of stems breaking is overestimated in the two stem breakage approaches tested. This overestimation could be attributed to neglecting the leaning of stems, which in effect would reduce the amount of wave load acting on the stem (Section 4.2.3). In order to take into account this overestimation, a correction factor for leaning is introduced, which varies depending on the flexibility of the vegetation species.

Sensitivity to wave height and seasonality of vegetation

A sensitivity analysis was performed for the wave energy balance model, for wave height as well as seasonal differences. With a bathymetry configuration of a gradual slope (1:40), the influence of wave height was tested by increasing the incident wave height by 0.2m for every model run. The result showed that with increasing incident wave height, more stem breakage occurred but at a decreasing rate. This behavior could be described from the increasing effect of depth-induced wave breaking that occurs due to the increase in wave height.

Sensitivity by season could also be observed based on the four different field measurement data sets from December 2014 to November 2015, that were obtained by NIOZ. The various measurement sets provided reasonable insight into how vegetation characteristics influence the behavior of stem breakage and consequent wave height variation in the foreshore. Among the two species, *Spartina anglica* was found to be more resilient to the same conditions, in other words, stems broke less than in the case of *Scirpus maritimus*. This could be attributed to the higher flexibility and hollow stem geometry of *Spartina anglica*. However, in the case where the stems did not break for both species, *Scirpus maritimus* showed a higher wave energy dissipation rate than that of *Spartina anglica*. The stronger wave energy dissipation in *Scirpus maritimus* could be attributed to the longer and thicker stems which is a characteristic feature of this species (Chapter 4).

Percentage stem breakage approach shows a more realistic behavior of stem density variation.

The first-order reliability method (FORM) is used in the probabilistic model to calculate the probability of dike failure. Multiple vegetation scenarios as well as differing correlation scenarios are tested.

Among the 5 vegetation scenarios, the most conservative and optimistic approach of no vegetation or strong (non-breaking) stems is modeled, and the models that include vegetation with stem breakage showed intermediate results, in between the most conservative and optimistic model approaches. The binary stem breakage approach (all/none of the stems break) is quite sensitive to the selection of stem strength and vegetation char-

acteristics, because the results often show that all stems in the entire foreshore broke. On the other hand, the percentage stem breakage approach showed a more gradual variation in stem breakage, and showed more realistic stem density variation along the foreshore.

Well-defined characteristic relations reduce the uncertainty of the probabilistic model.

Vegetation characteristics such as stem length, diameter and strength are related to each other, and including a relation between these vegetation characteristics would strengthen the results. Three different correlation scenarios were implemented which differ by: 1) no correlation - baseline scenario; 2) including Pearson correlation coefficients; 3) defining characteristic relations. In order to assess the differences between these correlation scenarios, the amount of uncertainty due to vegetation was analyzed. This analysis was done by comparing the sum of squared influence factors (α^2) of vegetation-related stochastic variables. It showed that including correlation coefficients did not necessarily reduce the amount of uncertainty due to vegetation, but rather slightly increased from the no correlation, baseline scenario. This could be attributed to the complex limit state function, as well as the difficulty to assess the variable's individual influence since the vegetation variables are no longer independent.

The correlation scenario that included characteristic relations instead of correlation coefficients was found to significantly reduce the amount of uncertainty due to vegetation. The characteristic relation is based on the physical relationship between two variables (stem diameter d and stem strength σ_{\max}), as well as includes a more specified relationship (linear relationship assumed between stem length and diameter) which are based on measurement and test data.

Among the individual influences of vegetation-related variables, the stem diameter (d) contributes the most uncertainty to the model, but this can be reduced by defining a characteristic relation.

The uncertainty contribution of individual vegetation-related variables were assessed based on its influence factor (α), and the stem diameter (d) was found to contribute the most uncertainty to the model results than other vegetation-related variables. All three vegetation-related equations (Table 4.1) are functions of stem diameter (d) with differing order of magnitudes. However, with the characteristic relation scenario, this uncertainty due to stem diameter significantly reduces by defining the relationship and including the relevant coefficients (a , b) as stochastic variables instead of (d).

Stem length may act as a resistance or load depending on its magnitude.

The influence factor for stem length is positive (+) for *Spartina anglica* and negative (-) for *Scirpus maritimus*. The positive and negative (+/-) sign generally indicates whether the variable acts as a resistance or a load. The differing effects of the two species can be attributed to its stem length. Wave energy dissipation due to vegetation (ϵ_v) is a resistance parameter and a linear function of stem length ($\propto L$), whereas the wave-induced stress (σ_{\max}) acts as a load parameter that breaks the stems, and it is a function of stem length to the power two ($\propto L^2$). For shorter stem lengths (*Spartina anglica*), the effect due to resistance is stronger, but for longer stems the power two of wave-induced stress

often has a more dominating effect (Chapter 5).

Overall, including stem breakage in quantifying the wave energy and probability of flooding showed reasonable results. This stem breakage approach is useful in that it can model the variation in stem density along the foreshore which depends on the vegetation characteristics as well as physical boundary conditions of the foreshore. The stem breakage approach can be implemented to various species as well as locations around the world, with the generic three-point bending test of the vegetation stems to quantify the strength of the stem, as well as by wave measurement data and bathymetry information, specific to the geographic location.

BIBLIOGRAPHY

- Allsop, W., Kortenhaus, a., and Morris, M. (2007). Failure Mechanisms for Flood Defence Structures. *FLOODsite publications*, (T04-05-01):693–702.
- Battjes, J. and Janssen, J. (1978). Energy Loss and Set-Up Due To Breaking of Random Waves. *Proceedings of 16th Conference on Coastal Engineering, ASCE*, (1):569–587.
- Bjerager, R. (1991). Methods for structural reliability computation. In Casciati, F. and Roberts, J., editors, *Reliability problems: general principles and applications in mechanics of solids and structures*, pages 89–136. Springer Vienna.
- Bosboom, J. and Stive, M. (2015). *Coastal Dynamics 1*. Delft Academic Press (VSSD-uitgeverij), Delft, The Netherlands, 0.5 edition.
- Bouma, T., Vries, M. D., and Herman, P. (2010). Comparing Ecosystem Engineering Efficiency of 2 Plant Species With Contrasting Growth Strategies. *Ecology*, 91(9):2696–2704.
- Bouma, T. J., de Vries, M. B., Low, E., Peralta, G., Tánczos, I. C., van de Koppel, J., and Herman, P. M. J. (2005). Trade-offs Related to Ecosystem Engineering: A Case Study on Stiffness of Emerging Macrophytes. *Ecology*, 86(8):2187–2199.
- Bouma, T. J., van Belzen, J., Balke, T., Zhu, Z., Airoidi, L., Blight, A. J., Davies, A. J., Galvan, C., Hawkins, S. J., Hoggart, S. P. G., Lara, J. L., Losada, I. J., Maza, M., Ondiviela, B., Skov, M. W., Strain, E. M., Thompson, R. C., Yang, S., Zanuttigh, B., Zhang, L., and Herman, P. M. J. (2014). Identifying knowledge gaps hampering application of intertidal habitats in coastal protection: Opportunities & steps to take. *Coastal Engineering*, 87:147–157.
- Cizelj, L., Mavko, B., and Riesch-Oppermann, H. (1994). Application of first and second order reliability methods in the safety assessment of cracked steam generator tubing. *Nuclear Engineering and Design*, 147(3):359–368.
- Dalrymple, R. A., ASCE, M., Kirby, J. T., and Hwang, P. A. (1984). Wave Diffraction Due To Areas of Energy Dissipation. *Journal of Waterway, Port, Coastal, and Ocean Engineering*, 110(1):67–79.
- Dean, R. G. and Bender, C. J. (2006). Static wave setup with emphasis on damping effects by vegetation and bottom friction. *Coastal Engineering*, 53(2-3):149–156.
- Deltares (2016). OpenEarth (<https://publicwiki.deltares.nl/display/OET/OpenEarth>) date accessed: 2016-03-10.

- Diermanse, E., den Heijer, K., and Hoonhout, B. (2016). Probabilistic methods in Open Earth Tools (<https://publicwiki.deltares.nl/display/OET/OpenEarth>) date accessed: 2016-06-02.
- Dijkstra, J. T. and Uittenbogaard, R. E. (2010). Modeling the interaction between flow and highly flexible aquatic vegetation. *Water Resources Research*, 46(12):1–14.
- Duarte, C. M., Losada, I. J., Hendriks, I. E., Mazarrasa, I., and Marbà, N. (2013). The role of coastal plant communities for climate change mitigation and adaptation. *Nature Climate Change*, 3(11):961–968.
- EurOtop, Pullen, T., Allsop, N., Bruce, T., Kortenhaus, A., Schüttrumpf, H., and Van der Meer, J. (2007). *EurOtop - Wave Overtopping of Sea Defences and Related Structures: Assessment Manual*.
- Fonseca, M. S. and Cahalan, J. A. (1992). A preliminary evaluation of wave attenuation by four species of seagrass. *Estuarine, Coastal and Shelf Science*, 35(6):565–576.
- Gautier, C. and Groeneweg, J. (2012). Achtergrondrapportage hydraulische belasting voor zee en estuaria. Technical report, Deltares.
- Kobayashi, N., Raichle, A., and Tshiyuki, A. (1993). Wave Attenuation by Vegetation. *Journal of Waterway, Port, Coastal, and Ocean Engineering*, 119(1):30–48.
- Koch, E. W., Barbier, E. B., Silliman, B. R., Reed, D. J., Perillo, G. M. E., Hacker, S. D., Granek, E. F., Primavera, J. H., Muthiga, N., Polasky, S., Halpern, B. S., Kennedy, C. J., Kappel, C. V., and Wolanski, E. (2009). Non-linearity in ecosystem services: Temporal and spatial variability in coastal protection. *Frontiers in Ecology and the Environment*, 7(1):29–37.
- Liffen, T., Gurnell, A. M., O’Hare, M. T., Pollen-Bankhead, N., and Simon, A. (2013). Associations between the morphology and biomechanical properties of *Sparganium erectum*: Implications for survival and ecosystem engineering. *Aquatic Botany*, 105:18–24.
- Mendez, F. J. and Losada, I. J. (1999). Hydrodynamics induced by wind waves in a vegetation field. *Journal of geophysical research*, 104(C8):18,383–18,396.
- Mendez, F. J. and Losada, I. J. (2004). An empirical model to estimate the propagation of random breaking and nonbreaking waves over vegetation fields. *Coastal Engineering*, 51(2):103–118.
- Möller, I., Kudella, M., Rupprecht, F., Spencer, T., Paul, M., van Wesenbeeck, B. K., Wolters, G., Jensen, K., Bouma, T. J., Miranda-Lange, M., and Schimmels, S. (2014). Wave attenuation over coastal salt marshes under storm surge conditions. *Nature Geoscience*, 7(September):727–731.
- Möller, I., Mantilla-Contreras, J., Spencer, T., and Hayes, A. (2011). Micro-tidal coastal reed beds: Hydro-morphological insights and observations on wave transformation from the southern Baltic Sea. *Estuarine, Coastal and Shelf Science*, 92(3):424–436.

- Ondiviela, B., Losada, I. J., Lara, J. L., Maza, M., Galván, C., Bouma, T. J., and van Belzen, J. (2014). The role of seagrasses in coastal protection in a changing climate. *Coastal Engineering*, 87:158–168.
- Paul, M. and Amos, C. L. (2011). Spatial and seasonal variation in wave attenuation over *Zostera noltii*. *Journal of Geophysical Research: Oceans*, 116(8):1–16.
- Puijalon, S., Bouma, T. J., Douady, C. J., van Groenendael, J., Anten, N. P. R., Martel, E., and Bornette, G. (2011). Plant resistance to mechanical stress: Evidence of an avoidance-tolerance trade-off. *New Phytologist*, 191(4):1141–1149.
- Rupprecht, F., Möller, I., Evans, B., Spencer, T., and Jensen, K. (2015). Biophysical properties of salt marsh canopies — Quantifying plant stem flexibility and above ground biomass. *Coastal Engineering*, (JUNE 2015).
- Schierreck, G. and Verhagen, H. (2012). *Introduction to Bed, Bank and Shore Protection*. VSSD, Delft, The Netherlands, 2 edition.
- Shepard, C. C., Crain, C. M., and Beck, M. W. (2011). The protective role of coastal marshes: A systematic review and meta-analysis. *PLoS ONE*, 6(11).
- Silinski, A., Heuner, M., Schoelynck, J., Puijalon, S., Schröder, U., Fuchs, E., Troch, P., Bouma, T. J., Meire, P., and Temmerman, S. (2015). Effects of wind waves versus ship waves on tidal marsh plants: A flume study on different life stages of *Scirpus maritimus*. *PLoS ONE*, 10(3):1–16.
- Suzuki, T., Zijlema, M., Burger, B., Meijer, M. C., and Narayan, S. (2012). Wave dissipation by vegetation with layer schematization in SWAN. *Coastal Engineering*, 59(1):64–71.
- TU Delft (2016). BE SAFE Bio-Engineering for SAFETY using vegetated foreshores (<http://www.citg.tudelft.nl/nl/over-faculteit/afdelingen/hydraulic-engineering/sections/hydraulic-structures-and-flood-risk/research/be-safe/?action=register>).
- Usherwood, J. R., Ennos, a. R., and Ball, D. J. (1997). Mechanical and anatomical adaptations in terrestrial and aquatic buttercups to their respective environments. *Journal of Experimental Botany*, 48(312):1469–1475.
- van der Doef, M., van Buren, R., Wagenaar, D., and Slootjes, N. D. (2014). *Factsheets - behorend bij technisch-inhoudelijke uitwerking van eisen aan primaire keringen*. Deltaprogramma, deelprogramma Veiligheid.
- Van der Meer, J., Janssen, J., and Delft Hydraulics (1994). *Wave run-up and wave overtopping at dikes and revetments*. Delft Hydraulics.
- Van Gelder, P. H. A. J. M. (2000). Statistical methods for the risk-based design of civil structures.
- van Slobbe, E., de Vriend, H. J., Aarninkhof, S., Lulofs, K., de Vries, M., and Dircke, P. (2013). Building with Nature: In search of resilient storm surge protection strategies. *Natural Hazards*, 66(3):1461–1480.

- Van Wesenbeeck, B. K., Mulder, J. P. M., Marchand, M., Reed, D. J., De Vries, M. B., De Vriend, H. J., and Herman, P. M. J. (2014). Damming deltas: A practice of the past? Towards nature-based flood defenses. *Estuarine, Coastal and Shelf Science*, 140:1–6.
- Vrijling, J., Bezuyen, K., Kuijper, H., van Baars, S., Molenaar, W., and Voorendt, M. (2015). *Manual Hydraulic Structures*. February 2 edition.
- Vuik, V., Jonkman, S. N., Borsje, B. W., and Suzuki, T. (2016). Nature-based flood protection: The efficiency of vegetated foreshores for reducing wave loads on coastal dikes. *Coastal Engineering*, 116:42–56.
- Vuik, V., Van Balen, W., and van Vuren, S. (2015). Fully probabilistic assessment of safety against flooding along the Dutch coast. *Journal of Flood Risk Management*, pages n/a–n/a.
- Yang, S. L., Shi, B. W., Bouma, T. J., Ysebaert, T., and Luo, X. X. (2012). Wave Attenuation at a Salt Marsh Margin: A Case Study of an Exposed Coast on the Yangtze Estuary. *Estuaries and Coasts*, 35(1):169–182.
- Ysebaert, T., Yang, S. L., Zhang, L., He, Q., Bouma, T. J., and Herman, P. M. J. (2011). Wave attenuation by two contrasting ecosystem engineering salt marsh macrophytes in the intertidal pioneer zone. *Wetlands*, 31(6):1043–1054.
- Zhao, Y. G. and Ono, T. (1999). A general procedure for first/order reliability method (FORM/SORM). *Structural Safety*, 21:95–112.

A

WAVE DYNAMICS

A.1. LINEAR WAVE THEORY

The linear wave theory is the basis to ocean and coastal engineering, of which waves are considered as sinusoidal and superimposed on top of each other. This is a simplification ignoring the non-linearities of ocean waves. A distinction is made between deep and shallow water depending on the relation between water depth and wave length (in deep water: L_0 , in shallow water: L_s). Refer to Table A.1. Here, wave number ($k=2\pi/L$) is also a function of wave length.

Shallow water			Deep water		
h/L_0	h/L_s	kh	h/L_0	h/L_s	kh
< 0.015	$< 1/20$	$< \pi/10$	> 0.5	> 0.5	π

Table A.1: Criteria for distinguishing between shallow and deep water in the linear wave theory, with an error of the order of 1% (Bosboom and Stive [2015]).

In this research, the vegetated foreshore is considered as shallow, and the deep water situation will not be discussed in detail. For more information about deep water and shallow water look-up table of wave characteristics, refer to [Bosboom and Stive, 2015] Table B-3.

The fluid motion underneath the water surface shows an orbital path, and in the linear wave theory, these orbital paths are assumed draw a closed circle (deep water) or ellipse (shallow water). In shallow water, water particles are more affected by the bottom surface, and therefore the horizontal displacement remains almost constant. The horizontal orbital velocity is assumed to be nearly constant throughout the vertical profile, as seen in figures A.1 to A.3.

A

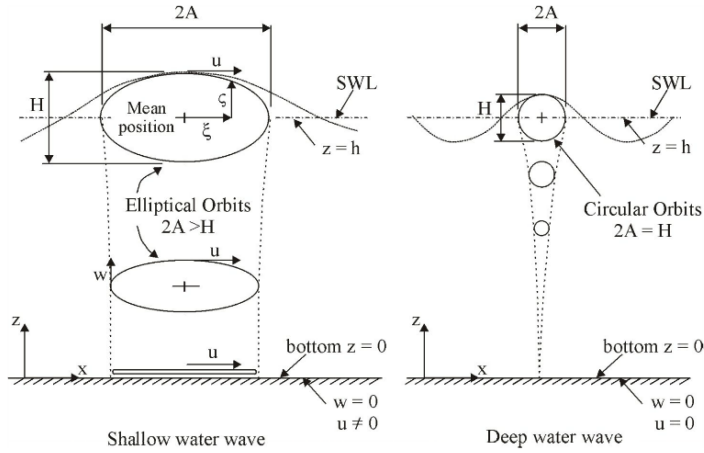


Figure A.1: Horizontal orbital velocity under shallow water wave and deep water wave. *Reprinted from Bosboom and Stive [2015] page 533. Figure B-2.

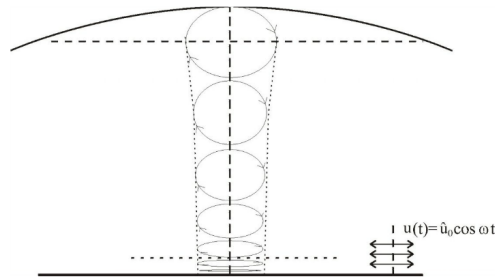


Figure A.2: Horizontal orbital velocity under shallow water. *Reprinted from Bosboom and Stive [2015] page 178. Figure 5-18.

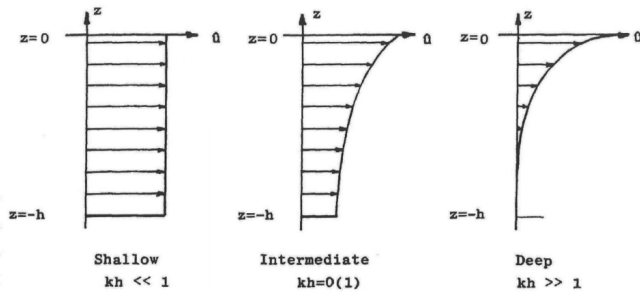


Figure A.3: Schematic drawing of vertical profiles of the horizontal velocity amplitude. $z=0$ indicates the location at water surface, and $z=-h$ indicates the location at the bottom. *Reprinted from Bosboom and Stive [2015] page 179. Figure 5-19.

A.2. SHORT-TERM WAVE STATISTICS

Waves in the sea have irregular shapes and widely varying sizes. When looking closely at waves in the sea, it can easily be concluded that the size and direction are unpredictable with its random orientation. Although the waves at sea are indeed irregular and random, in order to understand the behavior of these waves, short-term wave statistics is used (Bosboom and Stive [2015]). In short-term wave statistics, as its name implies, the waves are expressed in short-term variations in a statistical way in which the average value is taken for a short duration, and it is considered constant during that period of time (stationary). For instance, wave parameters such as the wave height, period, etc. are measured for a duration of 20 minutes every few hours, and the recordings from these 20 minutes are considered as representative (repeated) until the next 20 minute recordings.

In order to be representative of the sea state, the short-term recordings (20 minutes in the previous example) must be long enough to have reliable amount of data, yet short enough to be considered repetitive in time (statistically stationary). The adequate amount of time may vary by situation, but 15-30 minutes is often used at sea. In this re-research, in order to account for the varying motion including tidal variations near shore, an interval of 15 minutes is used: 7 minutes of wave recordings followed by 8 minutes of rest (Section 2.2).

There are two main methods to characterize wave records: 1) direct analysis of time series and 2) spectral analysis. The latter, spectral analysis is used in this research.

The spectral analysis treats the sea surface as a sum of an infinite number of sinusoidal waves each having its own amplitude, frequency, phase, and direction. A Rayleigh distribution can be used to demonstrate the wave heights in a short-term statistical distribution for waves that are not too steep. The Rayleigh distribution is a special type of Weibull distribution in statistical analysis with a scale parameter of 2, and it is often used to characterize wave heights and wind speeds.

The significant wave height is based on 1/3 of the highest wave heights, which is often denoted as H_{m0} . Certain characteristic relations hold between the significant wave height and other representative wave heights, which a few are showed in Table 4.1. For a more complete table of characteristic relations, refer to Bosboom and Stive [2015] Table 3-1.

B

PROBABILISTIC METHODS

B.1. FIRST-ORDER RELIABILITY METHOD (FORM)

Nowadays, probabilistic analysis is more frequently used across many fields in order to assess the probability of a certain event occurring. The advanced computational power allows more possibilities as the calculations have become faster and more robust. Of the many developments and approximation methods in probability assessment, one of the most reliable computational methods is considered to be the first-order reliability method (FORM), Bjerager [1991].

A limit state function ($Z=R-S$) as mentioned earlier in Section 2.6 is used, where again R is the resistance (strength of system) and S is the load (unfavorable force acting on the system). For Z greater than zero, the strength of the system is greater than the load, and the system is in tact. However as the load (S) increases, the point at which $Z=0$ is when the system starts to fail. For Z less than or equal to zero, failure occurs (example: structure breaks, flooding occurs, etc.).

A design point is defined as the point (single combination of variables) with the highest contribution towards the probability of failure. In the variable space, the design point can be found by locating a point on the failure surface ($Z=0$) with the shortest distance to the origin of the variable space (Cizelj et al. [1994], Diermanse et al. [2016], Zhao and Ono [1999]), as can be seen from Figure B.1. This distance is also equivalent to the reliability index, β (distance from the origin). A first order (linear) approximation of the Taylor expansion is used to find the design point, as part of an iterative procedure.

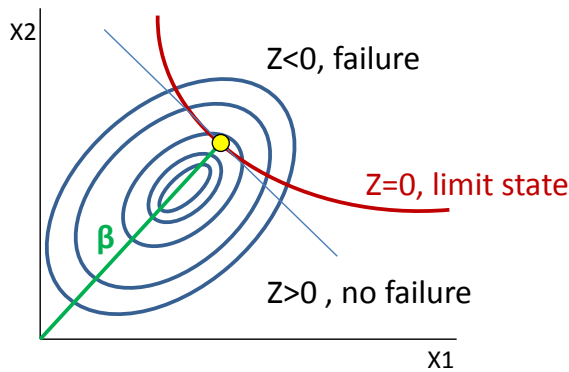


Figure B.1: Representation of a normalized variable space, for first-order reliability method (FORM). The blue ovals indicate the multivariate probability distribution function (PDF) contours of the system; the red line is the failure surface, i.e. limit state function at which $Z=0$; the area above the red line indicates $Z<0$, indicating failure of the system; the area below the red line indicates $Z>0$, in which the the system has not failed; the yellow point is the design point with the shortest distance from origin to failure surface ($Z=0$); this distance is represented by the green line which is the reliability index β .

The first order reliability method (FORM) is used to approximate the design point on the limit state function (Z), which may not necessarily be a straight line, but rather random or curvy. This limit state function is linearized in order to make the first order approximation of the design point.

FORM method takes all the variables in the limit state function and converts them to normally distributed variables. Based on the newly distributed variables, the limit state function is consequently also normally distributed, and a linear approximation is taken in order to find the shortest distance between the failure state ($Z=0$) and the origin of the variable space, also called the reliability index (β). Since the design point is not immediately known, an iterative procedure is used to locate the design point.

Two important factors are calculated from FORM, which are the reliability index (β) and influence factor (α).

1. **Reliability index β :** Minimum distance from failure plane ($Z=0$) to origin of variable space. This distance is also the length between the design point and the origin, and can be calculated with the quotient of mean value over the standard deviation of each variable.

$$\beta = \frac{\mu_z}{\sigma_z} \quad (\text{B.1})$$

2. **Influence factor α_i :** Variable(X_i)'s relative contribution to the uncertainty (variance) of the limit state function. In general, resistance parameters have a positive value of alpha, whereas load parameters have negative values of alpha. However, the sign may not always be representative of whether the variable acts as a load or resistance in cases of complicated limit state functions with multiple relations. A larger magnitude of alpha means the respective variable has a larger uncertainty contribution towards the limit state function. The influence factor α is calculated by:

$$\alpha_i = \frac{a_i \sigma_i}{\sigma_z} \quad (\text{B.2})$$

Here, a_i is calculated by the first order Taylor expansion, and σ_i and σ_z represent the standard deviation of the variable X_i and limit state function (Z), respectively. The influence factors are used for analysis of the FORM results of the probability of overtopping and flooding.

C

VEGETATION CHARACTERISTICS

C

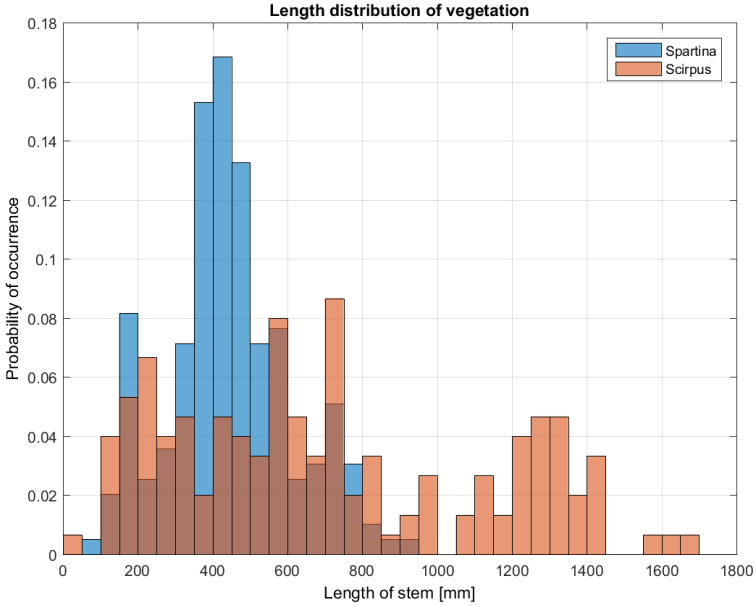


Figure C.1: Distribution of vegetation stem length for species: *Spartina anglica* and *Scirpus maritimus*. Samples are from four different measurement periods in 2014 December, 2015 April, 2015 September, 2015 November

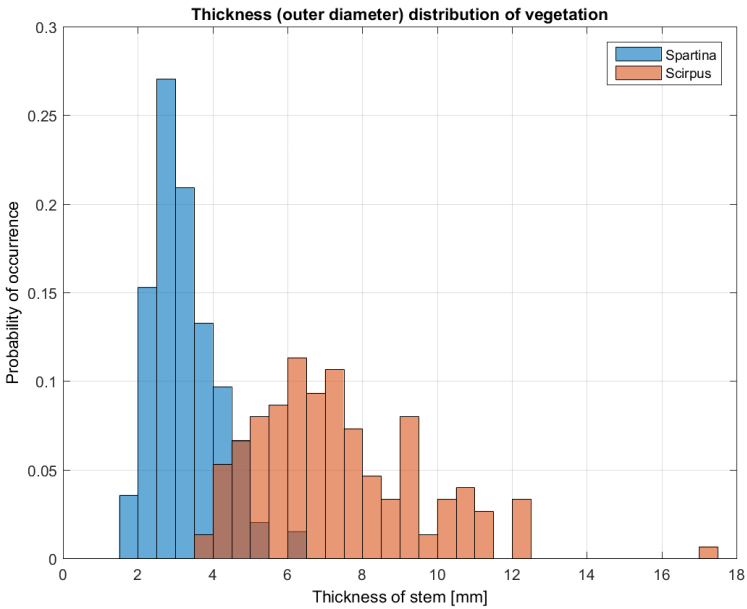


Figure C.2: Distribution of vegetation stem thickness (outer diameter) for species: *Spartina anglica* and *Scirpus maritimus*. Samples are from four different measurement periods in 2014 December, 2015 April, 2015 September, 2015 November

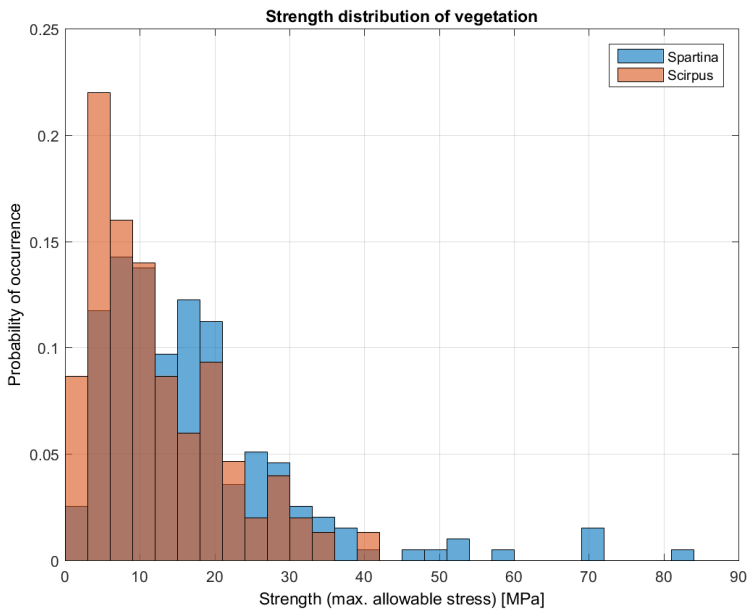


Figure C.3: Distribution of vegetation stem strength (maximum flexure stress from three-point bending tests) for species: *Spartina anglica* and *Scirpus maritimus*. Samples are from four different measurement periods in 2014 December, 2015 April, 2015 September, 2015 November

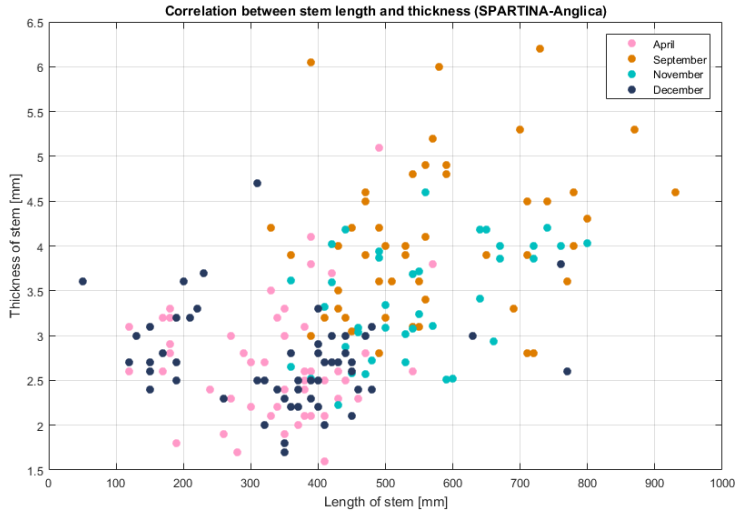


Figure C.4: Correlation between stem length and thickness for species: *Spartina anglica* from four different measurement periods in 2014 December, 2015 April, 2015 September, 2015 November

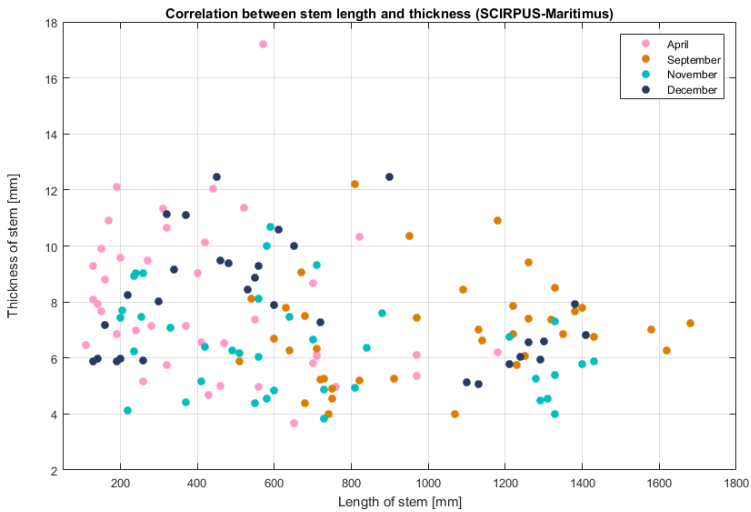


Figure C.5: Correlation between stem length and thickness for species: *Scirpus maritimus* from four different measurement periods in 2014 December, 2015 April, 2015 September, 2015 November

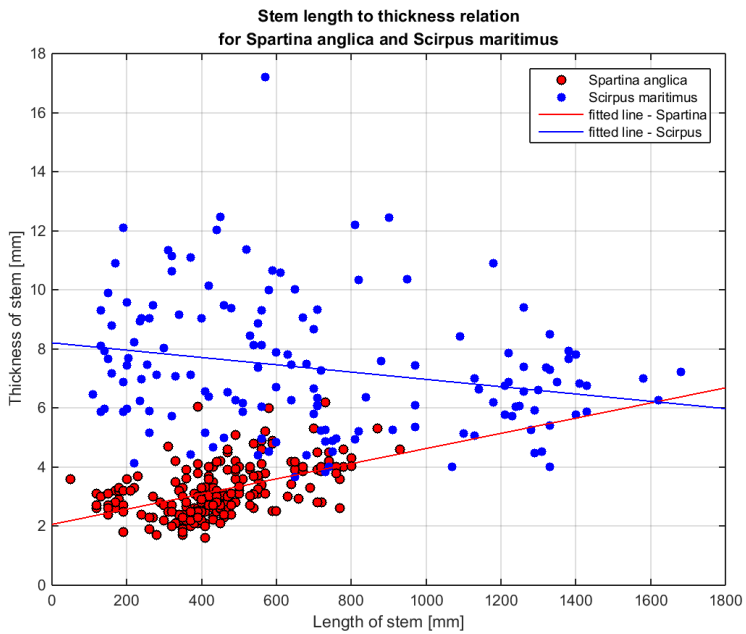


Figure C.6: Stem length to thickness relation for both species: *Spartina anglica* and *Scirpus maritimus* from four different measurement periods in 2014 December, 2015 April, 2015 September, 2015 November

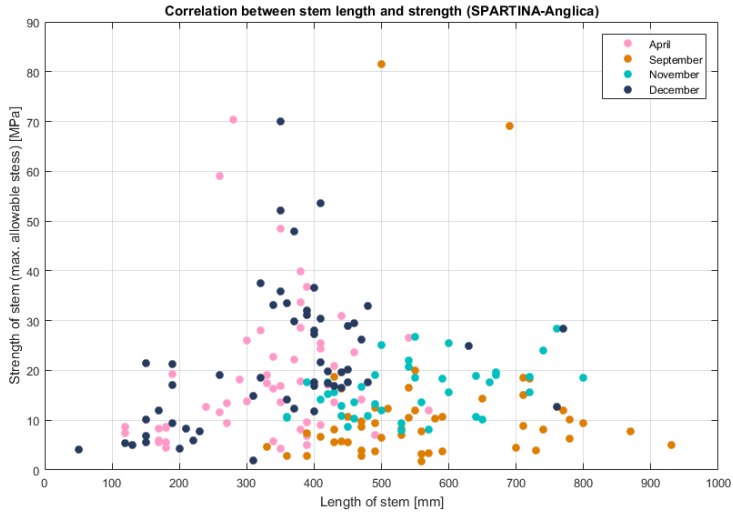


Figure C.7: Correlation between stem length and strength (stress) for species: *Spartina anglica* from four different measurement periods in 2014 December, 2015 April, 2015 September, 2015 November

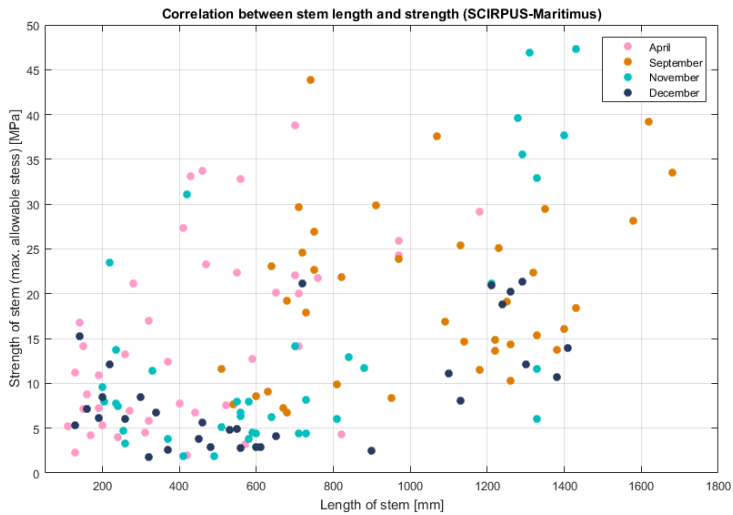


Figure C.8: Correlation between stem length and strength (stress) for species: *Scirpus maritimus* from four different measurement periods in 2014 December, 2015 April, 2015 September, 2015 November

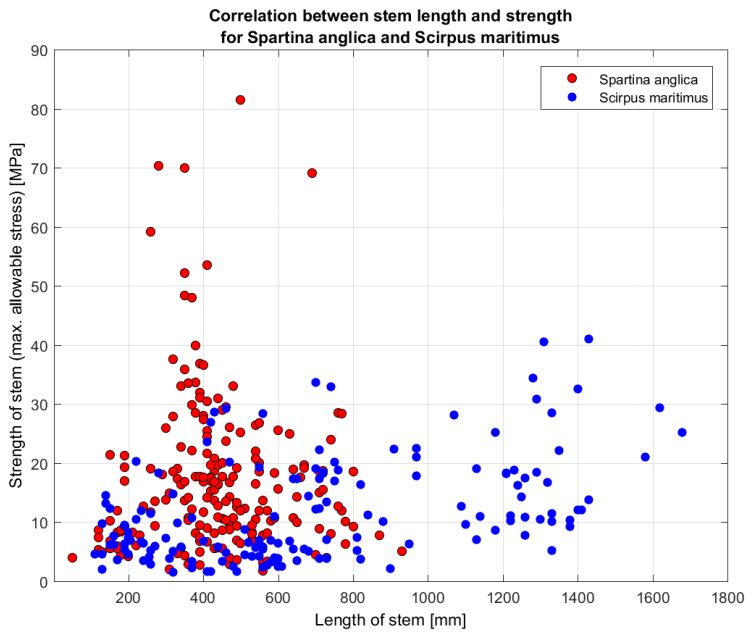


Figure C.9: Correlation between stem length and strength (stress) for both species: *Spartina anglica* and *Scirpus maritimus* from four different measurement periods in 2014 December, 2015 April, 2015 September, 2015 November

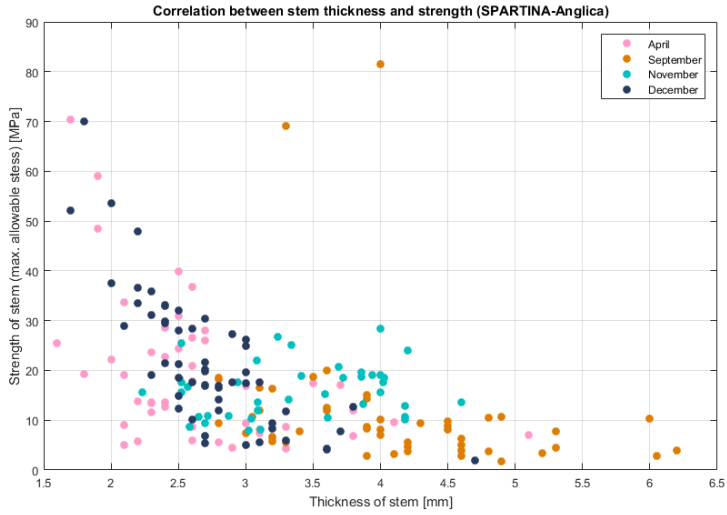


Figure C.10: Correlation between stem thickness and strength (stress) for species: *Spartina anglica* from four different measurement periods in 2014 December, 2015 April, 2015 September, 2015 November

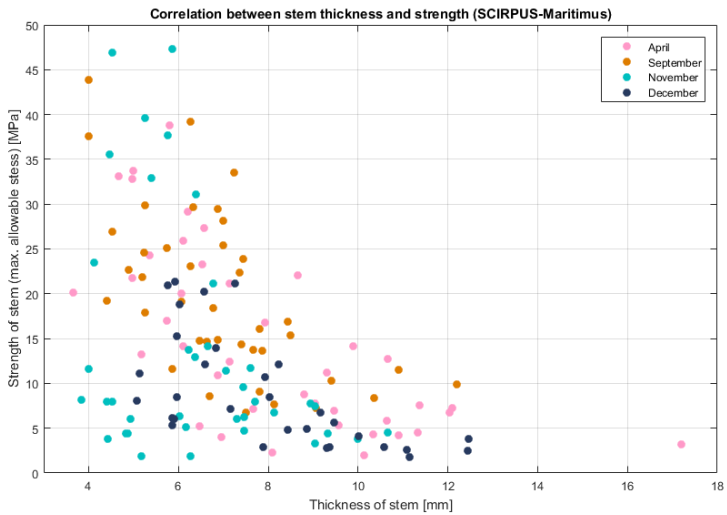


Figure C.11: Correlation between stem thickness and strength (stress) for species: *Scirpus maritimus* from four different measurement periods in 2014 December, 2015 April, 2015 September, 2015 November

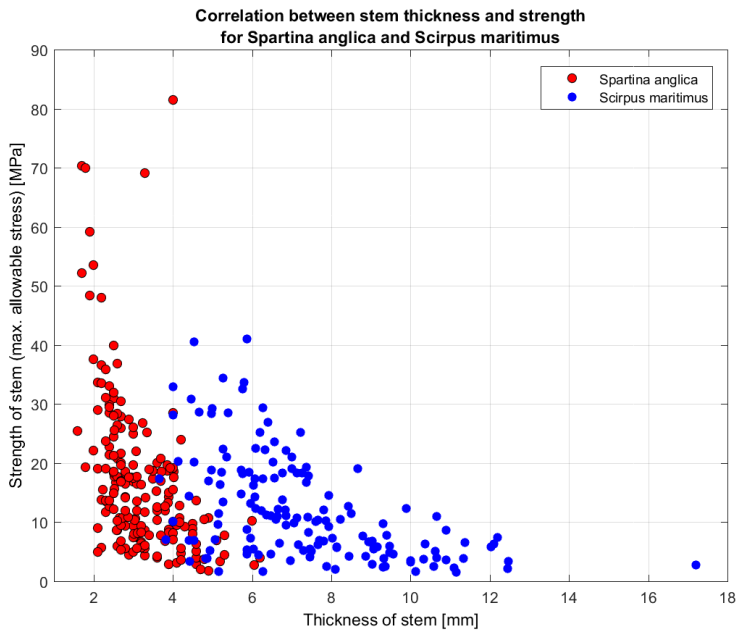


Figure C.12: Correlation between stem thickness and strength (stress) for both species: *Spartina anglica* and *Scirpus maritimus* from four different measurement periods in 2014 December, 2015 April, 2015 September, 2015 November